

# Oncology and Translational Medicine

Volume 6 • Number 1 • February 2020

## Clinical characteristics and survival outcomes of perianal Paget's disease: A SEER population-based study

Hui Peng, Zhimin Liu, Roshan Ara Ghoorun, Xianglin Yuan 1

## Efficacy and safety of anlotinib plus S-1 as thirdly-line or later-line treatment in advanced non-small cell lung cancer

Heng Cao, Kai Liang (Co-first author), Peng Liu (Co-first author), Jing Wang, Yuanyuan Ji, Lujuan Xu, Weilong Wu, Shengnan Guo, Xuekun Song, Yonggui Hong 10

## Cisplatin selects for CD133+ cells in lung cancer cells

Jiaheng Li, Mei Jiang, Xiaoting Zhao, Ziyu Wang, Meng Gu, Weiyang Li 16

## A study on melanoma treatment using dendritic cells loaded with antigens purified from melanoma cell lines

Yanwei Gao, Xia Chen, Weishi Gao, Xiangji Lu, Lin Peng 21

## Proton pump inhibitors and stomach neoplasm

Jinkun Guo, Zhongyin Zhou 26

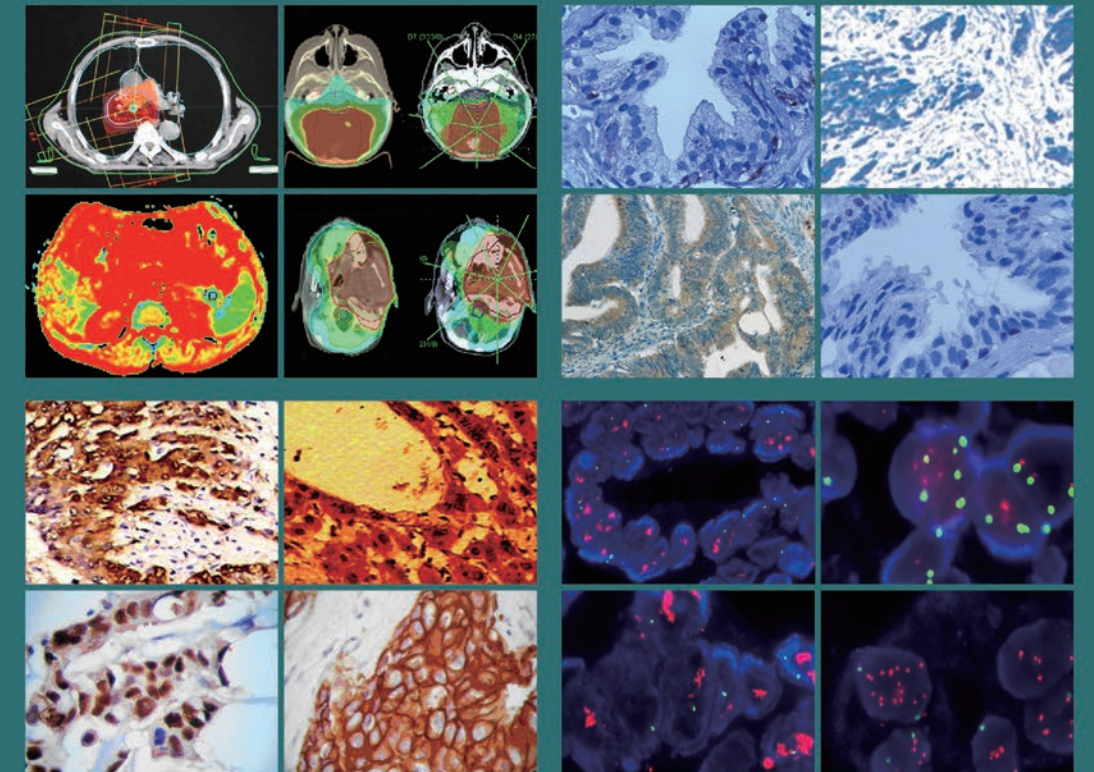
Oncology and Translational Medicine

Volume 6 • Number 1 • February 2020

pp 1-45

ISSN 2095-9621  
CN 42-1865/R

# Oncology and Translational Medicine



**Online First**  
Immediately Online

[otm.tjh.com.cn](http://otm.tjh.com.cn)

Faster  
publication!

邮发代号: 38-121

ISSN 2095-9621



GENERAL INFORMATION  
>> [otm.tjh.com.cn](http://otm.tjh.com.cn)

Volume 6  
Number 1  
February 2020





## Honorary Editors-in-Chief

W.-W. Höpker (Germany)  
Mengchao Wu (China)  
Yan Sun (China)

## Editors-in-Chief

Anmin Chen (China)  
Shiying Yu (China)

## Associate Editors

Yilong Wu (China)  
Shukui Qin (China)  
Xiaoping Chen (China)  
Ding Ma (China)  
Hanxiang An (China)  
Yuan Chen (China)

## Editorial Board

A. R. Hanauske (Germany)  
Adolf Grünert (Germany)  
Andrei Iagaru (USA)  
Arnulf H. Hölscher (Germany)  
Baoming Yu (China)  
Bing Wang (USA)  
Binghe Xu (China)  
Bruce A. Chabner (USA)  
Caicun Zhou (China)  
Ch. Herfarth (Germany)  
Changshu Ke (China)  
Charles S. Cleeland (USA)  
Chi-Kong Li (China)  
Chris Albanese (USA)  
Christof von Kalle (Germany)  
D Kerr (United Kingdom)  
Daoyu Hu (China)  
Dean Tian (China)  
Di Chen (USA)  
Dian Wang (USA)  
Dieter Hoelzer (Germany)  
Dolores J. Schendel (Germany)  
Dongfeng Tan (USA)  
Dongmin Wang (China)  
Ednin Hamzah (Malaysia)  
Ewerbeck Volker (Germany)  
Feng Li (China)  
Frank Elsner (Germany)  
Gang Wu (China)  
Gary A. Levy (Canada)  
Gen Sheng Wu (USA)  
Gerhard Ehninger (Germany)  
Guang Peng (USA)  
Guangying Zhu (China)  
Gunther Bastert (Germany)  
Guoan Chen (USA)

Guojun Li (USA)  
Guoliang Jiang (China)  
Guoping Wang (China)  
H. J. Biersack (Germany)  
Helmut K. Seitz (Germany)  
Hongbing Ma (China)  
Hongtao Yu (USA)  
Hongyang Wang (China)  
Hua Lu (USA)  
Huaqing Wang (China)  
Hubert E. Blum (Germany)  
J. R. Siewert (Germany)  
Ji Wang (USA)  
Jiafu Ji (China)  
Jianfeng Zhou (China)  
Jianjie Ma (USA)  
Jianping Gong (China)  
Jihong Wang (USA)  
Jilin Yi (China)  
Jin Li (China)  
Jingyi Zhang (Canada)  
Jingzhi Ma (China)  
Jinyi Lang (China)  
Joachim W. Dudenhausen (Germany)  
Joe Y. Chang (USA)  
Jörg-Walter Bartsch (Germany)  
Jörg F. Debatin (Germany)  
JP Armand (France)  
Jun Ma (China)  
Karl-Walter Jauch (Germany)  
Katherine A Siminovitch (Canada)  
Kongming Wu (China)  
Lei Li (USA)  
Lei Zheng (USA)  
Li Zhang (China)  
Lichun Lu (USA)  
Lili Tang (China)  
Lin Shen (China)  
Lin Zhang (China)  
Lingying Wu (China)  
Luhua Wang (China)  
Marco Antonio Velasco-Velázquez (Mexico)  
Markus W. Büchler (Germany)  
Martin J. Murphy, Jr (USA)  
Mathew Casimiro (USA)  
Matthias W. Beckmann (Germany)  
Meilin Liao (China)  
Michael Buchfelder (Germany)  
Norbert Arnold (Germany)  
Peter Neumeister (Austria)  
Qing Zhong (USA)  
Qinghua Zhou (China)

Qingyi Wei (USA)  
Qun Hu (China)  
Reg Gorczynski (Canada)  
Renyi Qin (China)  
Richard Fielding (China)  
Rongcheng Luo (China)  
Shenjiang Li (China)  
Shenqiu Li (China)  
Shimosaka (Japan)  
Shixuan Wang (China)  
Shun Lu (China)  
Sridhar Mani (USA)  
Ting Lei (China)  
Ulrich Sure (Germany)  
Ulrich T. Hopt (Germany)  
Ursula E. Seidler (Germany)  
Uwe Kraeuter (Germany)  
W. Hohenberger (Germany)  
Wei Hu (USA)  
Wei Liu (China)  
Wei Wang (China)  
Weijian Feng (China)  
Weiping Zou (USA)  
Wenzhen Zhu (China)  
Xianglin Yuan (China)  
Xiaodong Xie (China)  
Xiaohua Zhu (China)  
Xiaohui Niu (China)  
Xiaolong Fu (China)  
Xiaoyuan Zhang (USA)  
Xiaoyuan (Shawn) Chen (USA)  
Xichun Hu (China)  
Ximing Xu (China)  
Xin Shelley Wang (USA)  
Xishan Hao (China)  
Xiuyi Zhi (China)  
Ying Cheng (China)  
Ying Yuan (China)  
Yixin Zeng (China)  
Yongjian Xu (China)  
You Lu (China)  
Youbin Deng (China)  
Yuankai Shi (China)  
Yuguang He (USA)  
Yuke Tian (China)  
Yunfeng Zhou (China)  
Yunyi Liu (China)  
Yuquan Wei (China)  
Zaide Wu (China)  
Zefei Jiang (China)  
Zhangqun Ye (China)  
Zhishui Chen (China)  
Zhongxing Liao (USA)

# Oncology and Translational Medicine

February 2020 Volume 6 Number 1

## Contents

Clinical characteristics and survival outcomes of perianal Paget's disease:  
A SEER population-based study

*Hui Peng, Zhimin Liu, Roshan Ara Ghoorun, Xianglin Yuan 1*

Efficacy and safety of anlotinib plus S-1 as thirdly-line or later-line treatment in  
advanced non-small cell lung cancer

*Heng Cao, Kai Liang (Co-first author), Peng Liu (Co-first author), Jing Wang, Yuanyuan Ji, Lujuan Xu, Weilong Wu, Shengnan Guo, Xuekun Song, Yonggui Hong 10*

Cisplatin selects for CD133+ cells in lung cancer cells

*Jiaheng Li, Mei Jiang, Xiaoting Zhao, Ziyu Wang, Meng Gu, Weiyang Li 16*

A study on melanoma treatment using dendritic cells loaded with antigens purified from  
melanoma cell lines

*Yanwei Gao, Xia Chen, Weishi Gao, Xiangji Lu, Lin Peng 21*

Proton pump inhibitors and stomach neoplasm

*Jinkun Guo, Zhongyin Zhou 26*

Radiation-induced brain injury after a conventional dose of intensity-modulated radiotherapy  
for nasopharyngeal carcinoma: a case report and literature review

*Qian Zhang, Jie Tang, Jiayu Du, Xiaojie Ma 30*

Glioblastoma multiforme with metastasis to lung, bone, and chest wall:  
a case report

*Guobo Du, Qian Zhou, Xinyao He, Long Cheng, Jing Zhou 36*

The application of 3D printing in the development of RECIST standard for  
evaluating tumor efficacy

*Xiaodan Yang, Tao Han (Co-first author), Yue Zhang, Yanming Zhang, Gao Li, Yongye Liu, Zhaozhe Liu, Zhendong Zheng 39*

Adrenal endothelial cyst associated with adrenocortical adenoma:  
a case report and literature review

*Yuxiang Hong, Qingtao Yang, Junhong Zheng, Gaoming Hou 43*

# Oncology and Translational Medicine

## Aims & Scope

**Oncology and Translational Medicine** is an international professional academic periodical. The Journal is designed to report progress in research and the latest findings in domestic and international oncology and translational medicine, to facilitate international academic exchanges, and to promote research in oncology and translational medicine as well as levels of service in clinical practice. The entire journal is published in English for a domestic and international readership.

## Copyright

Submission of a manuscript implies: that the work described has not been published before (except in form of an abstract or as part of a published lecture, review or thesis); that it is not under consideration for publication elsewhere; that its publication has been approved by all co-authors, if any, as well as – tacitly or explicitly – by the responsible authorities at the institution where the work was carried out.

The author warrants that his/her contribution is original and that he/she has full power to make this grant. The author signs for and accepts responsibility for releasing this material on behalf of any and all co-authors. Transfer of copyright to Huazhong University of Science and Technology becomes effective if and when the article is accepted for publication. After submission of the Copyright Transfer Statement signed by the corresponding author, changes of authorship or in the order of the authors listed will not be accepted by Huazhong University of Science and Technology. The copyright covers

the exclusive right and license (for U.S. government employees: to the extent transferable) to reproduce, publish, distribute and archive the article in all forms and media of expression now known or developed in the future, including reprints, translations, photographic reproductions, microform, electronic form (offline, online) or any other reproductions of similar nature.

## Supervised by

Ministry of Education of the People's Republic of China.

## Administered by

Tongji Medical College, Huazhong University of Science and Technology.

## Submission information

Manuscripts should be submitted to:  
<http://otm.tjh.com.cn>  
[dmedizin@sina.com](mailto:dmedizin@sina.com)

## Subscription information

ISSN edition: 2095-9621  
CN: 42-1865/R

### ■ Subscription rates

Subscription may begin at any time. Remittances made by check, draft or express money order should be made payable to this journal. The price for 2020 is as follows: US \$ 30 per issue; RMB ¥ 28.00 per issue.

## Database

**Oncology and Translational Medicine** is abstracted and indexed in EM-BASE, Index Copernicus, Chinese Science and Technology Paper Citation Database (CSTPCD), Chinese Core Journals Database, Chinese Journal Full-text Database (CJFD), Wanfang

Data; Weipu Data; Chinese Academic Journal Comprehensive Evaluation Database.

## Business correspondence

All matters relating to orders, subscriptions, back issues, offprints, advertisement booking and general enquiries should be addressed to the editorial office.

## Mailing address

Editorial office of  
*Oncology and Translational Medicine*  
Tongji Hospital  
Tongji Medical College  
Huazhong University of Science and Technology  
Jie Fang Da Dao 1095  
430030 Wuhan, China  
Tel.: +86-27-69378388  
Email: [dmedizin@sina.com](mailto:dmedizin@sina.com)

## Printer

Changjiang Spatial Information Technology Engineering Co., Ltd. (Wuhan)  
Hangce Information Cartography Printing Filial, Wuhan, China  
Printed in People's Republic of China

## Managing director

Jun Xia

## Executive editors

Yening Wang  
Jun Xia  
Jing Chen  
Qiang Wu

# Clinical characteristics and survival outcomes of perianal Paget's disease: A SEER population-based study\*

Hui Peng<sup>1</sup>, Zhimin Liu<sup>2</sup>, Roshan Ara Ghoorun<sup>2</sup>, Xianglin Yuan<sup>1</sup> (✉)

<sup>1</sup> Department of Oncology, Tongji Hospital, Tongji Medical College, Huazhong University of Science and Technology, Wuhan 430030, China

<sup>2</sup> Department of Colorectal Surgery, The Sixth Affiliated Hospital of Sun Yat-sen University (Gastrointestinal and Anal Hospital), Guangzhou 510655, China

## Abstract

**Objective** The aim of the study was to analyze the clinical features of patients with perianal Paget's disease (PPD) and investigate prognosis risk factors.

**Methods** The SEER\*Stat software was used to identify 116 PPD patients from 1975 to 2015 in the SEER research database. The Kaplan-Meier method was used to conduct a univariate analysis for PPD patients. The differences in survival rates were evaluated using the log-rank test. The differences in the clinicopathological features of PPD patients with or without anorectal carcinoma were compared using the chi-square test.

**Results** The median survival time of PPD patients was 44 months. The median age of onset was 73 years old. The 43.10% of the patients were alive at the end of follow up, and only 12.93% of the patients died of PPD. Elderly (age > 70 years;  $\chi^2 = 9.453$ ,  $P = 0.002$ ), poor differentiation ( $\chi^2 = 46.557$ ,  $P = 0.000$ ) and abdominal perineal resection (APR;  $\chi^2 = 46.557$ ,  $P = 0.000$ ) were unfavorable risk factors of prognosis. Nearly 50% of PPD had combined with other malignancies, and over 22.41% of those had multiple primary neoplasms (3 or more). PPDs predisposed concurrent malignancy, and 48.21% of PPD patients with other malignancies combined with anorectal carcinoma in the study. Stage ( $\chi^2 = 10.127$ ,  $P = 0.018$ ), and surgical method ( $\chi^2 = 12.245$ ,  $P = 0.007$ ) were statistically significant in the PPD patients with or without anorectal carcinoma. The 16.07% of patients had multiple lesions of Paget's.

**Conclusion** Patients with PPD have a favorable survival, while the disease-specific mortality is low. Diagnosed age, differentiation, and surgical methods were the influence factors of prognosis in PPD patients. PPDs with anorectal carcinoma is of most important in further investigation.

**Key words:** perianal Paget's disease (PPD); extramammary Paget's disease; SEER database; survival analysis

Received: 7 January 2020

Revised: 1 February 2020

Accepted: 20 February 2020

Paget's disease (PD), first described by Sir James Paget in 1874<sup>[1]</sup>, was initially found in the breast. Two decades later, in 1889, Crocker reported extramammary Paget's disease (EMPD) of a genital site<sup>[2]</sup>. In 1893, perianal Paget's disease (PPD) was discovered<sup>[3]</sup>. Since then, less than 200 cases have been mentioned in the literature. Due to its rarity, and frequent association with concurrent malignancies, its management remains challenging. Wietfeldt<sup>[4]</sup> summarized a number of PPD

cases and established a treatment guideline for different situations. However, these cases were mostly from papers with small sample sizes, which inevitably results in selective bias. Up to now, the largest study<sup>[5]</sup> came from the Memorial Sloan-Kettering Cancer Center, which involved 65 patients over a 6 year follow-up period. Other than that, most papers have been case series. Several papers have focused on EMPD using the SEER database. Initially, Karam and Dorigo<sup>[6]</sup> asserted that the

✉ Correspondence to: Xianglin Yuan. Email: xlyuan1020@163.com

\* Supported by grants from the Scientific Research Staring Foundation for the Returned Overseas Scholars and the Scientific Research Foundation of Tongji Hospital, Tongji Medical College, Huazhong University of Science and Technology (No. 2019A16).

© 2020 Huazhong University of Science and Technology

disease-specific survival of invasive EMPD is generally favorable. Later, they identified that patients had a long-term increased risk of developing secondary malignancies of invasive EMPD and suggested a prolonged follow-up period [7]. Yao *et al* [8] found that vaginal lesions, older age, concurrent malignancy, distant metastasis, and being male are risk factors of EMPD survival and that surgery is a protective factor. However, EMPD is a group of diseases that encompasses multiple lesion sites, including the perianus.

As far as we know, this is the first paper that focusses on PPD using the SEER database and is one of the largest population-based studies about PPD. Although the study was retrospectively conducted, we believe that the large sample size will help to improve our understanding of this rare onset disease and offer interesting insights that can be used in clinical practice and surgical management.

## Materials and methods

### Data source

The SEER database is one of the world's largest open cancer databases. Representing almost 30% of the population of the United States of America, the database contains data on cancer incidence and mortality from 18 population-based registries. We signed the SEER research data agreement to access the SEER database. The SEER database and SEER-stat software (SEER\*Stat 8.3.5) were used to search for PPD patients between 1975 and 2015 with a known age ( $\geq 18$  years). Year of diagnosis, sex, race, primary site, differentiation grade, stage, histological type, surgery, cause of death, total number of *in situ*/malignant tumors, reason for no cancer-directed surgery, radiation, chemotherapy, number of PPD(s), and sequence at diagnosis were extracted from the SEER database.

### Statistical analysis

Baseline patient demographic characteristics and tumor information were compared using the Pearson's chi-square test for categorical variables. Overall survival (OS) was measured from the date on which the first definite diagnosis was made until the date of death, the date last known to be alive, or to 2015. Disease-specific survival (DSS) was measured from the date of diagnosis to the date of deaths, which were associated with PPD. Survival curves were generated according to the Kaplan-Meier method and compared using the log-rank test in a univariate analysis. All the statistical analyses were performed using SPSS statistical software, version 25.0 (IBM Corp, Armonk, NY). All *P*-values were two-sided. A *P*-value of  $< 0.05$  was considered statistically significant.

## Results

### Characteristics of all the PPD patients included in this study

A total of 116 patients diagnosed with PPD in the SEER database from 1975 to 2015 were included in this study. The median follow-up time was 45.5 months, with the longest follow-up time being 340 months. The 63.79% of the patients were  $> 70$  years old, and 50.0% of the patients were males. The 84.48% of the patients were white, while 2.59% were black. The anus was the most common primary site, affecting 56.90% of the patients, followed by the anal canal at 31.03%, and the overlap rectum at 12.07%. Localized PPD covered 42.24%. 49.14% of the patients had one *in situ*/malignant tumors, while 28.45% and 22.41 % of the patients had two and more than two *in situ*/malignant tumors, respectively. The 69.83% of the patients underwent a surgical resection, followed by excisional biopsy, local tumor excision, and abdominal perineal resection (APR) in 56.79% and 16.05% of the patients, respectively. Surgery was not recommended in 77.14% of the patients who did not undergo surgery. The 43.10% of the patients were alive at the end of follow up, and only 12.93% of the patients died of PD. The characteristics of the patients with PPD are shown in Table 1.

### Prognosis analysis of the PPD patients

The median survival time of the 116 patients diagnosed with PPD was 44 months. The 1-year survival rate was 70.69%, while the 3-year, 5-year, 10-year, and 15-year survival rates were 48.28%, 31.03%, 10.34%, and 3.45%, respectively. The overall survival curve and disease-specific survival curve are shown in Fig. 1. The univariate survival analysis of the clinical and pathological factors indicated that age at diagnosis ( $\chi^2 = 9.453$ ,  $P = 0.002$ , optimal cutoff value was 70 years old), grade of differentiation ( $\chi^2 = 46.557$ ,  $P = 0.000$ ), and surgical method ( $\chi^2 = 4.790$ ,  $P = 0.029$ ) had a significant influence on the survival of patients with PPD (Fig. 2). Sex, race, primary site, stage, and other factors were not significantly related to prognosis (Table 2).

### Characteristics of the PPD patients with anorectal carcinoma

In the selected database, 27 patients were diagnosed with PPD and anorectal carcinoma. The median follow-up time in these patients was 39 months, the longest follow-up time was 199 months, and the shortest follow-up time was 2 months. The 62.96% of the patients were  $> 70$  years old, and 59.26% of the patients were male. The 81.48% of the patients were white, while 3.70% were black people. The anus was the most common primary site, affecting 59.26% of the patients, followed by the

**Table 1** Characters of perianal Paget's disease patients included in this study

Clinical characteristics	Number	Percentage (%)
Total number	116	100.00
Age at diagnosis (years)		
≤ 70	42	36.21
> 70	74	63.79
Sex		
Male	58	50.00
Female	58	50.00
Race		
White	98	84.48
Black	3	2.59
Other	15	12.93
Primary site		
Anus	66	56.90
Anal canal	36	31.03
Overlap rectum	14	12.07
Stage		
Localized	49	42.24
Regional	21	18.10
Distant	5	4.31
Unknown	41	35.34
Total number of <i>in situ</i> /malignant tumors for patient		
1	60	51.72
2	30	25.86
≥ 3	26	22.41
Surgery		
Yes	81	69.83
No	35	30.17
Surgical method		
Excisional biopsy, local tumor excision	46	56.79
APR	13	16.05
Polypectomy	1	1.23
Others	21	25.93
Reason of no cancer-directed surgery		
Not recommend	27	77.14
Recommend, but not performed	8	22.86
Survival status		
Alive	50	43.10
Paget's disease	15	12.93
Others (not by Paget's disease)	51	43.97
Cause of death		
Rectum and rectosigmoid junction malignancy	20	30.30
Colon malignancy	5	7.58
Other malignancy (anus, breast, lung, bronchus, non-melanoma skin malignancy or Hodgkin lymphoma)	14	21.21
Cardio-cerebrovascular disease	12	18.18
Urogenital diseases (urinary bladder, vulva, or prostate disease)	3	4.55
Septicemia	3	4.55
Chronic liver disease	1	1.52
Other causes	8	12.12

anal canal at 18.52% and overlap rectum at 22.22%. The 40.74% of the patients had one *in situ*/malignant tumor, while 25.93% and 33.33 % of the patients had two and more than two *in situ*/malignant tumors, respectively. About 74.07% of the patients were synchronous, while only 18.52% were metachronous. The 77.78% of the patients underwent surgery, followed by excisional biopsy, local tumor excision, and APR in 76.19% and 19.05% of the patients, respectively. The 83.33% of those that did not undergo surgery was because it was not recommended. The 77.78% of the patients did not undergo radiation or cancer-directed radiation, while 33.33% of the patients received chemotherapy. The 40.74% of the patients were alive at the end of follow up, and only 14.81% of the patients died of PD. Characters of the patients with PPD and anorectal carcinoma are shown in Table 3.

**Analysis of the influencing factors on PPD patients with anorectal carcinoma**

The stage ( $\chi^2 = 10.127, P = 0.018$ ), and surgical method ( $\chi^2 = 12.245, P = 0.007$ ) were statistically significant in the PPD patients with or without anorectal carcinomas. Age at diagnosis, sex, race, cause of death, number of tumors, the total number of benign/borderline tumors, the total number of *in situ*/malignant tumors, and reason for not undergoing cancer-directed surgery was not statistically significant between PPD patients with or without anorectal carcinomas (Table 4).

**Characteristics of PPD patients with other malignant tumors**

In the study, a total of 56 patients diagnosed with PPD and other malignant tumors in the SEER database from 1975 to 2015 were included. The median follow-up time was 70 months, the longest follow-up time was 340 months, and the shortest follow-up time was 2 months. The 48.21% of the patients were > 70 years old, and 55.36% of the patients were male. The 83.93% of the patients were white, while 5.36% were black. The 55.36% of the patients had two *in situ*/malignant tumors, while 32.14%, 10.71%, and 1.79% of the patients had 3, 4, and 5 *in situ*/malignant tumors, respectively. The 83.93% of the patients had one PPD, while 14.29% and 1.79% of the patients had 2 and 4 PPDs, respectively. PPD and the other malignant tumors were diagnosed at the same time in 53.57% of the patients, while only PPD was initially diagnosed in 14.29% of the patients. The 35.71% of the patients were alive at the end of the follow-up period. Only 17.86% of the patients died of PD, while 46.43% of the patients died from other causes. Characteristics of the patients with PPD and other malignant tumors are shown in Table 5.

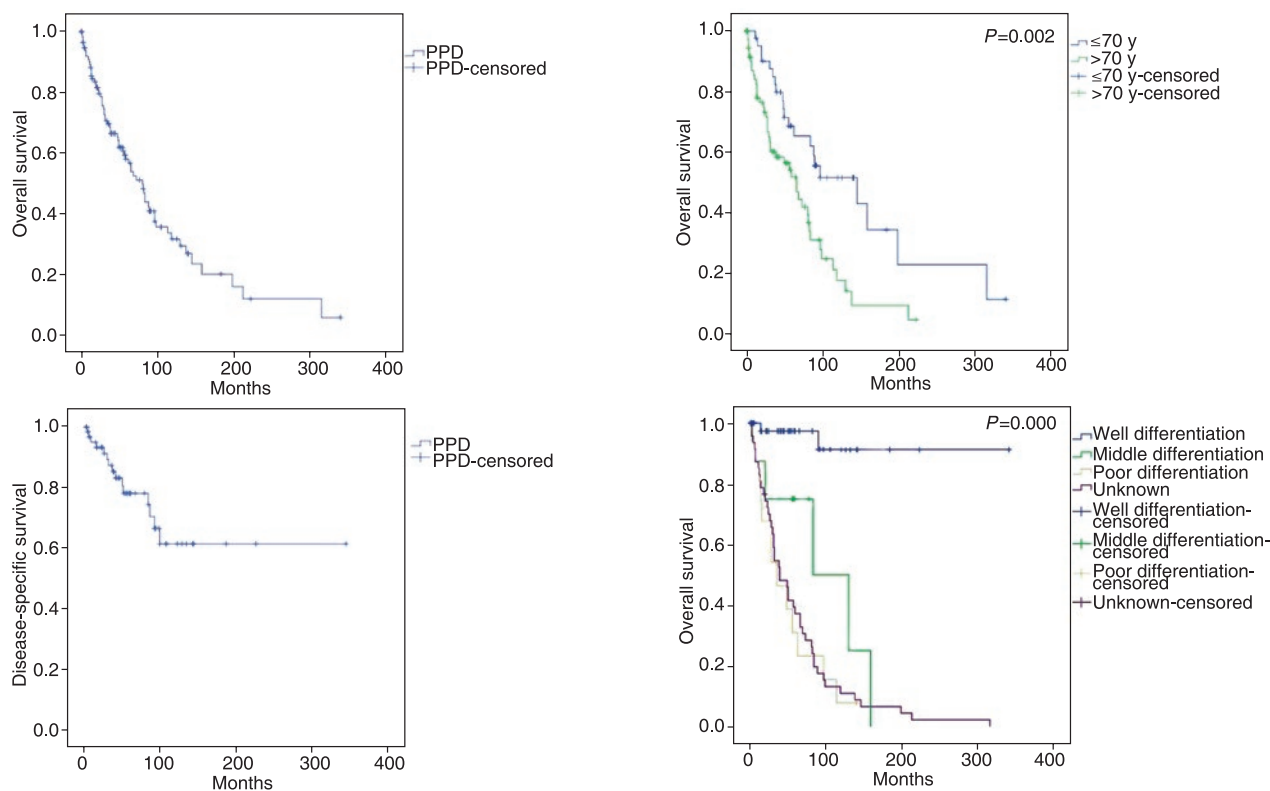


**Fig. 1** Overall survival and disease-specific survival of patients with perianal Paget's disease (PPD)

## Discussion

Although it is the second most common site of EMPD [5, 9], PPD is still rare. To examine the clinical features of PPD, we went through the SEER database and found 116 patients over 40 years old (1975–2015) with PPD. As far as we know, this is the largest study on PPD. The majority of patients were elderly, with the median age of onset being 73 years old. PPD is generally accepted to occur in older people [10]. Our results had an equal gender distribution (50% were male, and 50% were female). Since it is a nationwide population-based study, we do not observe the same female gender predominance as some studies [11–12].

We found that age, grade of differentiation, and surgical method were the risk factors of the overall survival of PPD patients. Patients older than 70 years old had a reduced survival rate. Older patients have a higher incidence of comorbidities and lower performance status or Karnofsky score, which might be the underlying reason for their inferior survival. The grade was the only pathology stratification included in the database. The survival rates of different grades showed satisfactory discrimination, where better-differentiated tumors resulted in more prolonged survival. Several studies have

**Fig. 2** Prognosis analysis of patients with perianal Paget's disease (PPD). Age at diagnosis, grade of differentiation, and surgical method had a significant influence on the survival of patients with PPD

emphasized the important role of pathology. Invasive malignancy was seen to result in reduced survival [10, 13]. Takamichi [14] investigated 155 EMPDs and indicated that a tumor thickness of more than 3 mm was the cutoff point for survival.

EMPD is well known for being associated with concurrent malignancies [9, 13]. Among all anatomic sites of EMPD, PPD is an intractable neoplasm and is more frequently associated with other malignant diseases than any other EMPD. Along with the findings of our study, nearly 50% of those with PPD (56/116) have other malignancies, and over 22.41% of those have

**Table 2** Prognosis analysis of all the PPD patients

Clinical characteristics		1-year survival rate [% (n)]	3-year survival rate [% (n)]	5-year survival rate [% (n)]	10-year survival rate [% (n)]	15-year survival rate [% (n)]	$\chi^2$	P
Total number		70.69 (82)	48.28 (56)	31.03 (36)	10.34 (12)	3.45 (4)		
Age at diagnosis (years)	≤ 70	95.24 (40)	78.57 (33)	50.00 (21)	23.81 (10)	9.52 (4)	9.453	0.002
	> 70	77.03 (57)	47.30 (35)	29.73 (22)	6.76 (5)	2.70 (2)		
Sex	Male	84.48 (49)	56.90 (33)	36.21 (21)	12.07 (7)	5.17 (3)	1.768	0.184
	Female	82.76 (48)	60.34 (35)	37.93 (22)	13.79 (8)	5.17 (3)		
Race	White	83.67 (82)	57.14 (56)	36.73 (36)	12.24 (12)	4.08 (4)	0.204	0.903
	Black	100.00 (3)	66.67 (2)	66.67 (2)	0 (0)	0 (0)		
	Other	85.71 (12)	71.43 (10)	42.86 (6)	21.43 (3)	14.29 (2)		
Primary site	Anus	81.82 (54)	56.06 (37)	33.33 (22)	10.61 (7)	4.55 (3)	2.821	0.244
	Anal canal	80.56 (29)	52.78 (19)	36.11 (13)	8.33 (3)	2.78 (1)		
	Overlap rectum	100.00 (14)	85.71 (12)	57.14 (8)	35.71 (5)	14.29 (2)		
Grade	I (well diff)	75.00 (3)	50.00 (2)	50.00 (2)	0 (0)	0 (0)	46.557	0.000
	II (mid diff)	100.00 (4)	100.00 (4)	50.00 (2)	25.00 (1)	0 (0)		
	III (poor diff)	100.00 (8)	50.00 (4)	37.50 (3)	12.50 (1)	0 (0)		
Stage	Localized	83.67 (41)	65.31 (32)	36.73 (18)	14.29 (7)	6.12 (3)	3.920	0.270
	Regional	85.71 (18)	61.90 (13)	38.10 (8)	9.52 (2)	0 (0)		
	Distant	60.00 (3)	60.00 (3)	40.00 (2)	0 (0)	0 (0)		
	Unknown	85.37 (35)	48.78 (20)	36.59 (15)	14.63 (6)	7.32 (3)		
Surgical method	APR	76.92 (10)	53.85 (7)	23.08 (3)	0 (0)	0 (0)	4.790	0.029
	not APR	84.47 (87)	59.22 (61)	38.83 (40)	14.56 (15)	6.80 (7)		
Survival status	Alive	86.00 (43)	68.00 (34)	38.00 (19)	16.00 (8)	6.00 (3)		
	Paget's disease	80.00 (12)	46.67 (7)	26.67 (4)	0 (0)	0 (0)		
	Others	82.35 (42)	52.94 (27)	39.22 (20)	13.73 (7)	5.88 (3)		
Total number of <i>in situ</i> malignant tumors for patient	< 3	82.22 (74)	54.44 (49)	34.44 (31)	11.11 (10)	3.33 (3)	3.755	0.053
	≥ 3	88.46 (23)	73.08 (19)	46.15 (12)	19.23 (5)	11.54 (3)		

multiple primary neoplasms (3 or more). We discovered 56 PPDs with different concurrent diseases, including anorectal carcinoma (27/56), urogenital tumor (11/56), breast cancer (6/56), gynecologic tumor (6/56), and colon cancer (3/56). The most common malignancy was rectal adenocarcinoma. Grow *et al*<sup>[15]</sup> reported that 76% of those with PPD had underlying rectal carcinoma. However, we assume that this is overestimated because our data did not show such a high prevalence (21/116, 18.1%). Derived from a well-regarded system, we believe that this incidence rate is more objective and closer to the accurate morbidity<sup>[16]</sup>.

Two types of PPD are typically identified<sup>[17]</sup>. Primary PPD is an *in situ* cutaneous intraepithelial neoplasm of the Paget's cell with CK7<sup>+</sup>/CK20<sup>-</sup>/GCDFP15<sup>+</sup><sup>[18]</sup>. Secondary PPD shows endodermal differentiation of the gastrointestinal glands with CK7<sup>±</sup>/CK20<sup>±</sup>/GCDFP15<sup>-</sup> and is considered to be the epidermotropic spread of concurrent primary malignancy<sup>[18-19]</sup>. Although we could not access the detailed pathological information, we did have access to the PPD sequence and whether the patient had concurrent anorectal carcinoma. About 74.07% (20/27) of the patients were synchronous, while only 18.52% (5/27) were metachronous. We assume that those synchronous patients had secondary PPD.

For most patients that have PPD without anorectal carcinoma, wide local excision is the recommended procedure. However, 2 steps of screening are still useful. Step 1: carefully search for the presence of primary gastrointestinal lesions to avoid a misdiagnosis. Step 2: closely follow up and be aware of the possibility of metachronous gastrointestinal cancer. Wietfeldt *et al* developed a guideline for various perianal malignancies, including treatment recommendations for PPD according to the different status of the lesion and other associated malignancies<sup>[4]</sup> (Table 6). However, these are not evidence-based treatment strategies. The number of patients treated in each instance is small, which means that the use of these modalities in treating PPD remains controversial. Based on the cause of death, anorectal carcinoma is more life-threatening than PPD (9/27 vs. 4/27). However, it is interesting to find that not all the candidates were following the management plan recommended. Sixteen (76.19%) patients underwent local excision of the lesion, while only 4 patients underwent APR. Surprisingly, the 4 patients who underwent APR treatment showed an inferior survival rate to the others. The underlying reason might be a histopathological error. However, more in-depth research is required. Although we were not able to check the TNM stage or histopathology, it is uncertain

**Table 3** Characters of PPD patients with anorectal carcinoma included in this study

Clinical characteristics	Number	Percentage (%)
Total PPD patients with anorectal carcinoma	27	100.00
Age at diagnosis (years)		
≤ 70	10	37.04
> 70	17	62.96
Sex: Male	16	59.26
Female	11	40.74
Race: White	22	81.48
Black	1	3.70
Other	4	14.81
Primary site: Anus	16	59.26
Anal canal	5	18.52
Overlap rectum	6	22.22
Stage		
Localized	9	33.33
Regional	10	37.04
Distant	2	7.41
Unknown	6	22.22
Total number of <i>in situ</i> /malignant tumors for patient		
1	11	40.74
2	7	25.93
≥ 3	9	33.33
Surgery		
Yes	21	77.78
No	6	22.22
Surgical method		
Excisional biopsy, local tumor excision	16	76.19
APR	4	19.05
Polypectomy	1	4.76
Reason of no cancer-directed surgery		
Not recommend	5	83.33
Recommend, but not performed	1	16.67
Radiation		
No radiation and/or cancer-directed surgery	21	77.78
Ratiation after surgery	4	14.81
Ratiation before and after surgery	1	3.70
Ratiation prior to surgery	1	3.70
Chemotherapy		
Yes	9	33.33
No/unknown	18	66.67
Survival status		
Alive	11	40.74
Paget's disease	4	14.81
Others (not by Paget's disease)	12	44.44
Cause of death		
Rectum and rectosigmoid junction malignancy	7	43.75
Anus malignancy	2	12.50
Cerebrovascular disease	2	12.50
Vulva disease	1	6.25
Chronic liver disease	1	6.25
Other causes	3	18.75
Sequence at diagnosis		
Synchronous	20	74.07
Anorectal carcinoma ahead	2	7.41
PPD ahead	5	18.52

**Table 5** Characters of PPD patients with other malignant tumor(s) included in this study

Clinical characteristics	Number	Percentage (%)
Total number	56	100.00
Age at diagnosis (years)		
≤ 70	29	51.79
> 70	27	48.21
Sex		
Male	31	55.36
Female	25	44.64
Race		
White	47	83.93
Black	3	5.36
Other	6	10.71
Sequence at diagnosis		
PPD ahead	8	14.29
Other malignant carcinoma ahead	18	32.14
Synchronous	30	53.57
Survival status		
Alive	20	35.71
Paget's disease	10	17.86
Others	26	46.43
Total number of <i>in situ</i> /malignant tumors for patient		
2	31	55.36
3	18	32.14
4	6	10.71
5	1	1.79
Number of PPD(s)		
1	47	83.93
2	8	14.29
4	1	1.79
With other malignant tumor(s)		
Carcinoma (rectum)	21	37.50
Adenocarcinoma (anal canal)	4	7.14
Adenocarcinoma (anus)	2	3.57
Clear cell adenocarcinoma (kidney)	1	1.79
Adenocarcinoma (prostate)	7	12.50
Carcinoma (bladder)	3	5.36
Adenocarcinoma (breast)	6	10.71
Adenocarcinoma (corpus uteri)	2	3.57
Granulosa cell tumor (ovary)	2	3.57
Mucinous adenocarcinoma (vagina)	1	1.79
Adenocarcinoma (vulva)	1	1.79
Adenocarcinoma (colon)	3	5.36
Adenocarcinoma (splenic flexure)	1	1.79
Chronic lymphocytic leukemia/small lymphocytic lymphoma (bone)	1	1.79
<i>In situ</i> (trunk)	2	3.57
Large cell carcinoma (lung)	2	3.57
Malignant melanoma (shoulder)	1	1.79
Adenocarcinoma (pancreas)	1	1.79
Gastrointestinal stromal sarcoma (stomach)	1	1.79
<i>In situ</i> (overlapping lesion of skin)	1	1.79
Lentigo maligna melanoma (ear)	1	1.79
Extranodal marginal zone lymphoma of mucosal-assoc. lymphoid tissue-MALT	1	1.79

**Table 4** Analysis of influencing factors of PPD patients with anorectal carcinoma

Clinical characteristics		PPD with anorectal carcinoma [% (n)]	PPD without anorectal carcinoma [% (n)]	$\chi^2$	P
Total number		100.00 (27)	100.00 (89)		
Age at diagnosis (years)	≤ 70	37.04 (10)	35.96 (32)	0.010	0.918
	> 70	62.96 (17)	64.04 (57)		
Sex	Male	59.26 (16)	47.19 (42)	1.207	0.272
	Female	40.74 (11)	52.81 (47)		
Race	White	81.48 (22)	85.39 (76)	0.304	0.859
	Black	3.70 (1)	2.25 (2)		
	Other	14.81 (4)	12.36 (11)		
Primary site	Anus	59.26 (16)	56.18 (50)	4.817	0.090
	Anal canal	18.52 (5)	34.83 (31)		
	Overlap rectum	22.22 (6)	8.99 (8)		
Stage	Localized	33.33 (9)	44.94 (40)	10.127	0.018
	Regional	37.04 (10)	12.36 (11)		
	Distant	7.41 (2)	3.37 (3)		
	Unknown	22.22 (6)	39.33 (35)		
Total number of <i>in situ</i> malignant tumors for patient	1	40.74 (11)	38.20 (34)	3.408	0.182
	2	25.93 (7)	42.70 (38)		
	≥ 3	33.33 (9)	19.10 (17)		
Surgery	Yes	77.78 (21)	91.01 (81)	12.245	0.007
	No	22.22 (6)	39.33 (35)		
Surgical method	Excisional biopsy, local tumor excision	76.19 (16)	37.04 (30)	0.157	0.692
	APR	19.05 (4)	11.11 (9)		
	Polypectomy	4.76 (1)	0 (0)		
	Others	0 (0)	25.93 (21)		
Reason of no cancer-directed surgery	Not recommend	83.33 (5)	62.86 (22)	0.144	0.931
	Recommend, but not performed, patient refused	16.67 (1)	20.00 (7)		
Survival status	Alive	40.74 (11)	43.82 (39)	8.977	0.254
	Paget's disease	14.81 (4)	12.36 (11)		
	Others (not by Paget's disease)	44.44 (12)	43.82 (39)		
Cause of death	Rectum and rectosigmoid junction malignancy	43.75 (7)	26.00 (13)		
	Colon malignancy	0 (0)	10.00 (5)		
	Other malignancy (anus, breast, lung, bronchus, non-melanoma skin malignancy or Hodgkin lymphoma)	12.50 (2)	24.00 (12)		
	Cardio-cerebrovascular disease	12.50 (2)	20.00 (10)		
	Urogenital diseases (urinary bladder, vulva, or prostate disease)	6.25 (1)	4.00 (2)		
	Septicemia	0 (0)	6.00 (3)		
	Chronic liver disease	6.25 (1)	0 (0)		
	Other causes	18.75 (3)	10.00 (5)		

**Table 6** Staging and treatment for perianal Paget's disease<sup>[4]</sup>

Stage	Description	Therapy
I	Paget's cells found in perianal epidermis and adnexa without primary carcinoma	Wide local excision
IIA	Cutaneous Paget's disease without associated adnexal carcinoma	Wide local excision
IIB	Cutaneous Paget's disease with associated anorectal carcinoma	Abdominoperineal resection
III	Paget's disease in which associated anorectal carcinoma has spread to regional nodes	Inguinal node dissection, abdominal perineal resection
IV	Paget's disease with distant metastases of associated carcinoma	Chemotherapy, radiotherapy, local palliative treatment

whether APR is the standard treatment of PPD with/without anorectal carcinoma.

More patients underwent chemotherapy (9/27) than radiotherapy (6/27) after surgical excision. Radiation therapy has been proposed as an adjuvant or salvage treatment of PPD [20–21]. Chemoradiotherapy and/or systemic chemotherapy are usually used for treating invasive or metastases diseases [22–25]. However, no improvements in survival were found when chemoradiotherapy was used. Karam [6] reported a surprising result of short disease-specific survival of EMPD after the application of radiotherapy. These poor adjuvant treatment results warrant further investigation. Lian *et al* [26] reported 8 cases of PPD with anorectal carcinoma, in which mucinous adenocarcinomas and signet ring cell cancer were the common histopathologic features. Highly aggressive subtypes might be indirect evidence that radio-chemotherapy has a limited effect on prolonging survival. Based on the homology with breast cancer and a similar regimen [27], Watanabe [28] has reported a successful case of EMPD with trastuzumab monotherapy on an HER-2 positive lesion after surgery. The application of a monoclonal antibody might be helpful in the future.

The 16.07% (9/56) of the patients with PPD had multiple lesions. Takamichi *et al* [14] reported that 12.4% of those with EMPD had multiple lesions or tumors spreading over two anatomic sites. No difference was found in the survival analysis by comparing these with single lesion PPD and multiple PPDs along with Paget's in other sites. However, local recurrence may be higher [14] and has been seen to be as high as 60% for a single lesion.

Any investigation of PPDs as a separate entity is very challenging because of the relative rarity of the condition. This limits the ability to detect statistically significant survival differences among subgroups. The main limitation of this study is that the SEER database lacks detailed pathology and incomplete information on the TNM stage, surgical method, and chemo/radiotherapy regimen. These factors should be taken into account when examining the results of this study.

In summary, the disease specific mortality of patients with PPD is low. Being elderly (> 70 years old), the grade of differentiation and surgical method (APR) were unfavorable risk factors to prognosis. Although PPD predisposed concurrent malignancy, no survival difference was found between those patients with one PPD and those with multiple lesions. Further investigation of patients with PPD and anorectal carcinoma is required due to a lack of research, the empirical guideline, and controversy surrounding adjuvant treatment.

## Conflicts of interest

The authors indicated no potential conflicts of interest.

## References

1. Paget J. On disease of the mammary areola preceding cancer of the mammary gland. St Bartholomew's Hospital Reprints, 1874,10: 87–89.
2. Lloyd J, Flanagan AM. Mammary and extramammary Paget's disease. *J Clin Pathol*, 2000, 53: 742–749.
3. Zhang N, Gong K, Zhang X, *et al*. Extramammary Paget's disease of scrotum – report of 25 cases and literature review. *Urol Oncol*, 2010, 28: 28–33.
4. Wietfeldt ED, Thiele J. Malignancies of the anal margin and perianal skin. *Clin Colon Rectal Surg*, 2009, 22: 127–135.
5. Perez DR, Trakansanga A, Shia J, *et al*. Management and outcome of perianal Paget's disease: a 6-decade institutional experience. *Dis Colon Rectum*, 2014, 57: 747–751.
6. Karam A, Dorigo O. Treatment outcomes in a large cohort of patients with invasive Extramammary Paget's disease. *Gynecol Oncol*, 2012, 125: 346–351.
7. Karam A, Dorigo O. Increased risk and pattern of secondary malignancies in patients with invasive extramammary Paget disease. *Br J Dermatol*, 2014, 170: 661–671.
8. Yao H, Xie M, Fu S, *et al*. Survival analysis of patients with invasive extramammary Paget disease: implications of anatomic sites. *BMC cancer*, 2018, 18: 403.
9. Chanda JJ. Extramammary Paget's disease and occult hypernephroma. *J Am Acad Dermatol*, 1985, 13: 1053–1055.
10. McCarter MD, Quan SH, Busam K, *et al*. Long-term outcome of perianal Paget's disease. *Dis Colon Rectum*, 2003, 46: 612–616.
11. Sarmiento JM, Wolff BG, Burgart LJ, *et al*. Paget's disease of the perianal region – an aggressive disease? *Dis Colon Rectum*, 1997, 40, 1187–1194.
12. Beck DE, Fazio VW. Perianal Paget's disease. *Dis Colon Rectum*, 1987, 30: 263–266.
13. Lam C, Funaro D. Extramammary Paget's disease: Summary of current knowledge. *Dermatol Clin*, 2010, 28: 807–826.
14. Ito T, Kaku Y, Nagae K, *et al*. Tumor thickness as a prognostic factor in extramammary Paget's disease. *J Dermatol*, 2015, 42: 269–275.
15. Grow JR, Kshirsagar V, Tolentino M, *et al*. Extramammary perianal Paget's disease: report of a case. *Dis Colon Rectum*, 1977, 20: 436–442.
16. Isik O, Aytac E, Brainard J, *et al*. Perianal Paget's disease: three decades experience of a single institution. *Int J Colorectal Dis*, 2016, 31: 29–34.
17. Weedon D. Tumor of cutaneous appendages. In: Weedon D, ed. *Weedon's Skin Pathology*. Philadelphia, PA: U.S. Churchill Livingstone Elsevier, 2010. 788–790.
18. Goldblum JR, Hart WR. Perianal Paget's disease: a histologic and immunohistochemical study of 11 cases with and without associated rectal adenocarcinoma. *Am J Surg Pathol*, 1998, 22: 170–179.
19. Ohnishi T, Watanabe S. The use of cytokeratins 7 and 20 in the diagnosis of primary and secondary extramammary Paget's disease. *Brit J Dermatol*, 2000, 142: 243–247.
20. Guerrieri M, Back MF. Extramammary Paget's disease: role of radiation therapy. *Australas Radiol*, 2002, 46: 204–208.
21. Brown RS, Lankester KJ, McCormack M, *et al*. Radiotherapy for perianal Paget's Disease. *Clin Oncol (R Coll Radiol)*, 2002, 14:

- 272–284.
22. Watanabe Y, Hoshiai H, Ueda H, *et al.* Low-dose mitomycin C, etoposide, and cisplatin for invasive vulvar Paget's disease. *Int J Gynecol Cancer*, 2002, 12: 304–307.
  23. Balducci L, Athar M, Smith GF, *et al.* Metastatic extramammary Paget's disease: dramatic response to combined modality treatment. *J Surg Oncol*, 1988, 38: 38–44.
  24. Thirlby RC, Hammer CJ Jr, Galagan KA, *et al.* Perianal Paget's disease: successful treatment with combined chemoradiotherapy. Report of a case. *Dis Colon Rectum*, 1990, 33: 150–152.
  25. Yamazaki N. Chemotherapy for advanced adenocarcinoma of the skin: experience with combination chemotherapy and a review of the literature. *Gan To Kagaku Ryoho (Japanese)*, 1997, 24: 30–36.
  26. Lian P, Gu WL, Zhang Z, *et al.* Retrospective analysis of perianal Paget's disease with underlying anorectal carcinoma. *World J Gastroenterol*, 2010, 16: 2943–2948.
  27. Guo JF, Liu ZZ, Zhang GJ, *et al.* Efficiency and safety of trastuzumab plus chemotherapy in Her-2 overexpressing metastatic breast cancer patients. *Chinese-German J Clin Oncol*, 2014, 13: 555–559.
  28. Watanabe S, Takeda M, Takahama T, *et al.* Successful human epidermal growth receptor 2-targeted therapy beyond disease progression for extramammary Paget's disease. *Invest New Drugs*, 2016, 34: 394–396.

**DOI 10.1007/s10330-020-0400-0**

**Cite this article as:** Peng H, Liu ZM, Ghoorun RA, *et al.* Clinical characteristics and survival outcomes of perianal Paget's disease: A SEER population-based study. *Oncol Transl Med*, 2020, 6: 1–9.

# Efficacy and safety of anlotinib plus S-1 as thirdly-line or later-line treatment in advanced non-small cell lung cancer\*

Heng Cao<sup>1</sup>, Kai Liang (Co-first author)<sup>2</sup>, Peng Liu (Co-first author)<sup>2</sup>, Jing Wang<sup>1</sup>, Yuanyuan Ji<sup>1</sup>, Lujian Xu<sup>1</sup>, Weilong Wu<sup>1</sup>, Shengnan Guo<sup>1</sup>, Xuekun Song<sup>3</sup>, Yonggui Hong<sup>1</sup> (✉)

<sup>1</sup> Department of Oncology, Anyang Tumor Hospital, The Fourth Affiliated Hospital of Henan University of Science and Technology, Anyang 455000, China

<sup>2</sup> Department of Surgical Oncology, Anyang Tumor Hospital, The Fourth Affiliated Hospital of Henan University of Science and Technology, Anyang 455000, China

<sup>3</sup> Henan University of Chinese Medicine, Zhengzhou 450000, China

## Abstract

**Objective** Anlotinib, an oral vascular endothelial growth factor receptor 2 (VEGFR2) inhibitor, has confirmed antitumor activity in lung cancer in both *in vitro* and *in vivo* assays, and has been recommended as third-line treatment agent in non-oncogene driven non-small cell lung cancer (NSCLC). This prospective study aimed to investigate the efficacy and safety of anlotinib plus S-1 for third- or later-line treatment in patients with advanced NSCLC.

**Methods** Patients with histologically or cytologically confirmed NSCLC, and documented disease progression following second-line chemotherapy, and/or epidermal growth factor receptor-tyrosine kinase inhibitor (EGFR-TKI) treatment were enrolled in this study. The patients were treated anlotinib (8 mg daily d 1–14) and S-1 (60 mg/m<sup>2</sup> d 1–14) and the treatment was repeated every 3 weeks. Treatment was continued until disease progression or unacceptable toxicity occurred. The objective response rate (ORR), disease control rate (DCR), progression-free survival (PFS), and adverse events (AEs) were reviewed and evaluated.

**Results** Forty-one patients were enrolled in the study between June 2018 and December 2018. The total ORR and DCR were 26.8% and 80.5%, respectively. The median PFS was 5.2 months [95% confidence interval (CI), 3.9 to 6.6 months]. In the univariate analysis, there was a significant difference in the median PFS between patients with brain metastases and those without brain metastases (4.8 months vs 5.9 months, respectively;  $P = 0.039$ ). The Eastern Cooperative Oncology Group (ECOG) performance status ( $P = 0.002$ ), lines of therapy ( $P = 0.015$ ), and therapeutic evaluation ( $P = 0.014$ ) were independent factors that influenced PFS. The most common AEs were hypertension, proteinuria, myelosuppression, gastrointestinal reactions, fatigue, and mucositis.

**Conclusion** Anlotinib plus S-1 is an effective and safe regimen for advanced NSCLC as third- or later-line therapy.

**Key words:** non-small cell lung cancer (NSCLC); anlotinib; tegafur gimerac; advanced stage

Received: 23 July 2019  
Revised: 25 August 2019  
Accepted: 30 November 2019

Non-small cell lung cancer (NSCLC) is the leading cause of cancer morbidity and mortality worldwide [1]. Approximately 85% of lung cancers diagnosed are NSCLC, and more than half of the newly diagnosed patients present with metastatic disease [2]. The tyrosine kinase inhibitors (TKIs), such as gefitinib, afatinib, and

erlotinib, are recommended as first-line therapy for advanced NSCLC patients harboring EGFR mutations [3]. However, for the majority of the advanced NSCLC patients without identifiable oncogenic drivers, platinum-doublet chemotherapy is the first-line treatment [4]. However, advanced NSCLC may be resistant to targeted- and

✉ Correspondence to: Yonggui Hong. Email: hygsir168@126.com

\* Supported by a grant from the Youth National Science Foundation of China (No. 61702164).

© 2020 Huazhong University of Science and Technology

chemotherapies, and second-line chemotherapy has poor efficacy with median survival time (MST) of less than 10 months<sup>[5]</sup>. Nivolumab, Pembrolizumab, and Atezolizumab are new candidates for use in second- or later-line therapies of advanced NSCLC<sup>[6]</sup>. Immunosuppressants have low efficiency and high cost for clinical therapeutic purposes, so their practical applications are limited. The optimization of the selection of treatment in advanced NSCLC after second- or above-line therapy has become a hot topic of research.

Vascular endothelial growth factor (VEGF) A was identified as the main mediator of angiogenesis. In addition, the high expression of VEGF contributes to cancer growth and metastasis by directly targeting the tumor cells<sup>[7-8]</sup>. Neutralizing monoclonal antibodies against VEGF and small molecule TKIs targeting VEGFRs are efficient methods to inhibit the angiogenic activity and metastasis of tumor<sup>[9]</sup>. Based on this theory, anti-angiogenic drugs, such as bevacizumab, have a place in the treatment of advanced NSCLC. Anlotinib, an oral VEGFR2 inhibitor, has confirmed antitumor activity in lung cancer *in vitro* and *in vivo*, and has been recommended as a third-line agent in advanced NSCLC without driver oncogenes<sup>[10]</sup>. Tegafur/gimeracil (trade name S-1), is composed of tegafur, gimeracil, and oteracil potassium. It has definite curative effects and controllable side effects in the treatment of advanced NSCLC<sup>[11]</sup>. This prospective study aimed to investigate the efficacy and safety of anlotinib plus S-1 as third- or later-line therapy in patients with advanced NSCLC.

## Materials and methods

### Patients

Between June 1st, 2018 and December 30th, 2018, 41 advanced NSCLC patients in the Anyang Tumor Hospital, the Fourth Affiliated Hospital of Henan University of Science and Technology, China, who failed more than second-line chemotherapy and/or EGFR-TKI treatment, were enrolled in the study and received anlotinib plus S-1 as third- or later-line treatment. All patients had been cytologically or histologically diagnosed with advanced NSCLC. Detailed variables of age, gender, smoking history, pathological type, metastasis sites, and other clinical data were obtained from electronic medical record system. Patients were treated anlotinib (8 mg daily d 1–14) and S-1 (60 mg/m<sup>2</sup> d 1–14) and the treatment was repeated every 3 weeks.

### Therapeutic procedures

Treatment was interrupted or terminated under the following conditions: disease progression, serious adverse events (AEs), death of the patient, or voluntarily giving up. If grade 3 or 4 AEs occurred during anlotinib plus

S-1 treatment, the treatment was initially suspended for 1–2 weeks to alleviate the side effects; and then, anlotinib plus S-1 treatment was continued. Treatment interruption and S-1 dose reduction (up to 1 dose; 40 mg/m<sup>2</sup>) was permitted in case of drug-related AEs. If further dose reductions were required, then the patients were withdrawn from the study.

### Efficacy and safety assessments

The patients followed the imaging requirements of the Response Evaluation Criteria in Solid Tumors (RECIST 1.1). Progression-free survival (PFS) was defined as the time from the first administration of anlotinib plus S-1 to the date of disease progression or occurrence of unacceptable toxicity. The last follow-up date was June 30th, 2019. Complete response (CR) was defined as the disappearance of all target lesions. Partial response (PR) was recorded when the longest diameter of target lesion reduced by at least 30%. Progressive disease (PD) was recorded when that the longest diameter of the target lesion increased by at least 20%, or the appearance of new lesions. Stable disease (SD) was recorded when the longest diameter of the target lesion increased to less than PD, or reduced to less than PR. Disease control rate (DCR) = (CR + PR + SD) / total number of cases × 100%, and the objective response rate (ORR) = (CR + PR) / total number of cases × 100%. AEs were determined using the National Cancer Institute Common Toxicity Criteria for AEs version 4.0.

### Statistical analyses

PFS was assessed using the Kaplan-Meier method and compared using the log-rank test. Multivariate analysis of the independent prognostic factors was evaluated using the Cox regression model. Statistical analyses were performed using SPSS version 21.0.  $P < 0.05$  was considered to be statistically significant.

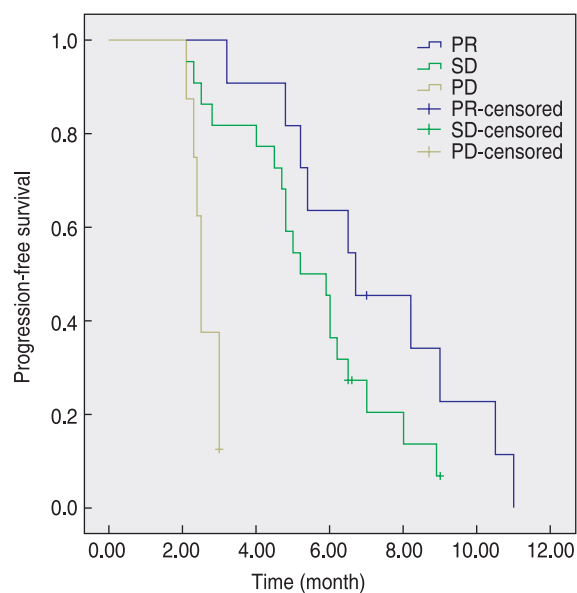
## Results

### Characteristics of patients

The demographic characteristics of 41 patients with advanced NSCLC are summarized in Table 1. The median age of the patients was 60 years, and there were 18 males and 23 females. Almost 51% of the patients had a favorable Eastern Cooperative Oncology Group (ECOG) performance status (0–1). A total of 23 patients received anlotinib plus S-1 as third-line therapy and 18 patients as further-line treatment. Thirty patients had adenocarcinoma and 11 had squamous cell carcinoma. Twelve patients presented with EGFR positive and 29 patients EGFR negative status. Nine patients had brain metastases. Thirteen patients had a previous smoking history, and 10 patients had a family history of cancer.

**Table 1** Comparison of clinical efficacy according to different characteristics

Category	Number (%)	ORR	$\chi^2$	<i>P</i>	DCR	$\chi^2$	<i>P</i>
Gender							
Male	18 (43.9)	22.2	0.347	0.556	83.3	0.165	0.684
Female	23 (56.1)	30.4			78.3		
Pathological type							
Adenocarcinoma	30 (73.2)	26.7	0.002	0.969	80.0	0.017	0.896
Squamous carcinoma	11 (26.8)	27.3			81.8		
Age (years)							
≤ 65	24 (58.5)	29.2	0.161	0.688	83.3	0.209	0.585
> 65	17 (41.5)	23.5			76.5		
EGFR mutation							
Positive	12 (29.3)	41.7	1.903	0.168	75.0	0.325	0.568
Negative	29 (70.7)	20.7			82.8		
Smoking status							
Ever	13 (31.7)	23.1	0.137	0.712	84.6	0.207	0.650
Never	28 (68.3)	28.6			78.6		
Family history of cancer							
Yes	10 (24.4)	30.0	0.068	0.795	80.0	0.002	0.964
No	31 (75.6)	25.8			80.6		
Lines of therapy							
Thirdly-line	23 (56.1)	34.8	1.688	0.194	87.0	1.396	0.237
Later-line	18 (43.9)	16.7			72.2		
Brain metastases							
Yes	9 (22.0)	11.1	1.451	0.228	77.8	0.054	0.816
No	32 (78.0)	31.3			81.3		
ECOG							
0–1	21 (51.2)	38.1	2.783	0.095	85.7	0.749	0.387
2	20 (48.8)	15.0			75.0		

**Fig. 1** The progression-free survival curves of NSCLC patients about therapeutic evaluation

### Clinical efficacy

As shown in the waterfall plot (Fig. 1), none achieved a CR. Eleven patients obtained PR, 22 patients obtained SD, and 8 patients obtained PD. The ORR and DCR were 26.8% and 80.5%, respectively. The median PFS was 5.2 months (95% CI, 3.8 to 6.6 months).

### Univariate and multivariate analyses

In univariate analysis (Table 2), patients with no brain metastases ( $P = 0.039$ ), ECOG performance status 0–1 ( $P = 0.002$ ), third-line of therapy ( $P = 0.015$ ), and good therapeutic evaluation ( $P = 0.014$ ) were associated with a longer PFS. However, in multivariate analysis (Table 2), patients with third-line of therapy ( $P = 0.015$ , HR = 0.383, 95% CI, 0.176 to 0.832), ECOG performance status 0–1 ( $P = 0.002$ , HR = 0.241, 95% CI, 0.098 to 0.593), PR vs PD ( $P = 0.005$ , HR = 0.124, 95% CI, 0.029 to 0.527), and SD vs PD ( $P = 0.006$ , HR = 0.127, 95% CI, 0.048 to 0.610) had significantly longer PFS.

### Toxicity

Most adverse reactions were mild and controllable (Table 3). A total of 5 patients were followed-up until

**Table 2** Progression-free survival of 41 NSCLC patients in univariate and multivariate analysis

Category	PFS (month)	P	
		Univariate	Multivariate
Gender			
Male	5.4 (3.9–6.9)	0.813	
Female	4.8 (3.8–5.8)		
Pathological type			
Adenocarcinoma	5.4 (4.4–6.4)	0.973	
Squamous carcinoma	4.7 (2.5–6.9)		
Age (years)			
≤ 65	5.4 (4.2–6.6)	0.920	
> 65	4.8 (2.1–7.5)		
EGFR mutation			
Positive	4.8 (0.1–10.2)	0.866	
Negative	5.2 (4.5–5.9)		
Smoking status			
Ever	5.2 (4.5–5.9)	0.730	
Never	5.2 (3.4–7.0)		
Family history of cancer			
Yes	4.8 (1.9–7.7)	0.488	
No	5.2 (4.4–6.0)		
Lines of therapy			0.015 (HR: 0.383,
Thirdly-line	6.2 (5.5–6.9)	0.012	95% CI: 0.176–0.832)
Later-line	4.5 (2.6–6.4)		1.00
Brain metastases			0.811 (HR: 1.115,
Yes	4.8 (3.2–6.5)	0.039	95% CI: 0.458–2.716)
No	5.9 (4.8–7.0)		1.00
ECOG			0.002 (HR: 0.241,
0–1	6.7 (5.3–8.1)	< 0.001	95% CI: 0.098–0.593)
2	4.0 (2.0–6.0)		1.00
Therapeutic evaluation			0.014
PR	6.7 (3.9–9.5)	< 0.001	0.005 (HR: 0.124,
SD	5.2 (4.1–6.3)		95% CI: 0.029–0.527)
PD	2.5 (2.4–2.6)		0.006 (HR: 0.172,
			95% CI: 0.048–0.610)
			1.00

**Table 3** Toxicities during treatment (n = 41)

Adverse events	All grade (n)	Grade I–II	Grade III
Hypertension	18	15 (36.6%)	3 (7.3%)
Proteinuria	13	11 (26.8%)	2 (4.9%)
Gastrointestinal reactions	20	19 (46.3%)	1 (2.4%)
Fatigue	15	13 (31.7%)	2 (4.9%)
Myelosuppression	12	11 (26.8%)	1 (2.4%)
Mucositis	7	7 (17.1%)	
Hand-foot syndrome	7	5 (12.2%)	2 (4.9%)
Elevation of aminotransferase	6	6 (14.6%)	
Hemoptysis	2	2 (4.9%)	1 (2.4%)
Hypothyroidism	1	1 (2.4%)	

June 30th, 2019. One patient terminated the treatment due to unacceptable toxicity and associated hemoptyses.

Three patients were treated with a reduced S-1 dose of 40 mg/m<sup>2</sup> d 1–14 due to development of myelosuppression and hand-foot syndrome. However, there was no reduction in the dosage of anlotinib during the treatment. The most common AEs of all levels were gastrointestinal reactions (48.8%), hypertension (43.9%), fatigue (36.6%), proteinuria (31.7%), myelosuppression (29.3%), mucositis (17.1%) and hand-foot syndrome (17.1%). The most frequently observed AEs of grade 3 were as follows: hypertension (7.3%), hand-foot syndrome (4.9%), proteinuria (4.9%), fatigue (4.9%), myelosuppression (2.4%), and hemoptyses (2.4%). No grade 4 AEs or treatment-related deaths were observed in this study.

## Discussion

Angiogenesis is a crucial characteristics of cancer. The growth of new vessels is important to supply the growing malignant tumor with oxygen and nutrients [12]. VEGF and its receptors including VEGFR-1, VEGFR-2, and VEGFR-3 which cooperate to activate the signal transduction cascade in response to VEGF ligand binding, are often overexpressed in tumors. Hence, several different strategies have been designed to target the VEGF signal transduction [13]. In the last decade, multiple inhibitors have been therapeutically validated in preclinical models and clinical trials. Neutralizing monoclonal antibodies against VEGF and small molecule TKIs targeting VEGFRs have been shown to block its angiogenic activity, resulting in tumor vascular regression, antitumor effects, and improvements in patient survival, including bevacizumab [14], ramoluzzumab [15], endostar [16], anlotinib [10] among others.

Anlotinib is a potent multi-tyrosine kinases inhibitor (TKI) which inhibits the activation of VEGFR2, PDGFRβ, and FGFR1 and their common downstream ERK signaling [17]. It inhibits angiogenesis *in vitro* and *in vivo* by inhibiting VEGF/PDGF-BB/FGF-2. Alotinib is a potential agent for inhibiting angiogenesis and can be used in tumor therapy. In the phase III ALTER-0303 trial [10], 439 patients were randomized, 296 to the anlotinib group and 143 to the placebo group. PFS was significantly longer in the anlotinib group compared to the placebo group (5.4 months vs 1.4 months; HR = 0.25, 95% CI, 0.19 to 0.31; P < 0.0001). A substantial increase in OS was noted in the anlotinib group compared to the placebo group (9.6 months vs 6.3 months; HR = 0.70, 95% CI, 0.55 to 0.89; P = 0.002). These findings suggest that anlotinib is a potential third- or later-line therapy for patients with advanced NSCLC.

This is the first study to evaluate anlotinib plus S-1 as third- or later-line treatment in advanced NSCLC patients for its efficacy and safety. The results demonstrated the efficacy of anlotinib plus S-1 as shown by an ORR of 26.8%

and DCR of 80.5% in the 41 patients. The SD from our study demonstrated that the median PFS was 5.2 months, which was superior to that of single agent apatinib in the third-line setting. In phase II trial (ALTER0302)<sup>[18]</sup>, PFS (4.8 months vs 1.2 months; HR = 0.32; 95% CI, 0.20 to 0.51;  $P < 0.0001$ ), and ORR (10.0%; 95% CI, 2.4 to 17.6% vs 0%; 95% CI, 0 to 6.27%;  $P = 0.028$ ) were better with anlotinib compared to the placebo. Currently, patients with brain metastases often receive radiotherapy. The median PFS of NSCLC patients with brain metastases was 3.0 to 3.7 months, and the median OS was only 7.4 to 12.2 months. Brain metastasis is one of the common and severe complications of lung cancer<sup>[19]</sup>. In this study, in the total of 9 patients with brain metastasis the data were as follows; PR (11.1%), SD (55.5%), PD (33.3%), and DCR was 66.6%. Within this subgroup, 5 patients had undergone brain radiotherapy before this study, including 4 patients with SD and 1 patient with PD, and the DCR was 80.0%. Four patients did not undergo any brain radiotherapy, including 1 patient with PR, 2 patients with SD, and 2 patients with PD, and the DCR was 60.0%. However, patients without brain metastases (HR = 0.421, 95% CI, 0.195 to 0.911;  $P = 0.028$ ) had longer PFS following anlotinib treatment, which was different from the results of our study<sup>[20]</sup>. It would be interesting to determine whether brain radiotherapy combined with anlotinib plus S-1 improves the DCR of brain metastasis. However, further studies with larger sample size is needed to validate this observation. However, in multivariate analysis, patients with ECOG 0–1 vs ECOG 2 (6.7 months vs 4.0 months; HR = 0.241, 95% CI, 0.098 to 0.593;  $P = 0.002$ ), third-line of therapy vs later-line of therapy (6.2 months vs 4.5 months; HR = 0.383, CI, 0.176 to 0.832;  $P = 0.015$ ), PR vs PD (6.7 months vs 5.2 months; HR = 0.124, 95% CI, 0.029 to 0.527;  $P = 0.005$ ), and SD vs PD (5.2 months vs 2.5 months; HR = 0.127, 95% CI, 0.048 to 0.610,  $P = 0.006$ ) had significantly longer PFS, which were similar to the results from other studies<sup>[20–21]</sup>. The results of another study indicated that an ECOG PS of 0–1 (HR = 0.152, 95% CI, 0.057 to 0.403;  $P = 0.001$ )<sup>[20]</sup>. Based on the above, we concluded that parallel use TKIs and chemotherapy drugs increases PFS, especially in patients with good performance status.

The most frequent AEs included hypertension, proteinuria, myelosuppression, gastrointestinal reactions, fatigue, and mucositis. The overall incidence of grade 3 AEs was 29.3%. One patient with advanced NSCLC was terminated due to grade 3 hemoptysis, whose was cured after symptomatic treatment. Antivascular targeted therapy should be more carefully monitored in patients with hilar lung cancer or tumors that invade the central blood vessels. According to the AEs reported in the ALTER-0303 trial<sup>[22]</sup>, the AEs observed in our study were expected of the treatment and could be controlled by

intervention, and dose modification. No grade 4 AEs or treatment-related deaths were observed in this study.

In summary, anlotinib plus S-1 may be recommended as a third- or later-line therapy in advanced NSCLC patients due to its better efficacy and tolerable toxicity, especially in patients with good performance status. However, further studies are needed to define the clinical treatment strategies using anlotinib alone or in combination treatments such as when chemotherapy or immunosuppressants are used along with antivascular therapy.

### Conflicts of interest

The authors indicated no potential conflicts of interest.

### References

1. Siegel RL, Miller KD, Jemal A. Cancer statistics, 2018. *CA Cancer J Clin*, 2018, 68: 7–30.
2. Ettinger DS, Akerley W, Borghaei H, *et al*. Non-small cell lung cancer. *J Natl Compr Canc Netw*, 2012, 10: 1236–1271.
3. Sebastian M, Schmittel A, Reck M. First-line treatment of EGFR-mutated nonsmall cell lung cancer: critical review on study methodology. *Eur Respir Rev*, 2014, 23: 92–105.
4. Schiller JH, Harrington D, Belani CP, *et al*. Comparison of four chemotherapy regimens for advanced non-small-cell lung cancer. *N Engl J Med*, 2002, 346: 92–98.
5. Lima AB, Macedo LT, Sasse AD. Addition of bevacizumab to chemotherapy in advanced non-small cell lung cancer: a systematic review and meta-analysis. *PLoS One*, 2011, 6: e22681.
6. Passiglia F, Galvano A, Rizzo S, *et al*. Looking for the best immune-checkpoint inhibitor in pre-treated NSCLC patients: An indirect comparison between nivolumab, pembrolizumab and atezolizumab. *Int J Cancer*, 2018, 142: 1277–1284.
7. Kojima H, Shijubo N, Yamada G, *et al*. Clinical significance of vascular endothelial growth factor-C and vascular endothelial growth factor receptor 3 in patients with T1 lung adenocarcinoma. *Cancer*, 2005, 104: 1668–1677.
8. Takizawa H, Kondo K, Fujino H, *et al*. The balance of VEGF-C and VEGFR-3 mRNA is a predictor of lymph node metastasis in non-small cell lung cancer. *Br J Cancer*, 2006, 95: 75–79.
9. Sia D, Alsinet C, Newell P, *et al*. VEGF signaling in cancer treatment. *Curr Pharm Des*, 2014, 20: 2834–2842.
10. Han B, Li K, Wang Q, *et al*. Effect of anlotinib as a third-line or further treatment on overall survival of patients with advanced non-small cell lung cancer: The ALTER 0303 phase 3 randomized clinical trial. *JAMA Oncol*, 2018, 4: 1569–1575.
11. Yumine K, Kawahara M. Phase II study of S-1, a novel oral fluorouracil, in advanced non-small-cell lung cancer. *Gan To Kagaku Ryoho (Japanese)*, 2006, 33 Suppl 1: 189–192.
12. Hoff PM, Machado KK. Role of angiogenesis in the pathogenesis of cancer. *Cancer Treat Rev*, 2012, 38: 825–833.
13. Shilpa P, Kaveri K, Salimath BP. Anti-metastatic action of anacardic acid targets VEGF-induced signaling pathways in epithelial to mesenchymal transition. *Drug Discov Ther*, 2015, 9: 53–65.
14. Gautschi O, Rothschild SI, Li Q, *et al*. Bevacizumab plus pemetrexed versus pemetrexed alone as maintenance therapy for patients with advanced nonsquamous non-small-cell lung cancer: Update from the

- Swiss group for clinical cancer research (SAKK)19/09 trial. *Clin Lung Cancer*, 2017, 18: 303–309.
15. Garon EB, Ciuleanu TE, Arrieta O, *et al.* Ramucirumab plus docetaxel versus placebo plus docetaxel for second-line treatment of stage IV non-small-cell lung cancer after disease progression on platinum-based therapy (REVEL): a multicentre, double-blind, randomised phase 3 trial. *Lancet*, 2014, 384: 665–673.
  16. Zhou S, Zuo L, He X, *et al.* Efficacy and safety of rh-endostatin (Endostar) combined with pemetrexed/cisplatin followed by rh-endostatin plus pemetrexed maintenance in non-small cell lung cancer: A retrospective comparison with standard chemotherapy. *Thorac Cancer*, 2018, 9: 1354–1360.
  17. Lin B, Song X, Yang D, *et al.* Anlotinib inhibits angiogenesis via suppressing the activation of VEGFR2, PDGFR $\beta$  and FGFR1. *Gene*, 2018, 654: 77–86.
  18. Han B, Li K, Zhao Y, *et al.* Anlotinib as a third-line therapy in patients with refractory advanced non-small-cell lung cancer: a multicentre, randomised phase II trial (ALTER0302). *Br J Cancer*, 2018, 118: 654–661.
  19. Sun ZY, Chen Y. Updates in the management of brain (leptomeningeal) metastasis of lung cancer. *Oncol Transl Med*, 2018, 4: 144–150.
  20. Wang J, Zhao Y, Wang Q, *et al.* Prognostic factors of refractory NSCLC patients receiving anlotinib hydrochloride as the third- or further-line treatment. *Cancer Biol Med*, 2018, 15: 443–451.
  21. Wu D, Nie J, Dai L, *et al.* Salvage treatment with anlotinib for advanced non-small cell lung cancer. *Thorac Cancer*, 2019, 10: 1590–1596.
  22. Si X, Zhang L, Wang H, *et al.* Management of anlotinib-related adverse events in patients with advanced non-small cell lung cancer: Experiences in ALTER-0303. *Thorac Cancer*, 2019, 10: 551–556.

**DOI 10.1007/s10330-019-0370-0**

**Cite this article as:** Cao H, Liang K, Liu P, *et al.* Efficacy and safety of anlotinib plus S-1 as thirdly-line or later-line treatment in advanced non-small cell lung cancer. *Oncol Transl Med*, 2020, 6: 10–15.

# Cisplatin selects for CD133+ cells in lung cancer cells

Jiaheng Li, Mei Jiang, Xiaoting Zhao, Ziyu Wang, Meng Gu, Weiyong Li (✉)

Department of Cellular & Molecular Biology, Beijing Chest Hospital, Capital Medical University, Beijing Tuberculosis and Thoracic Tumor Research Institute, Beijing 101149, China

## Abstract

**Objective** Platinum-based chemotherapy is the first-line treatment for non-small cell lung cancer, but the chemoresistance of tumor cells continues to be a considerable challenge in the management of NSCLCs, leading to recurrence of most patients. CD133 (prominin-1) is a five-transmembrane glycoprotein, and recent evidence suggests that CD133+ cells are the cause of drug resistance and tumor recurrence. In this study, the correlation between cisplatin and CD133+ cells was investigated systematically.

**Methods** Four lung cancer cell lines, including A549, H460, 801D and H1299, were treated with different concentrations of cisplatin. Cell viability was determined by MTT assay. Sphere-forming assay was performed to detect the capability of sphere-forming. CD133+ cells was detected by BD FACScaliber flow cytometer.

**Results** The results showed that cisplatin could increase the number of CD133+ cells in both time- and dose-dependent manner. The enrichment would weaken but the proportion of CD133+ cells was still higher than the basic level as incubation time extended after cisplatin was withdrawn. Compared with adherent culture, the proportion of CD133+ cells was higher when the cells were maintained suspension culture. The proportion of CD133+ cells significantly increased when cisplatin was provided in suspension culture.

**Conclusion** These results revealed that cisplatin induces the enrichment of CD133+ cells and CD133 is a new therapeutic target. Our data partially explained drug resistance to second-line chemotherapy in cisplatin-treated patients with NSCLCs.

**Key words:** CD133; Cisplatin; lung cancer cells

Received: 6 May 2019  
Revised: 25 May 2019  
Accepted: 10 June 2019

Lung cancer is the leading cause of cancer deaths worldwide because of its high incidence and mortality. Non-small cell lung cancer (NSCLC) has an estimated 10% 5-year survival rate [1]. Platinum-based chemotherapy is the standard first-line therapeutic approach to treat patients with NSCLCs. Although the overall median survival of patients who received platinum-based therapy has reached 9 to 12 months [2], the chemoresistance of tumor cells continues to be a considerable challenge in the management of NSCLCs. Tumor cells often show initial sensitivity to chemotherapy drugs, but resistance is acquired during treatment, leading to tumor recurrence and further tumor progression.

One emerging hypothesis that explains how cancer cells can withstand therapeutic assaults, acquire resistance, and establish distant metastasis, is the cancer stem cell (CSC) hypothesis. CSCs may be inherently resistant to the cytotoxic effect of chemotherapy because of their low proliferation rate and resistance mechanisms, including

the expression of multidrug transporters of the ATP-binding cassette (ABC) superfamily. However, there is no effective treatment strategy to override these transporters for clinical therapy.

CD133 (prominin-1), a five-transmembrane glycoprotein, was initially described as a marker specific to CD34+ human hematopoietic progenitor cells [3–4], the normal stem cells of the neural [5–6], epithelial [7–8], and endothelial lineages [9], and their tumor counterparts [10–14]. A recent study showed that the expression of CD133 is associated with levels of resistance-related proteins in patients with NSCLCs [15]. Furthermore, a combination of CD133 and ABCG2 can be used as an independent predictor of postoperative recurrence for patients with stage I NSCLCs [16]. Although the drug action of cisplatin has been widely explored [17], the correlation between cisplatin and CD133+ cells has not been systematically investigated. Here, we provide evidence showing that cisplatin treatment significantly increased the ratio of CD133+

cells. The proportion of CD133+ cells would increase as treatment time and dose increased. The enrichment would disappear after cisplatin was withdrawn and incubation time was extended but the proportion of CD133+ cells was still higher than normal levels. The proportions of CD133+ cells were significantly increased when cisplatin treatment and suspension culture coexisted. However, the high proportions only lasted a short time in culture and the high proportions disappeared as culture time extended. Cisplatin induces the enrichment of CD133+ cells. Based on our results, CD133 can be considered a new therapeutic target, suggesting that a new therapeutic strategy may be necessary to prevent the production of CSCs, whereas platinum-based chemotherapy is the standard of care for the management of NSCLCs.

## Materials and methods

### Cell lines and cisplatin

The human NSCLC cell lines, A549, H460, and H1299 were purchased from Peking Union Medical College Cell Center. The 801D cells were kindly provided by the People's Liberation Army General Hospital. A549, H460, 801D, and H1299 cell lines were maintained in RPMI-1640 supplemented with 10% FBS (Gibco Life Technologies, USA). Cell lines were maintained in a humidified incubator containing 5% CO<sub>2</sub> at 37°C. Cisplatin was purchased from Qilu Pharmaceutical Factory (China) and dissolved in saline to a final concentration of 0.3 mg/mL.

### Detection of CD133+ cells

After cisplatin treatment for 1 or 24 h, cells were washed with PBS. For some experiments, single cells were dissociated from tumor spheres and analyzed by this method. One million trypsinized cells were incubated with an anti-CD133 antibody or isotype control IgG (Miltenyi Biotec Inc., Miltenyi Biotec, Germany) for 10 min. The cells were washed and resuspended in a suitable amount of buffer (PBS) before analysis using a BD FACScaliber flow cytometer (BD Biosciences, USA).

### Cell proliferation assay

Tumor cells (3,000/well) were seeded in flat-bottom 96-well plates (NUNC, Denmark). Cell proliferation was evaluated by a 3-(4, 5-dimethyl-thiazol-2yl)-5-(3-carboxymethoxyphenyl)-2-(4-sulfophenyl)-2H-tetrazolium (MTS; Promega) assay, which was performed at a fixed time every day for 5 consecutive days. MTS (20 μL) was added to each well, followed by incubation for 3 h at 37°C. The absorbance was recorded at 490 nm using an EL-800 universal microplate reader (Bio-Tek Instruments, Winooski, VT, USA). This experiment was repeated in triplicate.

### Sphere-forming assay

Cells were expanded to spheres in a 10-cm ultra-low adhesion culture dish (Corning, USA) containing DMEM/F-12 with N2 supplement (Invitrogen, USA), 20 ng/mL EGF, and 20 ng/mL basic fibroblast growth factor (FGF; PeproTech, USA), referred to stem cell medium, for 2 weeks. The tumor sphere formation efficiency was calculated as the ratio of sphere number to the plated cell number.

### Statistical analysis

Data are presented as the mean ± SE. To analyze the results of the experiments in triplicate, quantitative variables were compared using one way analysis of variance.  $P \leq 0.05$  was considered statistically significant.

## Results

### Cisplatin treatment elevates the ratio of CD133+ cell

To determine whether cisplatin can elevate the ratio of CSCs in lung cancer, we first tested the cytotoxic effect of cisplatin in NSCLC cell lines. Four lung cancer cell lines, A549, H460, 801D, and H1299 were treated with different concentrations of cisplatin for 1 and 24 h, and cell viability was determined by MTT assay. With the increase of drug concentration, the cytotoxicity of cisplatin to the cell is stronger (Table 1). With the increase of drug concentration, the percentages of CD133+ cells were remarkably increased in all four cell lines when the treatment time was same (Table 2). With the increase of the drug concentration, the percentages of CD133+ cells were remarkably increased when the treatment time was different and cisplatin had the same killing effect. For example, the CD133 positive ratio of

**Table 1** The cisplatin concentration of IC<sub>50</sub> and IC<sub>80</sub> at different treatment times

Cells	24 h (μg/mL)		1 h (μg/mL)	
	IC <sub>50</sub>	IC <sub>80</sub>	IC <sub>50</sub>	IC <sub>80</sub>
A549	3.5 ± 0.3	5.0 ± 0.2	64.0 ± 3.6	128.0 ± 6.2
H460	1.5 ± 0.2	4.0 ± 0.1	40.0 ± 2.5	80.0 ± 3.2
H1299	3.0 ± 0.1	6.0 ± 0.3	64.0 ± 3.2	128.0 ± 5.5
801D	1.0 ± 0.1	3.0 ± 0.1	20.0 ± 2.5	35.0 ± 4.2

**Table 2** the ratios of CD133+ cells after cisplatin treatment

Cells	0 h (%)	24 h (μg/mL)		1 h (μg/mL)	
		IC <sub>50</sub>	IC <sub>80</sub>	IC <sub>50</sub>	IC <sub>80</sub>
A549	0.01	0.17±0.02	0.24±0.03	0.48±0.06	0.76±0.10
H460	0.03	0.07±0.02	0.10±0.01	0.16±0.06	0.19±0.02
H1299	0.02	0.11±0.02	0.19±0.02	0.20±0.04	0.19±0.05
801D	0.02	0.07±0.01	0.09±0.03	0.13±0.03	0.59±0.06

**Table 3** The ratios of CD133+ cells at high dose in different treatment time

Cells	Treatment concentration ( $\mu\text{g/mL}$ )	Action time (h)				
		0	12	24	48	72
H1299	128.00	0.02	0.02 $\pm$ 0.00	0.07 $\pm$ 0.02	0.07 $\pm$ 0.02	0.15 $\pm$ 0.05
801D	35.00	0.02	0.03 $\pm$ 0.01	0.05 $\pm$ 0.00	0.09 $\pm$ 0.02	0.59 $\pm$ 0.02
A549	128.00	0.01	0.04 $\pm$ 0.01	0.06 $\pm$ 0.01	0.50 $\pm$ 0.10	0.76 $\pm$ 0.06

**Table 4** The ratios of CD133+ cells at low dose in different treatment time

Cells	Treatment concentration ( $\mu\text{g/mL}$ )	Action time (h)				
		0	12	24	48	72
H1299	3.00	0.02	0.05 $\pm$ 0.01	0.11 $\pm$ 0.03	0.14 $\pm$ 0.02	0.15 $\pm$ 0.01
801D	1.00	0.02	0.04 $\pm$ 0.00	0.07 $\pm$ 0.01	0.09 $\pm$ 0.02	0.14 $\pm$ 0.02
A549	3.50	0.01	0.04 $\pm$ 0.00	0.17 $\pm$ 0.03	0.21 $\pm$ 0.03	0.23 $\pm$ 0.03

IC<sub>50</sub> to 24 h of drug treatment was lower than that of drug treatment for 1 h. The CD133 positive ratio of IC<sub>80</sub> to 24 h of drug treatment was lower than that of drug treatment 1 h of drug treatment. These suggested that high doses of cisplatin acting on cells for a short amount of time increased enrichment of CD133+ cells compared to low doses of cisplatin acting on cells for a long period of time. In other words, drug concentration plays a more important role in enriching CD133+ cells than length of treatment.

### The ratio of CD133+ cell depends on treatment time and dose of cisplatin

The above results suggested cisplatin treatment elevated the ratios of CD133+ cells in lung cancer cells. We also explore whether the change in ratio is related to the drug concentration and treatment time. In Table 1 and 2, the data showed that with the increase of drug concentration, the ratios of CD133+ cells increased in four lung cancer cell lines. Table 3 showed the conditions at a high dose and Table 4 showed the conditions at a low dose, which suggests that with the increase of treatment time, the ratios of CD133+ cells increased. In summary, the ratios of CD133+ cell depended on treatment times and dose levels of cisplatin.

### The proportion of CD133+ cell decreased, but was higher than the basal level with extended culture time after the withdrawal of cisplatin

The above results suggested that the ratio of CD133+ cells depended on treatment times and doses of cisplatin. The data suggest that drug concentration plays a more important role in enriching CD133+ cells. We used high dose cisplatin to treat cells for 1 h (Table 3). Cells were cultured for one month after removal of cisplatin and the proportion of CD133+ cells were examined. The data

**Table 5** The ratios of CD133+ cells after the removal of cisplatin

Cells	Before cisplatin treatment	Cisplatin treatment for 1 h	One month after removing cisplatin
H1299	0.02	0.19 $\pm$ 0.05	0.05 $\pm$ 0.01
801D	0.02	0.59 $\pm$ 0.06	0.04 $\pm$ 0.01
A549	0.01	0.76 $\pm$ 0.10	0.06 $\pm$ 0.02

**Table 6** The cisplatin concentration of IC<sub>50</sub> and IC<sub>80</sub> when culture time became long after the removal of cisplatin

Cells	1 h ( $\mu\text{g/mL}$ )		Culturing for 1 month after removing cisplatin	
	IC <sub>50</sub>	IC <sub>80</sub>	IC <sub>50</sub> ( $\mu\text{g/mL}$ )	IC <sub>80</sub> ( $\mu\text{g/mL}$ )
A549	64.0 $\pm$ 3.6	128.0 $\pm$ 6.2	85.0 $\pm$ 4.5	135.0 $\pm$ 5.3
H1299	64.0 $\pm$ 3.2	128.0 $\pm$ 5.5	80.0 $\pm$ 4.9	140.0 $\pm$ 6.2
801D	20.0 $\pm$ 2.5	35.0 $\pm$ 4.2	30.0 $\pm$ 3.5	60.0 $\pm$ 5.6

(Table 5) show the ratios of CD133+ cells decreased but were still higher than the basal level, which was observed when the culture time was extended after the withdrawal of cisplatin.

### Cells tolerated cisplatin when culture was extended after the removal of cisplatin

After being treated with cisplatin for 1 h, the cells were cultured for one month. Then we examined the response of cells to cisplatin. The results showed that the corresponding concentrations of IC<sub>50</sub> and IC<sub>80</sub> were higher than the previous concentrations in lung cancer cells (Table 6). These results suggested that the cells could tolerate cisplatin even if they were cultured for a long time after the removal of cisplatin.

### The ratio of CD133+ cell increased in sphere-forming assay when cells were treated by cisplatin

Some studies showed that CD133+ cells are highly tumorigenic, and are endowed with stem-like features; importantly, they are unaffected by cisplatin treatment [18]. Tumor-initiating cells (TICs) have been reported to grow in serum-free conditions to form spheres in several solid tumors; the sphere formation assay is widely used to detect TICs [19-20]. For this reason, we performed the sphere-forming assay. We used a high concentration of cisplatin to treat cells for 1 h and then removed it. Then cells were suspended in culture. When cells were cultured for 2 weeks, the ratios of CD133+ cells were higher than those of cells grown using adherent culture. The ratios of CD133+ cells after cisplatin treatment were higher than cells with no cisplatin treatment (Table 7). When the culture time was prolonged to 4 weeks, CD133+ ratios in cells treated with cisplatin reduced, but were higher than those in cells not treated with cisplatin (Table 8).

**Table 7** The ratios of CD133+ cells in sphere-forming assay when cisplatin was treated

Cells	Without cisplatin treatment (%)	After cisplatin treatment (%)
A549	0.17 ± 0.02	2.16 ± 0.23
H1299	0.12 ± 0.03	3.10 ± 0.12
801D	4.37 ± 0.10	21.50 ± 3.60
H460	0.54 ± 0.12	7.79 ± 1.20

**Table 8** The ratios of CD133+ cells in sphere-forming assay after the withdrawal of cisplatin

Cells	Without cisplatin treatment (%)	After cisplatin treatment (%)
A549	0.10 ± 0.02	1.12 ± 0.23
H1299	0.09 ± 0.01	0.19 ± 0.05
801D	0.14 ± 0.03	0.22 ± 0.06
H460	0.10 ± 0.02	1.61 ± 0.20

## Discussion

Platinum-based combination chemotherapy is a standard first-line treatment for advanced NSCLCs. Despite the efficacy of first-line chemotherapy, tumor recurrence is common in most cases<sup>[4]</sup>. Here, we provide direct evidence that cisplatin enriches CD133+ cells, which exhibit stem-like properties. Our data partially explained drug resistance to second-line chemotherapy in cisplatin-treated patients with NSCLCs. The proportion of CD133+ cells was reduced but was still higher than the normal levels as incubation time was extended. Our results showed that even a small rise of treatment concentration could increase the tolerance of cells to cisplatin. We explored whether this tolerance is due to cisplatin selecting resistant cells rather than selecting CD133+ cells. Studies showed that the treatment of H460 and H661 cells with cisplatin could enrich CD133+ cells. This cisplatin-induced enrichment of CD133+ cells was mediated through Notch signaling, as evidenced by increased levels of cleaved Notch1<sup>[21]</sup>. CD133+ tumor cells represent a group of cells that are not sensitive to radiotherapy and chemotherapy. These drug resistant cells are the source of tumor recurrence after radiotherapy and chemotherapy<sup>[18, 22]</sup>.

In previous studies with gastric TICs, cells were cultured on non-adherent substrata to form floating spheres<sup>[10]</sup>, and a substratum was used to induce their differentiation into non-tumorigenic cells. This induction effect could not have resulted from the elimination of CD133- cells—which are more sensitive to cisplatin—and preservation of the existing CD133+ cells before treatment because a limited number of cells were killed by a low dose of cisplatin—around the IC<sub>20</sub>—for each cell line during treatment. However, a high-dose (>

IC<sub>50</sub>) of paclitaxel, which induced significant cell death, showed no effect on the CD133+ cell number in the H460 and H661 cell lines. These results indicated that cisplatin might induce dedifferentiation of NSCLCs. Cells were treated with cisplatin and suspended in culture in this study. When cells were cultured for 2 weeks, the ratios of CD133+ cells were higher than those of a cells cultured under adherent conditions. The ratios of CD133+ cells after cisplatin treatment were higher than those in cells not treated with cisplatin. When the culture time was prolonged to 4 weeks, the CD133+ ratios of cells treated with cisplatin reduced, but were still higher than those of cells not treated with cisplatin.

In conclusion, we provided a direct evidence that cisplatin could enrich CD133+ cells. Compared with CD133- cells, the capability of sphere-forming increased in CD133+ cells. These results revealed that cisplatin induces the enrichment of CD133+ cells, and that CD133 could be a new, promising therapeutic target.

## Conflicts of interest

The authors indicated no potential conflicts of interest.

## References

- Jemal A, Siegel R, Ward E, *et al.* Cancer statistics, 2006. *CA Cancer J Clin*, 2006, 56: 106–130.
- Socinski MA. Clinical issues in the management of non-small-cell lung cancer and the role of platinum-based therapy. *Clin Lung Cancer*, 2004, 5: 274–289.
- Yin AH, Miraglia S, Zanjani ED, *et al.* AC133, a novel marker for human hematopoietic stem and progenitor cells. *Blood*, 1997, 90: 5002–5012.
- Miraglia S, Godfrey W, Yin AH, *et al.* A novel five-transmembrane hematopoietic stem cell antigen: isolation, characterization, and molecular cloning. *Blood*, 1997, 90: 5013–5021.
- Uchida N, Buck DW, He D, *et al.* Direct isolation of human central nervous system stem cells. *Proc Natl Acad Sci USA*, 2000, 97: 14720–14725.
- Lee A, Kessler JD, Read TA, *et al.* Isolation of neural stem cells from the postnatal cerebellum. *Nat Neurosci*, 2005, 8: 723–729.
- Corbeil D, Roper K, Hellwig A, *et al.* The human AC133 hematopoietic stem cell antigen is also expressed in epithelial cells and targeted to plasma membrane protrusions. *J Biol Chem*, 2000, 275: 5512–5520.
- Richardson GD, Robson CN, Lang SH, *et al.* CD133, a novel marker for human prostatic epithelial stem cells. *J Cell Sci*, 2004, 117: 3539–3545.
- Salven P, Mustjoki S, Alitalo R, *et al.* VEGFR-3 and CD133 identify a population of CD34+ lymphatic/vascular endothelial precursor cells. *Blood*, 2003, 101: 168–172.
- Collins AT, Berry PA, Hyde C, *et al.* Prospective identification of tumorigenic prostate cancer stem cells. *Cancer Res*, 2005, 65: 10946–10951.
- Ricci-Vitiani L, Lombardi DG, Pilozzi E, *et al.* Identification and expansion of human colon-cancer-initiating cells. *Nature*, 2007, 445: 111–115.
- O'Brien CA, Pollett A, Gallinger S, *et al.* A human colon cancer cell

- capable of initiating tumour growth in immunodeficient mice. *Nature*, 2007, 445: 106–110.
13. Yin S, Li J, Hu C, *et al.* CD133 positive hepatocellular carcinoma cells possess high capacity for tumorigenicity. *Int J Cancer*, 2007, 120: 1444–1450.
  14. Manoranjan B, Mahendram S, Almenawer SA, *et al.* The identification of human pituitary adenoma-initiating cells. *Acta Neuropathol Commun*, 2016, 4: 125.
  15. Salnikov AV, Gladkikh J, Moldenhauer G, *et al.* CD133 is indicative for a resistance phenotype but does not represent a prognostic marker for survival of non-small cell lung cancer patients. *Int J Cancer*, 2010, 126: 950–958.
  16. Li F, Zeng H, Ying K. The combination of stem cell markers CD133 and ABCG2 predicts relapse in stage I non-small cell lung carcinomas. *Med Oncol*, 2011, 28: 1458–1462.
  17. Siddik ZH. Cisplatin: mode of cytotoxic action and molecular basis of resistance. *Oncogene*, 2003, 22: 7265–7279.
  18. Bertolini G, Roz L, Perego P, *et al.* Highly tumorigenic lung cancer CD133+ cells display stem-like features and are spared by cisplatin treatment. *Proc Natl Acad Sci USA*, 2009, 106: 16281–16286.
  19. Pastrana E, Silva-Vargas V, *et al.* Eyes wide open: a critical review of sphere-formation as an assay for stem cells. *Cell stem cell*, 2011, 8: 486–498.
  20. Visvader JE, Lindeman GJ. Cancer stem cells in solid tumours: accumulating evidence and unresolved questions. *Nat Rev Cancer*, 2008, 8: 755–768.
  21. Liu YP, Yang CJ, Huang MS, *et al.* Cisplatin selects for multidrug-resistant CD133+ cells in lung adenocarcinoma by activating Notch signaling. *Cancer Res*, 2013, 73: 406–416.
  22. Fukamachi H, Seol HS, Shimada S, *et al.* CD49f(high) cells retain sphere-forming and tumor-initiating activities in human gastric tumors. *PloS one*, 2013, 8: e72438.

**DOI 10.1007/s10330-019-0355-5**

**Cite this article as:** Li JM, Jiang M, Zhao XT, *et al.* Cisplatin selects for CD133+ cells in lung cancer cells. *Oncol Transl Med*, 2020, 6: 16–20.

# A study on melanoma treatment using dendritic cells loaded with antigens purified from melanoma cell lines\*

Yanwei Gao<sup>1</sup>, Xia Chen<sup>2</sup>, Weishi Gao<sup>1</sup>, Xiangji Lu<sup>3</sup>, Lin Peng<sup>4</sup> (✉)

<sup>1</sup> Department of Surgical Oncology, Inner Mongolia People's Hospital, Hohhot 010017, China

<sup>2</sup> Department of Blood Components Preparation, Inner Mongolia Red Cross Blood Center, Hohhot 010010, China

<sup>3</sup> Department of Emergency, Inner Mongolia Armed Police Hospital, Hohhot 010010, China

<sup>4</sup> Department of Gastroenterology, Inner Mongolia People's Hospital, Hohhot 010017, China

## Abstract

**Objective** The aim of this study was to purify effective tumor peptide complexes from human melanoma cell lines to enhance the treatment effects on melanoma.

**Methods** We purified heat shock protein 70 (HSP70)-peptide complexes (PCs) from human melanoma cell lines A375, A875, M21, M14, WM-35, and SK-HEL-1. We named the purified product as M-HSP70-PCs and determined its immunological activities. Autologous HSP70-PCs purified from primary tumor cells of melanoma patients (9 cases) were used as controls. These two tumor antigenic complexes were loaded into dendritic cells (DCs) and used to stimulate an antitumor response against tumor cells in the corresponding patients.

**Results** Mature DCs pulsed with M-HSP70-PCs stimulated autologous T cells to secrete the same levels of type I cytokines as the autologous HSP70-PCs. Moreover, DCs pulsed with M-HSP70-PCs ended CIK cells with an equal ability as autologous HSP70-PCs to kill melanoma cells in the patients.

**Conclusion** M-HSP70-PCs may be used as an efficient and generalized tumor antigen in the treatment of DC-based malignant melanoma.

**Key words:** heat shock protein 70 peptide complexes; dendritic cells; CIK cells; melanoma; cellular immunotherapy

Received: 8 December 2019

Revised: 9 January 2020

Accepted: 23 February 2020

For melanoma, dendritic cell (DC) and CIK cell therapy is the earliest and most effective treatment method. At home and abroad, a combination of DC-CIK cells and immune reconstruction therapy has benefited a large number of patients with melanoma. It is well known that the effectiveness of DC-based cellular immunotherapy depends on the tumor antigens it carries, and obtaining comprehensive and effective autologous tumor antigens through fresh tumor tissue cells after surgery is considered the best choice. However, for advanced patients and most tumor patients who have undergone surgery, because of the inability to operate or postoperative specimens soaked in formalin, autoantigens cannot be obtained from

fresh tumor tissue, which greatly reduces the therapeutic effect. How to make such patients get better cellular immunotherapy has become an urgent problem.

Our previous research results showed that human-derived malignant tumor cell lines contain a large number of tumor-associated antigen peptides. At the same time, tumor antigen peptides can be isolated and purified by virtue of some characteristics of heat shock protein 70 (HSP70). This study will investigate whether HSP70-peptide complexes (PCs) purified from human melanoma cell lines can enhance the effect of adoptive immunotherapy for melanoma based on DCs.

✉ Correspondence to: Lin Peng. Email: penglinlaoshi@126.com

\* Supported by a grant from the National Natural Sciences Foundation of Inner Mongolia (No. 2017MS(LH)0847).

© 2020 Huazhong University of Science and Technology

## Materials and methods

### Cell culture

Human melanoma cell lines A375, A875, M21, M14, WM-35, and SK-HEL-1 were purchased from Peking Union Medical College. Cells were cultured according to the manufacturer's instructions.

### Purification of M-HSP70-PCs

M-HSP70-PCs were obtained from the above six cell lines by using the separation and purification scheme established previously<sup>[1]</sup>. The six melanoma cell lines were processed according to the following steps:

(1) Heat shock treatment. Cells were heated in 42 °C water bath for 12 h, and at 37 °C for 2 h.

(2) After incubation with a lysis solution on ice for 15 min, the cells were scraped with sterile cell scrapers to obtain a cell suspension. After counting,  $5 \times 10^6$  cells were taken from each group and then crushed with an ultrasonic crusher until there was no complete cell structure under the microscope.

(3) The crude cell extract was obtained through centrifugation at  $10000 \times g$  and 4 °C for 90 min.

(4) After dialyzing the cells in buffer at 4 °C overnight, the unconjugated parts were collected by ConA Sepharose affinity chromatography at 12 mL/h at room temperature.

(5) The unconjugated part of ConA Sepharose affinity chromatography column was dialyzed overnight at 4 °C. After the dialysis, the cell suspension was passed through ADP agarose affinity chromatography column at the rate of 10 mL/h at room temperature. The column was then washed with three steaming water and buffer solution in turns to the A280 value and returned to the baseline, and then the eluent was discarded.

(6) The column was eluted with buffer containing 3 mmol/L ADP until no protein was washed out. The eluate was then collected to obtain M-HSP70-PCs.

(7) Total protein was detected using the Lowry method.

(8) Endotoxin levels were detected with Limulus ameocyte lysate (LAL) assay.

### Primary melanoma cell culture

Surgical specimens were obtained from 15 patients who underwent resection of skin melanoma tumors at the Oncology Department, Inner Mongolia People's Hospital, in 2018. No patient received preoperative chemotherapy or radiotherapy.

(1) Fresh tumor tissue ( $1 \times 1$  cm<sup>2</sup> or more) was taken after the operation and immediately put into a 4 °C RPMI 1640 medium containing 100 µg/mL penicillin G and 100 µg/mL streptomycin, within half an hour and in a sterile sealed environment, and delivered to the laboratory. The following processes were performed on the tissue:

(2) Blood clots, skin, and fibrous tissues around the

specimen were removed, and the tumor tissue was washed twice with PBS. The specimen was cut into several small pieces ( $0.1 \times 0.1 \times 0.1$  cm) with sterile scissors and then put into a sterile culture dish. Next, 1% collagenase was added and shaken in a water bath at 37 °C for 1 h.

(3) The cell suspension was obtained after filtration with a 38 µm mesh. After dilution, the cells were inoculated in a 25 cm<sup>2</sup> cell culture flask and cultured at 37 °C in 5% CO<sub>2</sub> until the total number of cells reached more than  $1 \times 10^7$ .

### Purification of autologous HSP70-PCs

The autologous HSP70-PCs of patients were purified from  $5 \times 10^6$  primary cells according to the method described in "Purification of M-HSP70-PCs."

### Preparation of DCs and CIK cells

We extracted 50 mL of peripheral blood from the upper arms of healthy volunteers, diluted it twice with sterile heparinized normal saline, and slowly injected it into a centrifuge tube with a preset lymphocyte separation solution (relative density 1.077 g/mL). After density gradient centrifugation, peripheral blood mononuclear cells (PBMCs) were aspirated with a sterile bar pipette. The density of the PBMCs was adjusted to  $5 \times 10^6$  g/mL with RPMI 1640 medium containing 10% fetal bovine serum (FBS), 100 U/mL penicillin G, and 100 g/mL streptomycin. After placing it in a cell culture bottle for adherence for 2 h, non-adherent cells were washed away (for inducing CIK cells). Adherent cells were induced with RPMI 1640 medium containing 800 U/mL GM-CSF and 500 U/mL IL-4; the medium and cytokines were replaced every 3 days. DCs were obtained by adding 50 U/mL TNF-α on the 6th day of culture.

The non-adherent cells were resuspended in RPMI 1640 medium containing 10% FBS, 100 U/mL penicillin G, and 100 µg/mL streptomycin, and the density was adjusted to  $1 \times 10^6$  g/mL. On the day of culture, 1000 U/mL human recombinant IFN-γ, anti-CD3 monoclonal antibody 50 ng/mL, IL1-β 100 U/mL, and IL-2 300 U/mL were added. The cell density was adjusted every 3 days to  $2 \times 10^5$  g/mL. At the same time, new culture medium and 300 U/mL of IL-2 were added and cultured *in vitro* to obtain CIK cells.

### Preparation of tumor specific DC-CIK cells

At the sixth day of culture, the self-immature DCs of melanoma patients were divided into three groups ( $1 \times 10^5$  in each group). The following antigen complexes were added and incubated at room temperature for 12 h to prepare specific DC tumor vaccines. Group A received GM-CSF and IL-4 only, group B received 10 µg M-HSP70-PCs, and group C received 10 µg autologous HSP70-PCs purified from primary cells of each melanoma patient.

Similarly, CIK cells were divided into three groups ( $1 \times 10^6$  cells in each group) and mixed with the above three groups of DC tumor vaccines for one week to prepare tumor specific DC-CIK cells.

### Detection of cytokine secretion

The secretion of IFN- $\gamma$  is an important way for DC-CIK cells to kill tumor cells. Therefore, the level of IFN- $\gamma$  secretion indirectly reflects the antitumor activity of DC-CIK cells. In this study, the supernatant of DC-CIK cells in each group cultured together for 3 days was detected by IFN- $\gamma$  enzyme-linked immunosorbent kit to determine the level of IFN- $\gamma$  secreted by the cells in each group.

### In vitro cytotoxicity testing

The DC-CIK cells of the three groups were used as the effector cells, and the patient's primary cells were used as the target cells. The specific cytotoxic activity was detected by using LDH release method. The effector cells and target cells were incubated in RPMI 1640 medium containing 10% FBS at 37 °C for 4 h. The mixture was centrifuged at  $300 \times g$  for 10 min and the supernatant was collected. LDH release level of the cells in each group was detected by using an ELISA kit, and the target cell lysis rate was calculated.

### Statistical analysis

All values are expressed as mean  $\pm$  SD or percent (%). All analyses were conducted using the SPSS 17.0 software. The results were considered statistically significant when  $P < 0.05$ .

## Results

### Primary melanoma cell culture

The ages of 15 patients (10 males and 5 females) with melanoma ranged from 35–61 years. There were 12 patients with cutaneous melanoma and 3 patients with mucosal melanoma (MM). All patients did not receive any form of radiotherapy, chemotherapy, or targeted treatment before the operation. Part of the tissue was sent to the pathology department of our hospital for immunohistochemical detection to diagnose the disease. Another part of the tumor tissue was used to culture primary tumor cells. In the process of culture, four cells were polluted and two cells stopped growing for unknown reasons. In the other nine cases, the success rate was 60%.

### Antigen-specific IFN- $\gamma$ production induced by DC-CIK cells

DC and CIK cells co-culture can stimulate IFN- $\gamma$  secretion and kill tumor cells. The three groups of DC-CIK cells co-cultured for 3 days were tested for IFN- $\gamma$  secretion level using the IFN- $\gamma$  ELISA kit. The results

showed that the levels of IFN- $\gamma$  secreted by DC-CIK cells in groups B and C were significantly higher than those in group A ( $P < 0.01$ ), and there was no significant difference between the two groups ( $P > 0.05$ ) (Fig.1).

### In vitro cytotoxicity

The above three groups of tumor-specific DC-CIK cells co-cultured for one week were used as effector cells, and the primary tumor cells of MM patients were used as target cells. After 4 h of mixed culture at different target ratios (5:1, 10:1, 20:1), the LDH levels in the supernatants of each group were measured by the LDH release method to calculate the target cell lysis rate. The results showed that under different target-effector ratio conditions, the lysis rates of target cells in groups B and C were significantly higher than those in group A ( $P < 0.01$ ), and there was no significant difference between the two groups ( $P > 0.05$ ) (Fig. 2).

## Discussion

Melanoma is a kind of malignant tumor derived from the melanocytes of neural crest, which is often found in the skin and mucous membrane. In recent years, the incidence of malignant melanoma has been increasing year after year, and it has become one of the fastest-growing malignant tumors. The disease is characterized by high malignancy, occult incidence, insensitivity to radiotherapy and chemotherapy, and easy to have distant metastasis; therefore the mortality rate remains high. It has been found that the survival rate of patients with malignant melanoma is closely related to the degree of disease progression. Early patients can be completely controlled by surgery, while for late patients with

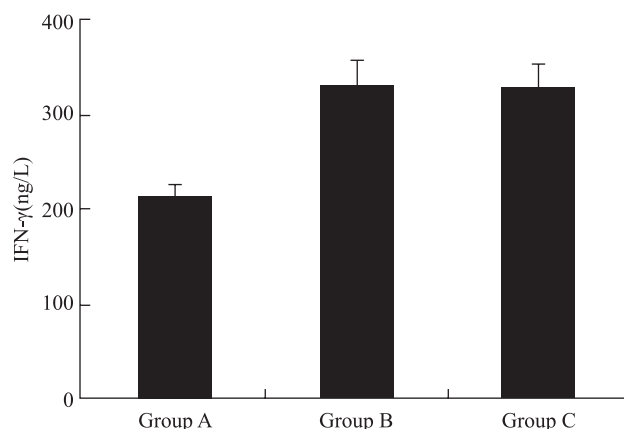


**Fig. 1** Secretion of IFN- $\gamma$  by T cells induced with autologous DCs. Group A is autologous DCs that received only GM-CSF and IL-4; Group B is autologous DCs pulsed with 10  $\mu$ g M-HSP70-PCs; Group C is autologous DCs pulsed with 10  $\mu$ g autologous HSP70-PCs. Assays were performed in triplicate. The results are expressed as the mean  $\pm$  SD

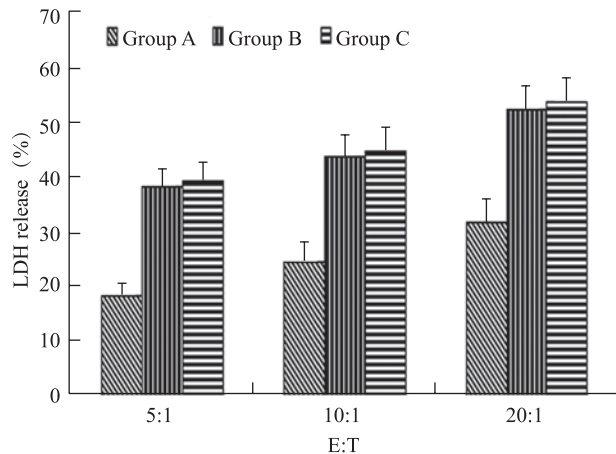


**Fig. 2** LDH release by CD8<sup>+</sup> T cells induced with autologous DCs. Primary tumor cells of melanoma patients were used as target cells, and three groups of effector cells were used. Group A is autologous DCs that received only GM-CSF and IL-4; Group B is autologous DCs pulsed with M-HSP70-PCs; Group C is autologous DCs pulsed with autologous HSP70-PCs. Assays were performed in triplicate. Results are expressed as the mean  $\pm$  SD

metastasis, the five-year survival rate is very low [2-4].

With the rapid development of tumor molecular biology and immunology, the emergence of some new treatment methods has gradually changed the treatment prospects of advanced malignant melanoma. A large number of studies have shown that the new immunotherapy and targeted therapy drugs alone or in combination can significantly improve the treatment effect of patients with advanced malignant melanoma and prolong the total survival period and progression free survival period [5-7]. However, a large number of late melanoma patients in China have not benefited from this. The reason is, firstly, the vast majority of patients are unable to afford the high cost of treatment. Secondly, the circulation channels of drugs are limited, and they cannot be obtained all the time, which affects the treatment cycle. Therefore, it is imperative to continue to develop cheap and efficient treatment methods. Cell immunotherapy based on DC and CIK cells is undoubtedly the best choice [8].

Studies have shown that the immune activity of tumor antigen peptide is the key to DC-CIK cell therapy [9]. Therefore, how to obtain the most comprehensive and effective autoantigen peptide of tumor patients, to achieve individualized treatment has become a research interest of DC based cellular immunotherapy in recent years. It is generally believed that the primary cells cultured in fresh tissue of tumor patients after operation are the best source for obtaining autoantigens. Unfortunately, this ideal treatment is difficult to implement and promote, for the following reasons: (1) Most patients with advanced cancer do not need or cannot tolerate surgical treatment and cannot get tumor tissue. (2) Pathological diagnosis

is needed in the postoperative tumor tissue routine, and primary cell culture cannot be carried out after formalin treatment. (3) Fresh tumor tissue should be preserved and transported in strict aseptic condition, and cell culture should be started immediately after *in vitro*. Most medical institutions do not meet this requirement. (4) The primary cell culture technology requires high level of efficiency and the success rate is low.

Subsequently, people continue to explore new antigen preparation methods. Because of the simple preparation method, the freeze-thaw of fresh tumor tissue of patients has become a common antigen source in clinic. However, the autogenous tumor tissue freeze-thaw contains high concentration of cytokines and normal tissue cell components, which has poor immunogenicity and is easy to induce autoimmune response, thus seriously affecting the treatment effect.

The heat shock protein (HSP) family is a group of highly conserved polypeptide protein molecular family, which widely exists in various cells. In normal condition, the content is low, and the expression is obvious in stress. It has been shown that HSP and tumor-related antigen peptide can form complexes by noncovalent bond in tumor cells. HSP tumor peptide complex can be obtained by separating and purifying HSP from tumor cells. By binding with HSP receptor on the surface of DC, it can effectively ingest tumor peptide and stimulate the body to produce antitumor response. Therefore, the separation and purification of HSP tumor peptide complex from tumor cells is an effective way to obtain tumor-associated antigens. In the HSP family, HSP70 has been studied the most and is the best candidate for the preparation of antigen complex [10-11].

In this study, we purified M-HSP70-PCs from six melanoma cell lines. We cultured primary tumor cells of melanoma patients and purified HSP70 tumor peptide complexes of patients. In addition, autologous DC-CIK cells were induced by the two complexes respectively. The results were exciting; there was no significant difference in IFN- $\gamma$  secretion level and the killing ability between M-HSP70-PCs and the autologous HSP70 tumor peptide complex of patients induced DC-CIK cells ( $P > 0.05$ ). It is suggested that M-HSP70-PCs may be used as an efficient and generalized tumor antigen in the treatment of malignant melanoma.

In the future, we will continue to focus on the study of tumor antigens. In the preparation of melanoma antigen, firstly, we will clarify the identity of tumor antigen peptides in the M-HSP70-PCs. Secondly, we will continue to carry out clinical trials, increase the number of patients, and evaluate the clinical treatment effect and side effects. At the same time, the clinical study of cellular immunotherapy combined with other treatment schemes for melanoma will be carried out. Finally, to increase the

types of human melanoma cell lines as antigen sources, and to explore the possibility of further enhancing the antitumor immune activity of melanoma antigen peptide complex.

### Conflicts of interest

The authors indicated no potential conflicts of interest.

### References

1. Gao Y, Chen X, Gao W, *et al.* A new purification method for enhancing the immunogenicity of heat shock protein 70-peptide complexes. *Oncol Rep*, 2012, 28: 1977–1983.
2. Kozar I, Marque C, Rothenqatter S, *et al.* Many ways to resistance: How melanoma cells evade targeted therapies. *Biochim Biophys Acta Rev Cancer*, 2019, 187: 313–322.
3. Dasgupta A, Katdare M. Ultraviolet radiation-induced cytogenetic damage in white, Hispanic and black skin melanocytes: a risk for cutaneous melanoma. *Cancers (Basel)*, 2015, 7: 1586–1604.
4. Reed JA, Shea CR. Lentigo maligna: melanoma in situ on chronically sun-damaged skin. *Arch PATHOL Lab Med*, 2011, 135: 838–841.
5. Awad MM, Sullivan RJ. Dabrafenib in combination with trametinib for the treatment of metastatic melanoma. *Expert Rev Clin Pharmacol*, 2015, 8: 25–33.
6. Deeks ED. Pembrolizumab: A review in advanced melanoma. *Drugs*, 2015, 76: 375–386.
7. Topalian SL, Sznol M, McDermott DF, *et al.* Survival, durable tumor remission, and long-term safety in patients with advanced melanoma receiving nivolumab. *J Clin Oncol*, 2014, 32: 1020–1030.
8. Redman JM, Gibney GT, Atkins MB. Advances in immunotherapy for melanoma. *BMC Med*, 2016, 14: 20.
9. Alaniz L, Rizzo MM, Mazzolini G. Pulsing dendritic cells with whole tumor cell lysates. *Methods Mol Biol*, 2014, 1139: 27–31.
10. Kim HS, Kang D, Moon MH, *et al.* Identification of pancreatic cancer-associated tumor antigen from HSP-enriched tumor lysate-pulsed human dendritic cells. *Yonsei Med J*, 2014, 55: 1014–1027.
11. Nahleh Z, Tfayli A, Najm A, *et al.* Heat shock proteins in cancer: targeting the chaperones. *Future Med Chem*, 2012, 4: 927–935.

DOI 10.1007/s10330-019-0396-6

Cite this article as: Gao YW, Chen X, Gao WS, *et al.* A study on melanoma treatment using dendritic cells loaded with antigens purified from melanoma cell lines. *Oncol Transl Med*, 2020, 6: 21–25.

# Proton pump inhibitors and stomach neoplasm

Jinkun Guo, Zhongyin Zhou (✉)

Department of Gastroenterology and Hubei Provincial Key Laboratory of Digestive Diseases, Renmin Hospital of Wuhan University, Wuhan 430060, China

## Abstract

This study aimed to explore the relationship between proton pump inhibitors (PPIs) and gastric tumors and determine the reasons behind these connections. We reviewed studies on PPIs and stomach tumors. We explored the relationship between PPIs and different types of gastric neoplasms according to the classification of gastric neoplasms. Long-term use of PPIs is associated with stomach infection, high gastrin levels, and rebound acid hypersecretion, which are directly or indirectly related to the development of gastric neoplasms. PPIs can increase the risk of gastric fundal polyps. Further evidence is needed to prove that it can increase the risk of gastric cancer.

Received: 15 October 2019  
Revised: 25 November 2019  
Accepted: 10 December 2019

**Key words:** proton pump inhibitor (PPI); stomach neoplasm; review

Gastric tumor is a tumor that develops in the gastric mucosa and gastric mucous membrane below the lymphatic tissue, including gastric benign and malignant tumors. Gastric cancer (GC) is the most common gastric malignancy [1]. In China, GC has the second highest incidence rate, after lung cancer, and has second highest mortality rate among all cancers [2]. A proton pump inhibitor (PPI) is widely used in the treatment of gastric acid-related diseases and considered a relatively safe drug. It is often used to treat peptic ulcer, offset gastroesophageal reflux, and *Helicobacter pylori* (HP) infection and prevent primary or recurrent peptic ulcer [3–4]. Moreover, peptic ulcer and HP infection are high-risk factors for gastric tumors. Therefore, PPIs have an inhibitory effect on the development of gastric tumors [5]. However, recently, researchers have found that there is an increased risk of gastric tumors among PPI users [6–7]. Therefore, we have reviewed relevant literature and summarized the relevant information in this study.

## Adverse reactions of the gastrointestinal tract in the clinical use of PPIs

PPIs, introduced in the 1980s, are effective stomach acid inhibitors that reduce stomach acid by inhibiting  $H^+K^+ATPase$  (proton pump) [8]. After absorption in the

blood, PPIs diffuse into the gastric parietal cells and irreversibly bind with  $H^+K^+ATPase$  in the parietal cells of the gastric mucosa, deactivating the proton pump. Gastric acid secretion resumes only when a new proton pump is formed. Therefore, PPIs are effective in inhibiting gastric acid secretion; they are widely used in diseases related to increased gastric acid secretion. A PPI has been regarded as a relatively safe drug with few adverse reactions since its inception. However, the adverse reactions of PPIs in the digestive, immune, endocrine, urinary, and nervous systems and other aspects have attracted the attention of many domestic and overseas scholars [9–10].

The adverse reactions related to gastrointestinal diseases have been summarized below.

### Infection

Long-term use of PPIs leads to non-HP infection in the stomach. Eusebi proposed that long-term acid inhibition would lead to an increase in gastric pH, reducing the bactericidal and bacteriostatic effect of gastric acid and causing microbial infection [11]. Additionally, according to Leonard and Bavishi, PPIs induces sodium hypochlorite damage, a natural defense mechanism of the human body against ingestion of bacteria, leading to bacterial colonization, gastrointestinal flora change, and increase in the risk of gastrointestinal infection. The relationship

between PPIs and gastrointestinal bacterial infection has also been confirmed in various studies [12–13].

### Increased blood gastrin levels

Several studies have found that long-term use of PPIs can increase serum gastrin levels, which is caused by a stress response of G cells in the gastric antrum to lower gastric acid concentration [7,10]. Gastrin has a proliferative effect on cell growth, especially gastrin hyperemia, and nutritional effect on enterochromaffin-like (ECL) cells. Long-term increase in gastrin levels will lead to gastric hyperplasia, further increasing the risk of gastric tumor [13–14].

### Rebound acid hypersecretion

When PPIs are abruptly discontinued, stomach acid production will be higher than that before PPI use, a phenomenon known as “rebound acid hypersecretion,” which causes rebound of gastrointestinal symptoms. This adverse reaction is more common in patients with poor compliance [15].

## PPIs and benign gastric tumor

### PPIs and gastric polyps

Gastric polyp refers to the papillary tissue developing on the surface of the gastric mucosa, which is a type of benign gastric tumor and related to a variety of risk factors [16]. PPI-related polyps are mainly fundic gland polyps.

A meta-analysis of 12 studies on the association between PPI use and gastric polyps by Tran-Duy found that the risk of gastric polyps was significantly increased in individuals who had been using a PPI for > 1 year, but the clinical significance of this increased risk was unclear [17]. Lundell integrated 16 studies and found that the blood gastrin level of individuals who had been using a PPI for > 3 years was 1 times higher than the upper limit of the normal range ( $\leq 100$  pg/mL) [7]. This increase was not associated with the presence or absence of HP infection, and the ECL cell density increased over time in PPI users during the treatment. However, Lundell believes there is insufficient evidence to link these changes. Further, a 5-year follow-up study by Fiocca showed that elevated gastrin levels in PPI users had a sustained drive to proliferate endocrine cell populations in the fundus gland [18]. This drive significantly increases the risk of polyps in the fundus glands, while PPI use increases the risk of non-HP infections in the stomach; inflammatory stimuli also increase the risk of polyps.

In combination with the abovementioned views, the risk of gastric polyps will be increased in individuals who have been using a PPI for a long time, which is mainly attributed to the fact that long-term PPI use can lead to gastrointestinal adverse reactions such as

increased blood gastrin levels and non-HP infection in the stomach [19].

### PPIs and other benign gastric tumors

Except for gastric polyps, there was no significant association between PPI use and other benign gastric tumors. Ezekwudo found the development of neuroendocrine tumors in patients treated with PPIs for a long time, but the cause of this phenomenon is unknown as it rarely occurs. Only a few cases have been reported; hence, these findings may be coincidental, and more cases are needed to confirm these results [19].

## PPIs and malignant gastric tumor

### PPIs and GC

GC is a multifactorial disease, which is affected by several factors during its development. After discovering that PPI use leads to elevated blood gastrin levels and increased risk of gastric polyps, many scholars have started exploring the relationship between PPI use and GC.

#### *PPIs can cause stomach cancer*

In a 2018 Hong Kong-wide retrospective cohort study by Cheung [20] on 63 397 patients who underwent radical treatment for HP infection, the incidence of GC in those who had been using a PPI for > 1 year was significantly higher than that in the control group, and the difference was more significant with longer period of PPI use. The risk of GC was also higher among individuals using PPIs than among those using H2 receptor blockers.

Moreover, in a cohort study based on the Swedish national population, Brusselsaers found that among 797 067 patients who received PPI treatment for at least 180 days [3], the standardized incidence ratio for GC was 3.38 and that the risk of GC increased, regardless of whether there were any signs of GC (e.g., chronic gastritis and HP infection). Meanwhile, the study also compared PPI users and H2 receptor blocker users and found that the incidence of GC did not significantly increase in H2 receptor blockers users. The study revealed that long-term use of PPIs is a risk factor for GC, although factors, such as reverse causality, can skew the results. Moreover, there were several scholars who agree with this point [21–22], Shichijo summarized the characteristics of GC in patients with HP eradication and reported that long-term PPI use in patients with HP eradication may be one of the causes of GC development [23]. Additionally, many researchers attempted to explain this phenomenon using the mechanism of action of PPIs that leads to GC.

(1) Hypergastrinemia theory. PPI use will increase the blood gastrin level, leading to the development of GC. Lundell found that PPI use can increase serum gastrin levels [7]. Moreover, a study by Smith on the relationship

between gastrin and GC showed that gastrin may activate the intracellular signal transduction pathway through the cholecystinin B receptor-mediated pathway and its own characteristics, such as angiogenesis and anti-apoptotic effects, resulting in the development of malignant tumors and GC [24]. Meanwhile, GC precancerous status was also observed after injection of gastrin into animal models [25]. Therefore, long-term use of PPIs may cause hypergastrinemia and further lead to the development of GC.

(2) Infection. PPI use leads to non-HP infection in the stomach, which causes GC. Long-term PPI use can cause gastrointestinal flora imbalance [8, 26] and increase the risk of non-HP infection. Such nonspecific infection will also cause inflammatory hyperplasia of the gastric mucosa. In the long-term development of gastric mucosa, atrophy, intestinal adenosis, polyp formation, and other precancerous lesions will develop, leading to GC [3]. Additionally, some studies have also shown that PPI treatment may promote the process of HP-inducing GC, inducing further malignant transformation of gastric glands [19, 27–28]. This hypothesis seems to explain the results of the previous study by Cheung [21].

#### *PPIs causing stomach cancer needs more evidence*

Although these hypotheses attempt to justify the long-term PPI use for GC, there are still many objections.

Some of these hypotheses have not been well explained. H2 receptor blockers mentioned in the Swedish national cohort study did not increase the risk of GC, but H2 receptor blockers can reduce acidity in the stomach, cause the reaction of G cells in the gastric antrum, and weaken the gastric defense mechanism, leading to infection. However, this phenomenon is explained by the author; they stated that H2 receptor blockers are not as effective as PPIs in inhibiting acid secretion. This explanation involves blood concentration, dose, medication use duration and body sensitivity to drugs which still to be confirmed by experiment [3], and many scholars have proposed that, although long-term PPI use is associated with precancerous lesions (e.g., gastric polyps and gastric mucosal hyperplasia), it cannot be regarded as an independent risk factor for GC [29–30]. In a meta-analysis of 11 studies, Ahn came to a conclusion contradictory to that reported in the Swedish national cohort study, suggesting that H2 receptor blockers increase the risk of GC, while PPIs are not significantly associated with the risk of GC [31]. This contrary conclusion suggests that more studies are needed to confirm the association between long-term PPI use and GC risk. Similarly, in the study by Brusselsaers, it was clearly stated that patients who had been using a PPI for a long time, regardless of the presence of HP infection, had an increased risk of GC [3]. This suggests that PPI use promotes GC development by inducing HP infections also needs to be extensively

investigated.

### **PPIs and gastric malignant lymphoma**

Gastric malignant lymphoma is the most common cancer, excluding GC [32]. Recently, many studies have found that gastric malignant lymphoma is associated with HP infection and that HP eradication plays an important role in the prevention and treatment of gastric malignant lymphoma. Therefore, several individuals regard HP eradication as the first treatment for gastric malignant lymphoma [33]. In HP eradication therapy, PPI use has not been associated with gastric malignant lymphoma.

### **PPIs and other malignant gastric tumors**

Gastric malignancies also include gastric malignant stromal and gastric carcinoid tumors. However, studies on the relationship between PPI use and gastric malignancies are extremely rare, and the relationship between PPI use and these cancers has not been explored.

## **Conclusion**

A PPI is an effective acid-inhibiting drug, which is widely used in clinical practice. Concurrently, PPI use and adverse reactions of the digestive tract have been paid more attention. PPI use can increase the risk of glandular polyps of the fundus, which is associated with hypergastrinemia and non-HP infection in the stomach. Meanwhile, PPI use can increase the risk of GC, which may be related to the development of gastric polyps, hypergastrinemia and infection. However, there are still speculations against this view; hence, more studies are needed to prove or overturn this view.

### **Conflicts of interest**

The authors indicated no potential conflicts of interest.

## **References**

1. Jiang K, Wu XY, Liu BY, *et al.* Primary gastric adenocarcinoma : a case report and literature review. *Oncol Transl Med*, 2019, 4: 188–191.
2. Chen W, Zheng R, Zhang S, *et al.* Report of incidence and mortality in China cancer registries, 2009. *Chin J Cancer Res*, 2013, 25: 10–21.
3. Brusselsaers N, Wahlin K, Engstrand L, *et al.* Maintenance therapy with proton pump inhibitors and risk of gastric cancer: a nationwide population-based cohort study in Sweden. *BMJ Open*, 2017, 7: 017739.
4. Boparai V, Rajagopalan J, Triadafilopoulos G. Guide to the use of proton pump inhibitors in adult patients. *Drugs*, 2008, 68: 925–947.
5. Karimi P, Islami F, Anandasabapathy S, *et al.* Gastric cancer: Descriptive epidemiology, risk factors, screening, and prevention. *Cancer Epidemiol Biomarkers Prev*, 2014, 23: 700–713.
6. Lee Y, Chiang C, *et al.* Association between *Helicobacter pylori*

- eradication and gastric cancer incidence: A systematic review and meta-analysis. *Gastroenterology*, 2016, 150: 1113–1124.
7. Lundell L, Vieth M. Systematic review: the effects of long-term proton pump inhibitor use on serum gastrin levels and gastric histology. *Aliment Pharmacol Ther*, 2015, 42: 649–663.
  8. Kinoshita Y, Ishimura N, Ishihara S. Advantages and disadvantages of long-term proton pump inhibitor use. *Gut*, 2018, 30, 24: 182–196.
  9. Cui Chen. Review: Adverse reactions of commonly used proton pump inhibitors. *Hei Long Jiang Med (Chinese)*, 2013, 4: 1004–5775.
  10. Haastrup P, Thompson W. Side effects of long-term proton pump inhibitor use: A review. *Basic Clin Pharmacol Toxicol*, 2018, 123: 114–121.
  11. Eusebi L, Rabitti S. Proton pump inhibitors: Risks of long-term use. *Gastroenterol Hepatol*, 2017, 32: 1295–1302.
  12. Leonard J, Marshall JK, Moayyedi P. Systematic review of the risk of enteric infection in patients taking acid suppression. *Am J Gastroenterol*, 2007, 102: 2047–2056.
  13. Bavishi C, Dupont HL. Systematic review: the use of proton pump inhibitors and increased susceptibility to enteric infection. *Aliment Pharmacol Therapeut*, 2011, 34: 11–12.
  14. Bjornsson E, Abrahamsson H, Simren M, *et al*. Discontinuation of proton pump inhibitors in patients on long-term therapy: a double-blind, placebocontrolled trial. *Aliment Pharmacol Therapeut*, 2006, 24: 945–954.
  15. Waldum HL, Qvigstad G, Fossmark R, *et al*. Rebound acidhypersecretion from a physiological, pathophysiological and clinical viewpoint. *Scandinav J Gastroenterol*, 2010, 45: 389–394.
  16. Stolte M, Sticht T, Eidt S, *et al*. Frequency, location, and age and sex distribution of various types of gastric polyp. *Endoscopy*, 1994, 26: 659–665.
  17. Tran-Duy, Spaetgens B. Use of proton pump inhibitors and risks of fundic gland polyps and gastric cancer: Systematic review and meta-analysis. *Clin Gastroenterol Hepatol*, 2006, 14: 1706–1719.
  18. Fiocca R, Mastracci L, Attwood SE, *et al*. Gastric exocrine and endocrine cell morphology under prolonged acid inhibition therapy: results of a 5-year follow-up in the LOTUS trial. *Aliment Pharmacol Ther*, 2012, 36: 959–971.
  19. Ezekwudo D, Tobi M. Letter: long-term use of proton pump inhibitors and risk of neuroendocrine tumours. *Aliment Pharmacol Ther*, 2016, 43: 749.
  20. Cheung KS, Chan EW, Wong AYS, *et al*. Long-term proton pump inhibitors and risk of gastric cancer development after treatment for *Helicobacter pylori*: a population-based study. *Gut*, 2018, 67: 28–35.
  21. Ko Y, Tang J. Safety of proton pump inhibitors and risk of gastric cancers: review of literature and pathophysiological mechanisms. *Expert Opin Drug Saf*, 2016, 15: 53–63.
  22. Waldum H, Sordal O, Fossmark R. Proton pump inhibitors (PPIs) may cause gastric cancer -clinical consequences. *Scand J Gastroenterol*, 2018, 53: 639–642.
  23. Shichijo S, Hirata Y. Characteristics and predictors of gastric cancer after *Helicobacter pylori* eradication. *World J Gastroenterol*, 2018, 24: 2163–2172.
  24. Smith JP, Nadella S, Osborne N. Gastrin and gastric cancer. *Cell Mol Gastroenterol Hepatol*, 2017, 4: 75–83.
  25. Walsh JH. Role of gastrin as a trophic hormone. *Digestion*, 1990, 47: 11–16.
  26. Takagi T, Naito Y. The influence of long-term use of proton pump inhibitors on the gut microbiota: an age-sex-matched case-control study. *Clin Biochem Nutr*, 2018, 62: 100–105.
  27. Filipe MI, Munoz N, Matko I, *et al*. Intestinal metaplasia types and the risk of gastric cancer: a cohort study in Slovenia. *Cancer*, 1994, 57: 324–329.
  28. Correa P, Cuello C, Duque E. Carcinoma and intestinal metaplasia in the stomach of Columbian migrants. *Natl Cancer Inst*, 1970, 44: 297–306.
  29. Song H, Zhu J, Lu D. Long-term proton pump inhibitor (PPI) use and the development of gastric pre-malignant lesions. *Cochrane Database Syst Rev*, 2014, (12): 010623.
  30. Eslami L, Nasseri-Moghaddam S. Meta-analyses: does long-term PPI use increase the risk of gastric premalignant lesions? *Arch Iran Med*, 2013, 16: 449–458.
  31. Ahn JS, Eom CS, Jeon CY, *et al*. Acid suppressive drugs and gastric cancer: a meta-analysis of observational studies. *World J Gastroenterol*, 2013, 19: 2560–2568.
  32. Wotherspoon AC, Doglioni C, Diss TC, *et al*. Regression of primary low-grade B-cell gastric lymphoma of mucosa-associated lymphoid tissue type after eradication of *Helicobacter pylori*. *Lancet*, 342: 575–577.
  33. Ono S, Ono Y, Sakamoto N. Diagnosis and treatment of gastric malignant lymphoma. *Nihon Shokakibyō Gakkai Zasshi*, 2017, 114: 1948–1956.

DOI 10.1007/s10330-019-0384-4

Cite this article as: Guo JK, Zhou ZY. Proton pump inhibitors and stomach neoplasm. *Oncol Transl Med*, 2020, 6: 26–29.

# Radiation-induced brain injury after a conventional dose of intensity-modulated radiotherapy for nasopharyngeal carcinoma: a case report and literature review\*

Qian Zhang<sup>1,3</sup>, Jie Tang<sup>1,3</sup>, Jiayu Du<sup>1,3</sup>, Xiaojie Ma<sup>1,2</sup> (✉)

<sup>1</sup> Department of Oncology, affiliated Hospital of North Sichuan Medical College, Nanchong 637000, China

<sup>2</sup> Medical Imaging College, North Sichuan Medical College, Nanchong 637000, China

<sup>3</sup> Department of Clinical Medicine, North Sichuan Medical College, Nanchong 637000, China

## Abstract

A 61-year-old female nasopharyngeal carcinoma patient was admitted to the hospital with sudden cognitive dysfunction one month after Volumetric Intensity Modulated Arc Therapy (VMAT) conventional dose radiotherapy, and the initial diagnosis was radiation-induced brain injury (RBI). After comprehensive treatment with steroid hormones, the patient's condition rapidly improved. Typically, in nasopharyngeal carcinoma patients treated with VMAT, the incidence of RBI is extremely low when the temporal lobe dose is less than 65 Gy or 1% of the volume is less than 65 Gy. When this limit is exceeded, RBI may occur in varying degrees. However, in this case, even though the temporal lobe dose was under the prescribed limit, the patient still experienced RBI. The rare observations in this case can be used as a reference, and clinicians should seriously consider the possibility of RBI in similar cases.

**Key words:** radiation-induced brain injury; nasopharyngeal carcinoma; VMAT

Received: 11 October 2019  
Revised: 8 December 2019  
Accepted: 29 December 2019

Radiation-induced brain injury (RBI) is caused by the radiotherapy for head and neck cancer, and presents as a radiation response syndrome in the brain tissue. The incidence of RBI at the conventional dose of Volumetric Intensity Modulated Arc Therapy (VMAT) in nasopharyngeal carcinoma radiotherapy is 0.9 to 4.8% [1–3]. The clinical manifestations vary due to the range and location of different lesions. The main clinical manifestations of the temporal lobe type are memory deterioration, visual, auditory, olfactory and taste hallucinations, multilingual or mental retardation, orientation disorders, and intracranial hypertension. The clinical manifestations of the brain-stem type are dizziness, speech disorder, and walking instability [4]. In clinical practice, Magnetic Resonance Imaging (MRI) is the most commonly used method for the examination

of RBI. Edema is the most common early manifestation of the injury. Late manifestations include brain atrophy, white matter necrosis, brain softening, and deposition of hemosiderin. The T1WI of the necrotic area shows a low signal and the T2WI shows a high signal [5]. Although with standardization of radiotherapy technology and dose, VMAT can significantly improve the local control rate of nasopharyngeal carcinoma with reduced exposure volume and dose for normal tissues, varying degrees of radiation brain damage are still possible. The main factors that determine the extent of RBI are radiation dose, divided dose, irradiation method and exposure volume, and individual radiotherapy sensitivity [6]. Nasopharyngeal carcinoma is different from brain tumor, for which radiation therapy is intended to be curative. The prescription dose is high, as the exposed brain tissue

✉ Correspondence to: Xiaojie Ma. Email: 992437730@qq.com

\* Supported by grants from the Sichuan Medical Research Youth Innovation Project (No. Q18031) and the 2018 City School Strategic Cooperation Research Project (No. 18SXHZ0542).

© 2020 Huazhong University of Science and Technology

is small in size, and the exposed area is usually located at a distance from important functional areas associated with sensory processes and motor. Generally, the dose limit for the brain tissue is relaxed to meet the dose coverage of the target area in the progress [7]. In clinical practice, the method of delineation of the temporal lobe is commonly used to limit the exposure dose for the brain. The dose limit for the temporal lobe is less than 65 Gy or 1% of the volume < 65 Gy, and radiation brain damage rarely occurs under this dose limit. However, we observed a rare case wherein a nasopharyngeal carcinoma patient who was recently admitted to our hospital developed RBI after intensity-modulated radiotherapy and administration of a sputum leaf dose of  $D_{max} < 60$  Gy. We hope to reduce complications of radiation therapy in the future by analyzing the cause of RBI in this case and provide evidence for the optimization of precision radiotherapy.

## Case history

A 61-year-old female patient was admitted to the Department of Radiation Oncology of the affiliated hospital of North Sichuan Medical College on August 30, 2018, one day after a diagnosis of nasopharyngeal carcinoma (T3N0M0 phase III), which required chemotherapy. The contraindications of radiotherapy were not considered after completing the relevant examinations, and radiotherapy was performed on the nasopharyngeal lesions and cervical lymphatic drainage areas on September 3, 2018.

In the first stage of treatment, the VMAT technique was used with a prescribed dose of P-GTVnx: 61.6 Gy/28Fx, P-GTVnd: 61.6 Gy/28Fx, P-CTV1: 60.2 Gy/28Fx, and P-CTV2: 50.4 Gy/28Fx. In the second stage, the dose prescribed was P-GTVnx: 11 Gy/5Fx. There was no atypical discomfort reported during the treatment, and the patient was discharged from the hospital on October 22, 2018.

On October 30, 2018, the patient was admitted to the Department of Neurology at our hospital for sudden cognitive impairment, concomitant with depression, gaze, slow reactions, physical decline, inability to calculate, confusion and memory loss, inability to recognize objects, and spatial and temporal orientation disorders among other symptoms. Physical examination showed the following: patient was conscious; the bilateral pupils were sensitive to light reflection; eyeball movement was normal; corneal reflex was present; symmetry of the bilateral frontal stria; nasolabial fold was symmetrical; no sag or drooping; tongue was centered; normal muscle tension; normal tendon reflex; mutual exercise and sensory system examination did not cooperate; and pathological signs were negative.

On October 30, 2018, the CT examination showed



**Fig. 1** Brain CT scan: Irregular slightly high-density shadow can be seen in the right temporal lobe

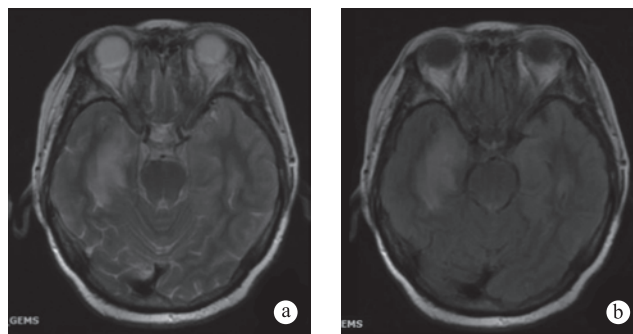


**Fig. 2** MRI scan: T2WI and FLAIR show slightly higher signal, T1WI shows slightly lower signal

that the right temporal lobe presented with irregular, high-density shadows, and large patches of low-density shadows could be seen around the region (Fig. 1).

On November 1, 2018, the MRI examination showed flaky abnormal signals in the bilateral temporal lobe; the T1WI showed a slightly low signal, the T2WI and fluid attenuated inversion recovery (FLAIR) showed a slightly high signal, and the DWI of the left island insular cortex showed a slightly higher signal in the cerebral gyrus than in the surrounding areas. There was a patchy enhancement at the bottom of the right temporal lobe (Fig. 2).

On November 12, 2018, the MRI examination showed that the bilateral frontal temporal lobes presented with scattered, patchy and small abnormal signal shadows. The T1WI showed low signal, the T2WI and FLAIR showed high signal, the bilateral hippocampus and left insular lobe, temporal lobe, and occipital lobe showed patchy abnormal signal shadows. The T1WI showed an equal signal, whereas the T2WI and FLAIR showed a slightly higher signal, and the DWI showed slightly high B value. There was no widening and deepening in the brain pool and the cerebral sulcus, and no displacement of the midline structure and no abnormal signals in the cerebellum and brainstem were found. Radioactive encephalitis was considered in the bilateral hippocampus,

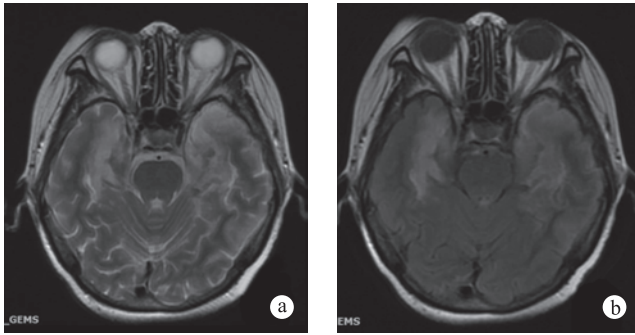


**Fig. 3** MRI scan: There was no widening and deepening in the brain pool and the cerebral sulcus, and no displacement of the midline structure and no abnormal signals in the cerebellum and brainstem were found

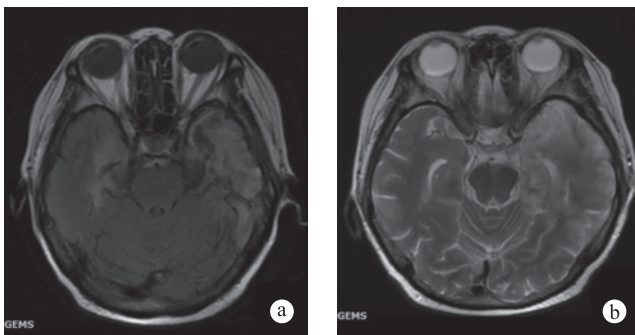


**Fig. 4** MRI scan: After one-month hormone shock therapy

left insular lobe, temporal lobe, and occipital lobe (Fig. 3).

At this time, the patient showed increased excitability, loss of appetite, dizziness, lethargy, memory loss, and slightly slow reactions. She could recognize familiar people, but could not recall names, whereas the symptoms of spatial and temporal disorientation were slightly improved.

On December 1, 2018, the MRI examination showed that the bilateral hippocampus, temporal lobe (sputum was extremely dominant, and left side was significantly larger than the right side), and the left-sided island leaf showed flaky abnormal signals, mainly on the left side of the lesion. The T1WI showed an equal signal compared with the dominant, whereas the right temporal lobe lesion showed a slightly higher patchy signal. The right temporal lobe and the left side of the lesion showed a slightly higher signal intensity; T2WI and T2-FLAIR also showed slightly higher signals; the DWI high B value was slightly higher; and the enhanced scan showed no obvious enhancement. The bilateral frontal and temporal lobes had scattered, spotted and patchy abnormal signals; the T1WI showed low signal, whereas the T2WI and T2-FLAIR showed high signals (Fig. 4).

The treatment plan included active dehydration with mannitol (125 mL q12h), dexamethasone (10 mg bid, lasting for four weeks), oxygen inhalation with a mask,

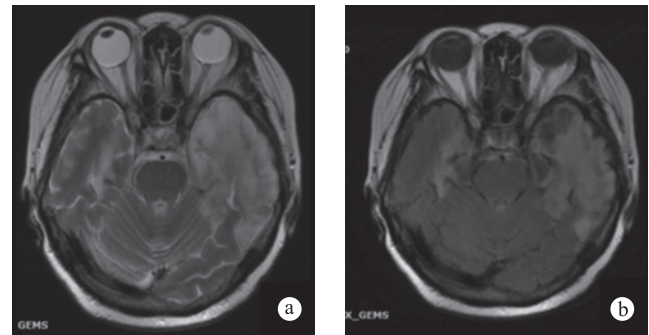


**Fig. 5** Re-examination of MRI

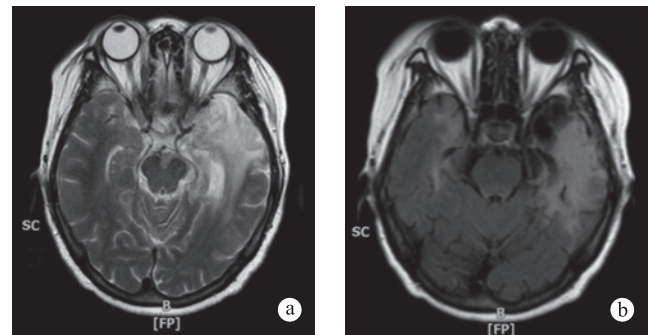


**Fig. 6** Re-examination of MRI

a single dose of ginseng polyphenol (200 mg qd) for promoting blood circulation and correcting blood stasis, butylphthalide (0.2 g tid) for improving nerve function, edaravone (30 mg bid) as a free radical scavenger, and cerebroside carnosine (5 mL qd) as a nutritional nerve supplement. This treatment proved to be effective, and the patient gradually recovered cognitive functions.

After one month of hormone shock therapy, the dose was gradually reduced. On December 9, 2018, the patient was discharged from the hospital and was treated with dexamethasone (6 mg bid, taken orally), and the reduction lasted for 3–4 months. The patient was requested to visit the hospital for regular follow-up cranial MRIs.

MRI examination on January 4, 2019 showed that the bilateral hippocampus, temporal lobe (sputum is extremely dominant, and left side is significantly larger than the right side), and left lobes presented with flaky abnormal signals, mainly to the left of the lesion. The T1WI showed equal signal compared with the dominant, whereas the right temporal lobe lesion showed a slightly higher patchy signal. The right temporal lobe and the left side of the lesion showed slightly higher signal intensities; the T2WI and T2-FLAIR also showed slightly higher signals; the DWI high B value was slightly higher; and the enhanced scan showed no significant enhancement (Fig. 5).

At this time, the general condition of the patient had

improved; there was no dizziness and sleepiness, patient had recovered memory, reactions were normal, and time and space orientation was normal. The patient's dexamethasone dose was maintained at 0.75 mg qd.

On March 25, 2019, the changes in the hippocampus and temporal lobe lesions were not obvious compared with the results on January 4. However, the patient's previous symptoms improved significantly, and no special discomfort was reported (Fig. 6).

## Discussion

### Pathogenesis

Most researchers believe that only a single factor cannot explain the complex pathological manifestations of RBI, and it is the result of multiple factors. There are several theories that may explain the underlying mechanism:

(1) Glial cell theory: Radiation directly damages brain tissue, mainly acting on the glial cells, which can cause a disorder in myelin phospholipid formation, myelin phospholipid loosening, and reactive glial proliferation in the white matter, as well as demyelination and white matter atrophy<sup>[9]</sup>.

(2) Autoimmune theory: Animal experiments have shown that oligodendrocytes and their enzyme systems produce autoantigens after radiotherapy, which induces autoimmune responses of the body, leading to demyelination of the brain glial cells, cerebral edema, and other pathological changes<sup>[5]</sup>.

(3) Free radical theory: The central nervous system is extremely sensitive to oxidative damage. Ionizing radiation causes ionization of macromolecular substances in the cells, causing the cells to form a large number of oxygen free radicals. This leads to the formation of peroxides due to lipid peroxidation of the cell membranes, causing cell damage.

(4) Theory of vascular injury: Shortly after radiotherapy, the volume of vascular endothelial cells in the brain increases, and their nuclei shrink and fragment, resulting in a large reduction of endothelial cells. This in turn leads to infiltration of inflammatory cells around the blood vessels, due to which there is an increase in vascular permeability, leading to edema of surrounding tissues. Such phenomena lead to microcirculation disorders, brain ischemia, and irreversible necrosis. In the late stage after irradiation, extensive capillary atrophy results in a large number of ischemic lesions in the brain, which accelerates liquefaction necrosis of the brain<sup>[10]</sup>.

### Diagnosis

The case characteristics of this patient are consistent with previous literature reports in our country and abroad. There was a clear history of radiotherapy,

relatively complex clinical manifestations, and lack of specificity. Plain CT scan in the acute and early-delayed response period showed extensive non-specific, low-density edema zones. MRI showed equal or low signals in the T1WI, and high signals in the T2WI and T2-FLAIR. One month after radiotherapy of the patient, the head CT showed an irregular, slightly high-density shadow in the right temporal lobe, and large patches of low-density shadow could be observed around the region. MRI showed abnormal patchy signals in the bilateral hippocampus and left insular lobe, temporal lobe, and occipital lobe; the T1WI showed equal signals, and T2WI and FLAIR showed slightly higher signals. The presence of typical symptoms (drowsiness, memory loss, irritability, and fatigue), time of onset of symptoms (1–6 months after irradiation), and effectiveness of the treatment (generally recoverable after treatment) confirmed the diagnosis of the early-delayed response period of RBI.

### Treatment

RBI is usually a progressive, irreversible chronic change, but timely intervention in the acute phase, for both early and late onset RBI, has a significant therapeutic effect. The treatment protocol that was followed has been given below:

(1) Glucocorticoids as the main treatment; Feng Qing *et al*<sup>[11]</sup> used glucocorticoids for radiation encephalopathy, which can effectively relieve clinical symptoms, reduce brain tissue damage and brain edema, and effectively repair brain metabolism and nerve cell function in patients<sup>[11]</sup>.

(2) Glycerol fructose or mannitol and torasemide were used to reduce brain edema and intracranial pressure<sup>[12]</sup>.

(3) High pressure oxygen absorption; hyperbaric oxygen can increase tissue oxygen partial pressure, stimulate endothelial growth factor production, and stimulate cell and vascular repair mechanisms<sup>[13]</sup>.

(4) Free radical scavengers; edaravone, a brain protectant, can not only scavenge free radical molecules, but also induce peroxidation reaction to alleviate the symptoms of brain edema.

(5) Warfarin and heparin can prevent and reverse vascular endothelial injury, improve microcirculation, and facilitate the repair of RBI.

(6) Simultaneously, the treatment was supplemented with vasodilators, nutrient supplements for nerves, large doses of vitamins, and blood circulation and stasis stimulus to improve brain function.

After the above treatment, the patient's symptoms improved and her cognitive function recovered significantly. However, the imaging results showed no obvious changes compared with the previous examination, and the patient required close observation and follow-up.

### Unique characteristics of the case: summary and relevance

In the first stage, the prescribed dose was P-GTVnx: 61.6 Gy/28Fx, P-GTVnd: 61.6 Gy/28Fx, P-CTV1: 60.2 Gy/28Fx, and P-CTV2: 50.4 Gy/28Fx. In the second stage, the prescribed dose was P-GTVnx: 11 Gy/5Fx. The maximum dose for the left temporal lobe was 5996.8 cGy, whereas the maximum dose for the right temporal lobe was 5751.1 cGy. Su *et al*<sup>[14]</sup> found that when the Dmax dose for the temporal lobe was greater than 64 Gy or D1cc was greater than 52 Gy, the incidence of RBI increased by approximately 2.5% with every 1 Gy increase in the dose. The recommended dose limits are Dmax < 68 Gy or D1cc < 58 Gy to ensure safety. Furthermore, Su *et al*<sup>[15]</sup> found that the absolute volume of the temporal lobe V40 (aV40) and the percentage of the temporal lobe V40 (rV40) were also independent risk factors for the occurrence of RBI. The recommended limits were rV40 < 10% and aV40 < 5 cc. In this patient's case, even though the radiation dose was significantly lower than the aforementioned cutoffs, radiation brain damage still occurred. The observations of this case report can be used for reference when developing radiation therapy protocols in the future.

### Conclusion

The occurrence of RBI is not only closely related to the radiation source, single dosage, total dose division, and total treatment time, but also related to other factors such as the patient's age, cancer pathology, clinical stage, individual sensitivity, cervical lymphadenopathy, neck and brain arteriosclerosis, and concurrent chemoradiotherapy. Moreover, there are no standard criteria for temporal lobe delineation, and there are numerous variations in protocols. We speculate that individual-specific factors may be the most important, as different individuals have different sensitivities to radiotherapy. Studies<sup>[16]</sup> have found that individuals with high radiosensitivity developed RBI earlier than those with low radiosensitivity. However, further studies are required to develop methods for determining an individual's sensitivity to radiotherapy before treatment.

The overall curative effect of RBI treatment is not satisfactory. Clinicians should focus on the prevention and reduction of the occurrence of RBI when performing head and neck radiotherapy. Similar to the results from the relevant body of literature, Lee *et al*<sup>[3]</sup> found that the incidence of RBI increased by 8.3% in patients with nasopharyngeal carcinoma treated with stereotactic radiotherapy compared to that in those treated with high-dose rate brachytherapy because brachytherapy did not involve an increase in the total dose of radiation to the temporal lobe. In the future, we should consider the use of close-range illumination instead of external

exposure. In addition, studies have found that intensity-modulated proton radiotherapy (IMPT) can further improve the dose distribution for tumors and normal tissues and reduce the incidence of RBI. Taheri-Kadkhoda *et al*<sup>[18]</sup> compared the dose-study of Intensity-modulated radiation therapy (IMRT) and IMPT simulations in patients with nasopharyngeal carcinoma. It was found that IMPT not only significantly optimized the coverage of tumor target areas but also reduced the average exposure of the temporal lobe to approximately 40% of the exposure during IMRT. This suggests that proton radiotherapy may have potential advantages over other techniques as it minimizes damage to the central nervous system. However, specific findings need to be confirmed with large-scale clinical trials.

In summary, factors specific to patients with nasopharyngeal carcinoma should be fully considered during radiotherapy. We should accurately design the target area according to individual differences, strictly limit the temporal lobe dose, strengthen the monitoring and follow-up of patients after radiotherapy, and develop advanced radiotherapy methods to reduce the incidence of RBI.

### Conflicts of interest

The authors indicated no potential conflicts of interest.

### References

1. Sun Y, Zhou GQ, Qi ZY, *et al*. Radiation-induced temporal lobe injury after intensity modulated radiotherapy in nasopharyngeal carcinoma patients: a dose-volume-outcome analysis. *BMC Cancer*, 2013, 13: 397.
2. Su SF, Huang Y, Xiao WW, *et al*. Clinical and dosimetric characteristics of temporal lobe injury following intensity modulated radiotherapy of nasopharyngeal carcinoma. *Radiother Oncol*, 2012, 104: 312–316.
3. Lee AW, Ng WT, Hung WM, *et al*. Major late toxicities after conformal radiotherapy for nasopharyngeal carcinoma-patient- and treatment-related risk factors. *Int J Radiat Oncol Biol Phys*, 2009, 15, 73: 1121–1128.
4. Greene-Schloesser D, Robbins ME, Peiffer AM, *et al*. Radiation-induced brain injury: A review. *Front Oncol*, 2012, 2: 73.
5. Chong VF, Fan YF, Mukherji SK. Radiation-induced temporal lobe changes CT and MR imaging characteristics. *AJR*, 2000, 175, 431–436.
6. Zeng L, Tian YM, Sun XM, *et al*. Late toxicities after intensity-modulated radiotherapy for nasopharyngeal carcinoma patient and treatment-related risk factors. *Br J Cancer*, 2014, 110: 49–54.
7. Ng WT, Lee MC, Chang AT, *et al*. The impact of dosimetric inadequacy on treatment outcome of nasopharyngeal carcinoma with IMRT. *Oral Oncol*, 2014, 50: 506–512.
8. Marks LB, Yorke ED, Jackson A, *et al*. Use of normal tissue complication probability models in the clinic. *Int J Radiat Oncol Biol Phys*, 2010, 76: S10–19.
9. Tofilon PJ, Fike JR. The radio response of the central nervous system: a dynamic process. *Radiat Res*, 2000, 153: 357–370.
10. Crossen JR, Garwood D, Glatstein E, *et al*. Neurobehavioral

- sequelae of cranial irradiation in adults: a review of radiation-induced encephalopathy. *J Clin Oncol*, 1994, 12: 627–642.
11. Kerob D, Kolb F, Marguis A, *et al*. Delayed cerebral radionecrosis following radiation therapy of cutaneous squamous cell carcinoma of the head. *Ann Dermatol Venereol*, 2002, 129: 41–45.
  12. Zeng L, Tian YM, Sun XM, *et al*. Late toxicities after intensitymodulated radiotherapy for nasopharyngeal carcinoma patient and treatment-related risk factors. *Br J Cancer*, 2014, 110: 49–54.
  13. Feldmeier JJ, Hampson NB. A systematic review of the literature reporting the application of hyperbaric oxygen prevention and treatment of delayed radiation injuries: an evidence based approach. *Undersea Hyperb Med*, 2002, 29: 4-30.
  14. Su SF, Huang Y, Xiao WW, *et al*. Clinical and dosimetric characteristics of temporal lobe injury following intensity modulated radiotherapy of nasopharyngeal carcinoma. *Radiother Oncol*, 2012, 104: 312–316.
  15. Su SF, Huang SM, Han F, *et al*. Analysis of dosimetric factors associated with temporal lobe necrosis (TLN) in patients with nasopharyngeal carcinoma (NPC) after intensity modulated radiotherapy. *Radiat Oncol*, 2013, 8: 17.
  16. Tang Y, Zhang Y, Guo L, *et al*. Relationship between individual radiosensitivity and radiation encephalopathy of nasopharyngeal carcinoma after radiotherapy. *Strahlenther Onkol*, 2008, 184: 510–514.
  17. Taheri-Kadkhoda Z, Björk-Eriksson T, Nill S, *et al*. Intensity-modulated radiotherapy of nasopharyngeal carcinoma: a comparative treatment planning study of photons and protons. *Radiat Oncol*, 2008, 3: 4.

**DOI 10.1007/s10330-019-0383-3**

**Cite this article as:** Zhang Q, Tang J, Du JY, *et al*. Radiation-induced brain injury after a conventional dose of intensity-modulated radiotherapy for nasopharyngeal carcinoma: a case report and literature review. *Oncol Transl Med*, 2020, 6: 30–35.

# Glioblastoma multiforme with metastasis to lung, bone, and chest wall: a case report

Guobo Du<sup>1</sup>, Qian Zhou<sup>2</sup>, Xinyao He<sup>3</sup>, Long Cheng<sup>1</sup>, Jing Zhou<sup>4</sup> (✉)

<sup>1</sup> Department of Oncology, Affiliated Hospital of North Sichuan Medical College, Nanchong 637000, China

<sup>2</sup> North Sichuan Medical College, Nanchong 637000, China

<sup>3</sup> North Sichuan Medical College, Nanchong 637000, China

<sup>4</sup> Department of Neurology, Affiliated Hospital of North Sichuan Medical College, Nanchong 637000, China

## Abstract

Glioblastoma multiforme (GBM) is a common brain tumor that rarely metastasizes extra-cranially. We present the case of a 40-year-old male with left temporal GBM who underwent craniotomy followed by radiotherapy and chemotherapy. Postoperative MRI scans at different time intervals demonstrated a good response. Eleven months after the initial diagnosis, there were no clinical or radiological signs suggesting recurrence. However, the tumor showed metastasis simultaneously to the chest wall, lungs, and bone, despite 2 cycles of chemotherapy. The patient developed paraplegia 14 months after the initial diagnosis and died due to systemic failure 19 months after diagnosis. Extracranial metastasis of GBM is extremely rare. We present the unusual case of a patient with GBM who showed simultaneous metastasis to the lungs, bone, and chest wall. The prognosis of patients with extracranial metastasis of glioblastomas is very poor, regardless of chemoradiotherapy. Newer approaches, such as immunotherapy and anti-angiogenic therapy, need to be further studied.

Received: 26 November 2019

Revised: 17 January 2020

Accepted: 29 January 2020

**Key words:** extracranial glioblastoma; glioblastoma multiforme; metastases

Glioblastoma multiforme (GBM) is an aggressive central nervous system (CNS) neoplasm associated with poor survival. Extracranial metastasis is rare, with the reported instances attributed to leptomeningeal involvement, cerebrospinal fluid (CSF) dissemination, direct seeding through craniotomy defects or shunt catheters, and very rarely, lymphatic or hematogenous spread to distant organs<sup>[1]</sup>. However, sporadic cases of GBM metastasis have been reported over the years<sup>[2]</sup>. This report details the unique case of a patient with GBM who showed post-surgical metastasis to the chest wall, lungs, and bone without local brain relapse and demonstrated an unfavorable chemotherapeutic response.

## Case history

A 40-year-old male complaining of pain in the right chest wall was admitted to our hospital. Twelve months

prior, he had a craniocerebral injury, and a solitary large (49 × 35 × 31 mm) left temporal lobe tumor was detected in the MRI scan (Fig. 1). He underwent a craniotomy and tumor debulking with satisfactory postoperative MRI. Histological examination confirmed a diagnosis of glioblastoma with oligodendrocytoma components. Immunohistochemical analysis demonstrated positive in situ expression of GFAP, OLig-2, EMA, Ki-67 (70%), S-100, and Vimentin. Genotyping revealed that the tumor was IDH-1 (isocitrate dehydrogenase-1) wild type. The patient underwent gross tumor resection followed by radiotherapy (60 Gy/30) with concomitant (6 cycles) and adjuvant temozolomide-based chemotherapy.

Eleven months following the initial diagnosis, he complained of progressive low back pain. CT scan revealed a mass in the right chest wall (73 mm × 54 mm), indicating multiple lung metastases (Fig. 2). MRI showed thoracic spine metastases from the primary GBM. Emission computed tomography (ECT) showed

✉ Correspondence to: Jing Zhou. Email: zj8126118@yeah.net

© 2020 Huazhong University of Science and Technology

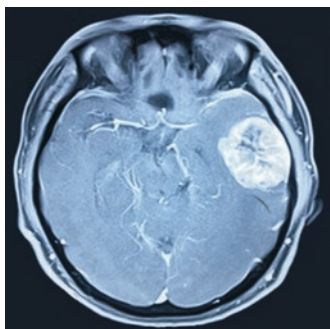


**Fig. 1** Contrast-enhanced T1 brain MRI

metastasis to the right rib 4-10, T10 vertebra, right ilium, right sacroiliac joint, bilateral upper humerus, and right superior femur.

Percutaneous biopsy of the right thoracic wall mass confirmed the diagnosis of GBM metastasis. Immunohistochemical analysis indicated the following profile of the metastasized tumors: CD34+ (vascular), GFAP-, olig-2+ (individual cells), s-100+, EMA-, IDH1-, ATRX+, P53+, ki-67+ (50%), and CK-. The patient received 2 cycles of chemotherapy with paclitaxel and cisplatin.

Fourteen months after the initial diagnosis, the patient presented with physical weakness and urinary incontinence. CT revealed enlargement of chest wall mass and the progression of lung and bone metastasis (Fig. 3). Response Evaluation Criteria in Solid Tumors (RECIST) score for the patient was progressive disease (PD), despite 2 cycles of chemotherapy. The patient refused to receive radiotherapy for the thoracic spine and other anti-tumor treatment strategies. He was discharged after two weeks of best supportive care. Subsequently, he developed paraplegia and died due to systemic failure, 19 months after the initial diagnosis.

## Discussion

GBM is the most malignant primary brain tumor with overall survival rates between 12-15 months [3]. Extracranial metastases from GBM are rare, with very few reports of lung [2, 4-5] and bone metastasis [5]. Furthermore, liver, lymph node, spleen, cardiac, orbit, meningeal, and surgical seeding/operative flap metastases have also been observed in some cases [6]. Davis [7] reported the first case of chest wall metastasis from GBM in 1928, but subsequent reports have been sparse. Our patient presented a rare case of GBM that exhibited simultaneous metastasis to the lungs, chest wall, and bone.

The overall paucity of documented extracranial GBM metastasis can be explained by the absence of cerebral lymphatics, early occlusion of veins, and short overall survival of the patients [2]. However, several cases of

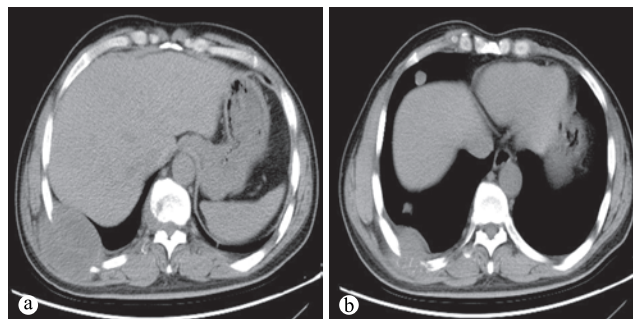


**Fig. 2** Bone destruction on the right side of the 6th and 9th rib. Localized soft tissue mass and bone destruction in the 10<sup>th</sup> thoracic vertebra (a). Multiple tumor metastases in both lungs (b)

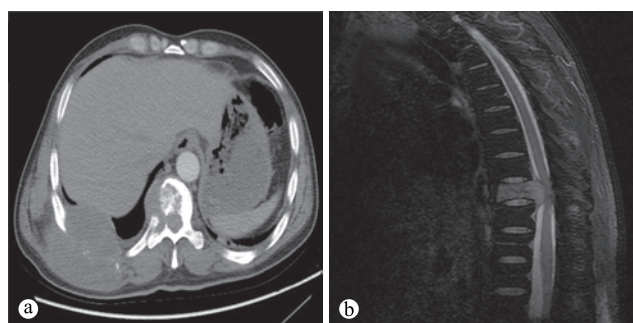


**Fig. 3** CT revealed enlargement of the chest wall mass and thoracic spinal metastasis (a). MRI revealed tumor metastasis to the thoracic spine, compressing the spinal cord (b)

extracranial metastasis of GBM have been reported in recent years, which could be the likely result of the lymphatic spread of tumor cells during surgery [5] due to mechanical disturbance of the lymph nodes. The risk of post-surgery metastasis is aggravated if the tumor lies in a region with extensive venous drainage. Hematogenous spread of GBM is unusual as the thin-walled intracerebral veins would probably collapse from compression before tumor invasion [8]. However, circulating tumor cells (CTCs) have been detected in the blood of GBM patients [9], which significantly contribute to GBM metastasis [8]. As our patient showed simultaneous metastasis to the chest wall, lungs, and bone, the metastasis was considered the result of hematogenous spread.

Current recommendations for newly diagnosed glioblastomas are maximum safe resection, followed by fractionated localized radiotherapy with daily concomitant temozolomide and adjuvant temozolomide [3, 10]. However, there is no standard treatment at present for extra-neural metastasis of glioblastoma. We introduced 2 cycles of chemotherapy with paclitaxel and cisplatin on account of the extensive nature of metastasis seen in our patient, which unfortunately was ineffective. As he refused radiotherapy for the thoracic spine, it is unclear whether paraplegia could have been delayed

with radiation therapy. However, in a similar case report of a GBM patient with extensive spinal metastasis who accepted adjuvant radiotherapy for the cervical spine in addition to chemotherapy, anti-angiogenic therapy, and immunotherapy with pembrolizumab and bevacizumab, death occurred 13.8 months after the initial diagnosis<sup>[11]</sup>.

Due to its highly aggressive nature, patients with glioblastomas have a poor prognosis, despite the use of radiotherapy and chemotherapy in patients who develop metastasis. The efficacy of immunotherapy and anti-vascular therapy require further study.

## Conclusion

GBM metastases have become more frequent in recent years due to post-surgery lymphatic and hematogenous dissemination, in addition to the usual route of the CSF. We present a rare case of a patient with GBM who showed simultaneous post-surgery metastasis to the lungs, bone, and chest wall, and died 19 months after the initial diagnosis. Novel treatment guidelines and therapeutic strategies need to be developed for recurrent and metastatic GBM.

## Conflicts of interest

The authors indicated no potential conflicts of interest.

## References

- Ginat DT, Schaefer PW. Imaging guidelines and findings of extracranial glioblastoma. *J Neurooncol*, 2014, 118: 9–18.
- Kumaria A, Teale A, Kulkarni GV, *et al.* Glioblastoma multiforme metastatic to lung in the absence of intracranial recurrence: case report. *Br J Neurosurg*, 2018: 1–3.
- Stupp R, Mason WP, van den Bent MJ, *et al.* Radiotherapy plus concomitant and adjuvant temozolomide for glioblastoma. *N Engl J Med*, 2005, 352: 987–996.
- Hoffman HA, Li CH, Everson RG, *et al.* Primary lung metastasis of glioblastoma multiforme with epidural spinal metastasis: Case report. *J Clin Neurosci*, 2017, 41: 97–99.
- Undabeitia J, Castle M, Arrazola M, *et al.* Multiple extraneural metastasis of glioblastoma multiforme. *An Sist Sanit Navar*, 2015, 38: 157–161.
- Piccirilli M, Brunetto GM, Rocchi G, *et al.* Extra central nervous system metastases from cerebral glioblastoma multiforme in elderly patients. Clinico-pathological remarks on our series of seven cases and critical review of the literature. *Tumori*, 2008, 94: 40–51.
- Davis L. Spongioblastoma multiforme of the brain. *Ann Surg*, 1928, 87: 8–14.
- Müller C1, Holtschmidt J, Auer M, *et al.* Hematogenous dissemination of glioblastoma multiforme. *Sci Transl Med*, 2014, 6: 247ra101.
- Chistiakov DA, Chekhonin VP. Circulating tumor cells and their advances to promote cancer metastasis and relapse, with focus on glioblastoma multiforme. *Exp Mol Pathol*, 2018, 105: 166–174.
- Liu X, Cui L, Dong H. Clinical observation in three-dimensional conformal radiotherapy (3D-CRT) with concurrent chemotherapy in treatment of postoperative cerebral gliomas. *Oncol Transl Med*, 2010, 4: 193–197.
- Schwartz C, Romagna A, Machegger L, *et al.* Extensive leptomeningeal intracranial and spinal metastases in a patient with a supratentorial glioblastoma multiforme, IDH-wildtype: A case report. *World Neurosurgery*, 2018, 120: 442–447.

DOI 10.1007/s10330-019-0393-3

Cite this article as: Du GB, Zhou Q, He XY, *et al.* Glioblastoma multiforme with metastasis to lung, bone, and chest wall: a case report. *Oncol Transl Med*, 2020, 6: 36–38.

# The application of 3D printing in the development of RECIST standard for evaluating tumor efficacy\*

Xiaodan Yang<sup>1</sup>, Tao Han<sup>1</sup> (Co-first author), Yue Zhang<sup>2</sup>, Yanming Zhang<sup>2</sup>, Gao Li<sup>3</sup>, Yongye Liu<sup>1</sup>, Zhaozhe Liu<sup>1</sup> (✉), Zhendong Zheng<sup>1</sup> (✉)

<sup>1</sup> Department of Oncology, Cancer Center, General Hospital of Northern Theater Command, Shenyang 110840, China

<sup>2</sup> Oncology Phymatology, Jinzhou Medical University, Jinzhou 121000, China

<sup>3</sup> Department of Clinical Pharmacy, Shenyang Pharmaceutical University, Shenyang 110840, China

## Abstract

Three-dimensional (3D) printing technology, as a novel technical method, can convert conventional computed tomography (CT) or magnetic resonance imaging (MRI) scans to computer-aided design files and develop a 2D spatial structure into a 3D imaging structure. In recent years, the technology has been widely used in numerous areas, including head and neck surgery, orthopedics, and bio-medicinal research. This article uses examples of 3D printed tumor models to develop Response Evaluation Criteria In Solid Tumors (RECIST) standards to evaluate the changes in tumors. RECIST standard is currently recognized as the standard for assessment of chemotherapy. Under the RECIST standard, changes occurring in tumors before and after the surgery, are evaluated. The assessment depends upon a CT evaluation of the changes in the lesions with the largest diameters. In addition, the disease progression and stability of remission is also assessed. Three-dimensional printing technology is more intuitive in the evaluation of changes to human tumors following chemotherapy and targeted therapy. However, a few reports are available.

Received: 19 August 2019  
Revised: 11 September 2019  
Accepted: 30 October 2019

**Key words:** Three-dimensional (3D) printing; RECIST standard; chemotherapy

Case 1: A 75-year-old man, diagnosed over half a month ago with a tumor in the left lung, was admitted to the hospital. In September 2015, obvious causes of cough, sputum, fever, and shortness of breath following activity, were not observed. In October 2015, the presence of a pulmonary hilar measuring 4.4 cm × 3.6 cm was detected in the left lung via a chest CT scan. (Fig. 1a). Multiple lymph node metastases were also noted. The pathological and immunohistochemical results were as follows: lower differentiation of adenocarcinoma, a wild-type EGFR gene, and an unfused EML4-ALK gene. Upon admission, no significant assessment result was noted, except for weak breathing sounds in the left lung. Based on clinical, pathologic, imaging, and preliminary assessment results, the patient was diagnosed with low differentiated adenocarcinoma of the left lung (IIIA, cT2N2M0). Pemetrexed, in combination with Endostar, was administered to the patient. The Chest CT results

indicated that the left hilar mass was significantly reduced after two cycles of treatment. A part remission was indicated by the RECIST standard efficacy rating. Comparison of the two 3D print results were shown in Fig. 1b and 1c.

Case 2: A 66-year-old woman, experiencing chest tightness and heavy expectoration for 6 months, was admitted to the hospital. In February 2015, no apparent cause of chest tightness and cough white foam sputum was observed, and no system treatment was found. In August 2015, the aforementioned symptoms worsened. A CT scan revealed the presence of hilar lesions in the left lung (Fig. 2a). A physical examination indicated no abnormalities. Baseline examinations and CT scan results revealed presence of lesions measuring approximately 4.0 cm × 3.3 cm, in the left pulmonary hilum and left lung leaf with approximately 2.1 cm × 1.4 cm nodules. Central-type lung cancer with left lung lobe metastasis was considered.

✉ Correspondence to: Zhaozhe Liu. Email: lzz\_summer@126.com  
Zhendong Zheng. Email: zhengzhong@163.com

\* Supported by a grant from the National Natural Science Foundation of China (No. 81702622).

© 2020 Huazhong University of Science and Technology

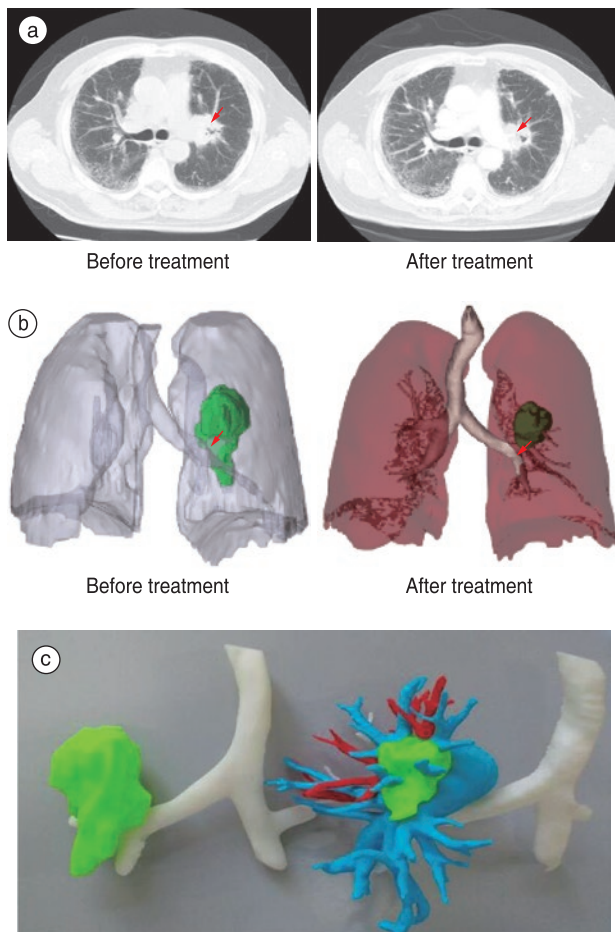


**Fig. 1** (a) CT showed a change in the left lung mass before and after treatment; (b) 3D print before and after the treatment of left lung hilar mass change; (c) 3D print entity model diagram

The preliminary diagnosis was, presence of a lesion in the left lung space, and double lung metastasis. The patient and her family refused to undergo a bronchoscopy biopsy and chemotherapy and requested an oral targeted therapy. The patient was discharged. After 2 months, the patient was readmitted to the hospital. The CT scan results revealed the presence of lesions measuring approximately 5.0 cm × 3.3 cm in the left lung hilum and nodules measuring approximately 2.1 cm × 1.4 cm in the left lung leaf. Comparison of the two 3D print results were shown in Fig. 2b and 2c.

### The cost and time of application of 3D printing technology

Approximately, one hour is required to design a 3D printing scheme on the computer. The printing of the 3D model requires approximately 3 to 5 h. The SD printing cost for each organ is approximately 3000 RMB.

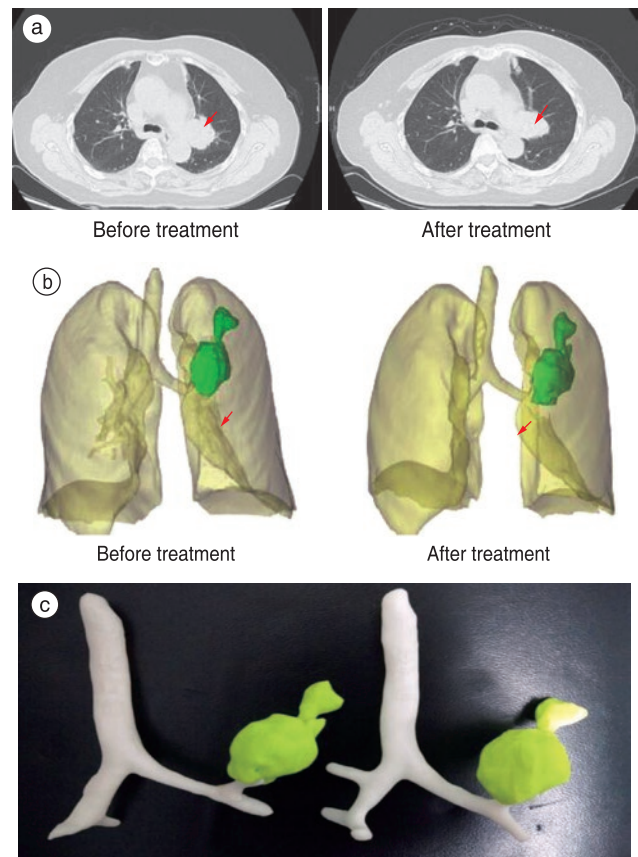


**Fig. 2** (a) CT showed a change in the left lung mass before and after treatment; (b) Print before and after the treatment of left lung hilar mass change; (c) 3D print model diagram

## Discussion

RECIST is a recognized assessment tool used to determine the changes in the tumors following chemotherapy and targeted therapy, and to evaluate the prognosis of patients. The assessment depends on CT imaging of target lesions with LD, and the sum of changes in patients with disease progression, and stable remission [1-2]. Provisions in the RECIST standard include a length of at least 2 slice thickness (10 mm) for a lesion (a thickness of less than 10 mm is considered to be normal in lymph nodes). However, due to the conditional difference of CT imaging, the LD, measured in accordance with LD recist standards, may not be credible. The measurements may be influenced by various factors, such as the shape of target lesions, and thus cannot be a true assessment of the patient's prognosis [2-4]. Moreover, the LD cannot be used to measure tumor invasion. In some cases, the target lesion is not a small tissue necrosis, and as a result, changes in the tumor cannot be measured [5-7].

Three-dimensional printing technology employs hierarchical processing, and gradually superimposes layer

upon layer to generate a 3D entity. The technique uses 3D software and tools to compile information from CT and MRI scans into a CAD file. The 2D cross section is then used to develop a 3D image<sup>[8]</sup>. The 3D printing technology, makes up for the lack of sensitivity of the RECIST standard in the evaluation of disease progression, remission, and stability<sup>[9]</sup>. Three-dimensional printing technology has been used in the field of medicine, as it captures the arbitrary complex geometry of the entity<sup>[9-11]</sup>. This technology allows the surgeon to understand the anatomy of the lesion<sup>[12]</sup>. The establishment of models of the head and neck, heart, pelvis, lung blood vessels, other related tissues and organs, as well as the in vitro simulation of the operating processes may improve the probability of a successful surgery<sup>[10-11, 13-15]</sup>. In medical oncology, 3D printing technology aids in the visualization of tumor volume and determination of tumor location and surrounding blood vessels. Moreover, it may enable the comprehension of blood flow distribution in the tumor and may provide a better observation index for the treatment<sup>[9, 14]</sup>. According to literature<sup>[16]</sup>, 3D printing can also be used as a tool to study metastatic lesions and assess drug sensitivity. The 3D printing technology allows a simulation of malignant tumors within the human body and facilitates an intuitive understanding of tumor volume changes directly with a specific anatomical model interaction. As a result, patients are better able to comprehend the changes in the tumor volume. This understanding limits the dependence on imaging science, and allows direct communication between patients and healthcare providers<sup>[9]</sup>. Moreover, 3D printing technology also requires less materials and reduces labor and production costs<sup>[8]</sup>.

In this paper, the CT results of two cases of lung tumor were compared with 3D printed models. The results indicate a more intuitive and comprehensive understanding of the effect of chemotherapy and targeted therapy on the changes to the tumor volumes, before and after the treatment. Among the two cases of clinical studies using 3D printed models of lung tumors, significant reduction in the volume of lung tumor of one patient was observed. However, in the second patient no significant change in the lung tumor volume was observed. However, the results indicated that a 3D printed model can provide better understanding of the volume changes in the tumor before and after the treatment. Three-dimensional printing is also more convenient and facilitates better communication between doctors and patients. With constant breakthroughs in technology and large-sample clinical research, 3D printing technology is expected to influence future treatments, probably in precision medicine. It can also enable the development of a customized treatment plan, tailored for the patient's specific conditions. The technology may also be extended

to other applications and become a routine procedure in the future. Three-dimensional printing, as a novel technology, has not been widely promoted. Its application requires additional clinical randomized control trials, large-sample control studies, and long-term prognosis and follow-up support.

### Conflicts of interest

The authors indicated no potential conflicts of interest.

### References

- Hu J, Tan BX, Liu M, *et al*. Late course three-dimensional conformal radiotherapy for esophageal carcinoma. *Chinese-German J Clin Oncol*, 2011, 10: 147-149.
- Therasse P, Arbuck SG, Eisenhauer EA, *et al*. New guidelines to evaluate the response to treatment in solid tumors. European Organization for Research and Treatment of Cancer, National Cancer Institute of the United States, National Cancer Institute of Canada. *J Natl Cancer Inst*, 2000, 92: 205-216.
- Nishino M, Cardarella S, Jackman DM, *et al*. RECIST 1.1 in NSCLC patients with EGFR mutations treated with EGFR tyrosine kinase inhibitors: comparison with RECIST 1.0. *AJR Am J Roentgenol*, 2013, 201: W64-W71.
- Beaumont H, Souchet S, Labatte JM, *et al*. Changes of lung tumour volume on CT - prediction of the reliability of assessments. *Cancer Imag*, 2015, 15: 17.
- Sakao Y, Kuroda H, Mun M, *et al*. Prognostic significance of tumor size of small lung adenocarcinomas evaluated with mediastinal window settings on computed tomography. *PLoS One*, 2014, 9: e110305.
- Sakao Y, Nakazono T, Tomimitsu S, *et al*. Lung adenocarcinoma can be subtyped according to tumor dimension by computed tomography mediastinal-window setting. Additional size criteria for clinical T1 adenocarcinoma. *Eur J Cardiothorac Surg*, 2004, 26: 1211-1215.
- Sakao Y, Miyamoto H, Sakuraba M, *et al*. Prognostic significance of a histologic subtype in small adenocarcinoma of the lung: the impact of nonbronchioloalveolar carcinoma components. *Ann Thorac Surg*, 2007, 83: 209-214.
- Eisenhauer EA, Therasse P, Bogaerts J, *et al*. New response evaluation criteria in solid tumours: revised RECIST guideline (version 1.1). *Eur J Cancer*, 2009, 45: 228-247.
- AlAli AB, Griffin MF, Butler PE. Three-dimensional printing surgical applications. *Eplasty*, 2015, 15: e37.
- Sodian R, Weber S, Markert M, *et al*. Pediatric cardiac transplantation: three-dimensional printing of anatomic models for surgical planning of heart transplantation in patients with univentricular heart. *J Thorac Cardiovasc Surg*, 2008, 136: 1098-1099.
- Witschey WR, Pouch AM, McGarvey JR, *et al*. Three-dimensional ultrasound-derived physical mitral valve modeling. *Ann Thorac Surg*, 2014, 98: 691-694.
- Schmauss D, Gerber N, Sodian R. Three-dimensional printing of models for surgical planning in patients with primary cardiac tumors. *J Thorac Cardiovasc Surg*, 2013, 145: 1407-1408.
- Chae MP, Rozen WM, McMenamin PG, *et al*. Emerging applications of bedside 3D printing in plastic surgery. *Front Surg*, 2015, 2: 25.
- Nakada T, Akiba T, Inagaki T, *et al*. Thoracoscopic anatomical subsegmentectomy of the right S2b + S3 using a 3D printing model with rapid prototyping. *Interact Cardiovasc Thorac Surg*, 2014, 19: 696-698.

15. Akiba T, Nakada T, Inagaki T. Simulation of the fissureless technique for thoracoscopic segmentectomy using rapid prototyping. *Ann Thorac Cardiovasc Surg*, 2015, 21: 84–86.
16. Zhu W, Holmes B, Glazer RI, *et al*. 3D printed nanocomposite matrix for the study of breast cancer bone metastasis. *Nanomedicine*, 2016, 12: 69–79.

**DOI 10.1007/s10330-019-0374-4**

**Cite this article as:** Yang XD, Han T, Zhang Y, *et al*. The application of 3D printing in the development of RECIST standard for evaluating tumor efficacy. *Oncol Transl Med*, 2020, 6: 39–42.

# Adrenal endothelial cyst associated with adrenocortical adenoma: a case report and literature review

Yuxiang Hong<sup>1,2</sup>, Qingtao Yang<sup>1</sup> (✉), Junhong Zheng<sup>1</sup>, Gaoming Hou<sup>1</sup>

<sup>1</sup> Department of Urology, Shantou University Medical College Second Affiliated Hospital, Shantou 515041, China

<sup>2</sup> Shantou University Medical College, Shantou 515041, China

## Abstract

We present a case of a middle-aged male Chinese patient who was asymptomatic with a large (6 × 7 cm) right adrenal mass was found in this patient upon routine health examination. He underwent laparoscopic right adrenalectomy after comprehensive evaluation, and the mass was finally diagnosed as right adrenal endothelial (vasculature) cyst associated with adrenocortical adenoma according to pathological and immunohistochemical studies. The puzzling image resemblance of a variation of adrenal cyst to carcinoma necessitated histological examination for confirmative diagnosis. The development of endothelial cyst is extremely rare, and its association with other adrenal neoplasms is even rarer. Herein, we report a new case of adrenal endothelial cyst associated with adrenocortical adenoma, which was almost indistinguishable from adrenocortical carcinoma, and hope that it would be helpful in the diagnosis of other similar cases.

**Key words:** adrenal; endothelial cyst; adenoma; urology

Received: 24 September 2019

Revised: 15 October 2019

Accepted: 25 November 2019

A 53-year-old man was hospitalized because of a large right adrenal mass that was incidentally found on plain and contrast-enhanced abdominal computed tomography (CT) scan upon routine health examination. The patient has type 2 diabetes for > 2 years, and blood glucose level was well controlled with regular use of glimepiride (4 mg once daily) and acarbose (50 mg thrice daily). He had no significant medical or family history. He did not show any Cushingoid features, such as moon face and skin atrophy, on physical examination. Body mass index was 26.1 kg/m<sup>2</sup> (height, 1.65 m; weight, 71 kg), and the pattern of fat deposition was generalized rather than centripetal. The preoperative blood pressure ranged from 114/78 mmHg to 133/89 mmHg, and the heart rate was from 73 beats/min to 88 beats/min. The laboratory examination results, including biochemical and hematological investigations, urinalysis, and coagulation, were within normal limits. Basal plasma levels of prostatic antigen Total Prostate Specific Antigen (TPSA) and Free Prostate Specific Antigen (FPSA), cortisol, aldosterone, urine 17-ketosteroid, and

3-methoxy 4-hydroxymandelic acid were within normal limits (Table 1). Abdominal CT scan (Fig. 1) demonstrated a huge (6 × 7 cm) circular low-density right adrenal mass. A multi-room separation can be observed inside the mass, and plaque-like high-density calcification can be observed on the wall of the capsule. The CT value is approximately 17 HU. There was no significant enhancement on contrast-enhanced CT. After comprehensive condition assessment, case discussions, and obtaining informed consent from the patient, the possibility that the tumor may be a nonfunctioning adrenocortical carcinoma (AC) was considered. Laparoscopic right adrenalectomy was performed. The specimen was sent for histopathological and immunohistochemical examination. The cystic mass (7.0 × 6.0 × 2.5 cm) has clear content, and the pale-yellow mass (5.0 × 1.0 × 1.0 cm) was noted outside the capsule wall, whose slice surface was yellowish and soft (Fig. 2). Microscopically, the cystic mass was composed of fibrous sac wall tissues with local calcification. Another mass with fibrous capsule outside the cystic wall

**Table 1** Summary of the preoperative laboratory data

Items	Unit names	Measured value	Range
TPSA	ng/mL	0.54	(0–4)
FPSA	ng/mL	0.2	(≤ 4)
Cortisol (4:00 pm)	μg/dL	4.9	(1.5–12)
Cortisol (12:00 am)	μg/dL	1.74	(1.5–8)
Cortisol (8:00 am)	μg/dL	8.19	(4.3–22.4)
Aldosterone (standing position)	ng/L	164.8	(65–295)
Aldosterone (supine position)	ng/L	128.95	(59–173)
17-OHCS	μmol/24h	9.1	(8.3–27.7)
VMA	μmol/25h	16	(0–68.6)
CEA	μg/L	1.9	(0–5)
AFP	μg/L	3.5	(< 9)
CA-125	IU/mL	4.6	(0–68)
CA-199	U/mL	16.87	(0–37)

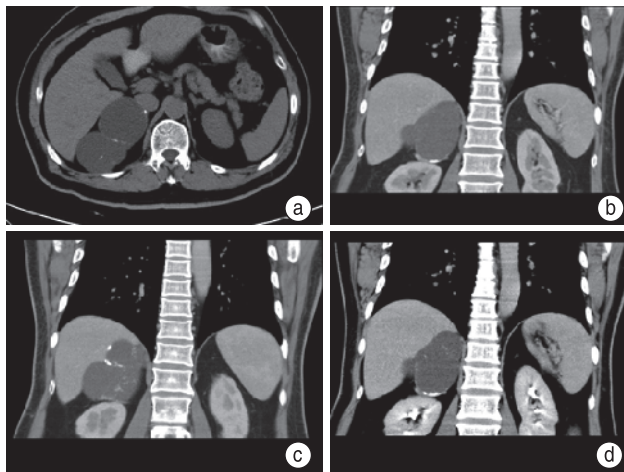


**Fig. 1** Transversal CT scanning. (a) 6 × 7 cm circular right adrenal mass. Coronal CT scanning; (b) Low-density mass, CT value 17 HU; (c) Multi-room separation inside the mass; (d) Plaque-like high-density calcification on cyst wall

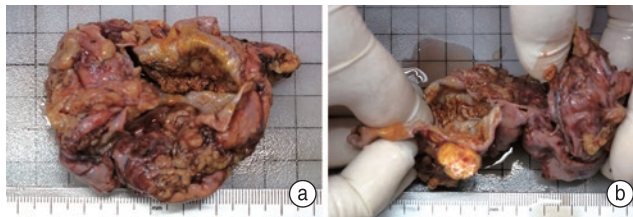


**Fig. 2** (a) Cystic mass (7.0 × 6.0 × 2.5cm) with clear content; (b) Pale-yellow mass (5.0 × 1.0 × 1.0cm) outside the capsule wall, with yellowish and soft slice surface

composed of bright and dark cells, which are arranged in acinar and flaky shapes, can be found, and a large and deformed nucleus was present in the foci. The result of immunohistochemistry shows that the cells stained positive for CD34 (angiomatic marker/+), D2-40 (lymph angiomatic marker/+), desmin(+), and SMA(+). (Fig. 3).

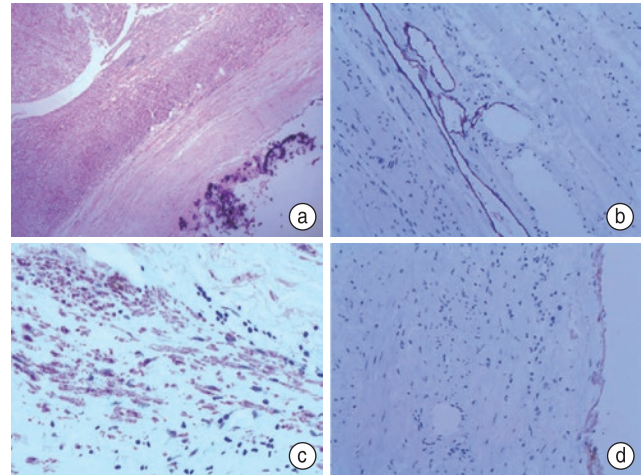


**Fig. 3** Microscopically (HE staining × 40), the junction of fibrous sac wall tissue and adrenocortical adenoma cells (a). The result of immunohistochemistry shows that the cells stained positive for D2-40 (b), SMA (c), and CD34 (d)

Based on the histological and immunohistochemical results, right adrenal endothelial (vasculature) cyst associated with adrenocortical adenoma was the final pathologic diagnosis. The patient had an uneventful hospital course and was discharged on the 13th postoperative day.

## Discussion

Incidental adrenal masses are common and develop in approximately 3%–7% of adults. They are more frequently detected because of increased utilization and improved spatial resolution of CT and magnetic resonance imaging (MRI). The pathological types of adrenal tumors include adenomas, myelolipomas, pheochromocytomas, ACs, adrenal lymphoma, and cysts. The most frequent type is a benign, non-hyperfunctioning adenoma<sup>[1]</sup>.

An adenoma is usually incidentally found on imaging and exhibits no hormonal activity. When hormonally active, it may produce cortisol or aldosterone. Adenomas can be accompanied by the following clinical syndromes: hypercortisolism (Cushing's syndrome) and hyperaldosteronism<sup>[2]</sup>. Generally, adenomas can be divided into two groups: lipid-rich and lipid-poor adenomas. This determines the appearance of adenomas on CT and MRI<sup>[3]</sup>.

Cysts are a rare pathological type of adrenal glands. The number of patients with adrenal cystic lesions determined by autopsy is approximately 14 per 20,000, which constitutes 0.074% of the general population<sup>[4]</sup>. Since most adrenal cysts are asymptomatic, they are usually incidental findings on imaging studies or discovered incidentally during surgery performed for

other abdominal pathologies. Their diagnostic rate has increased in the last two decades due to the widespread use of imaging studies with improved techniques [5]. The sensitivity of a CT for an abdominal hydatid cyst is 97%. To identify a hydatid cyst, CT or MRI can reveal a cystic lesion and the presence of daughter cysts [6]. The radiological features of cystic lesions are diverse because of the heterogeneous texture within the cysts. Classifications have been proposed, and that by Barron and Emanuel in 1961 is now widely accepted. They categorized adrenal cystic lesions into pseudocysts, epithelial cysts, endothelial cysts, and parasitic cysts [7].

The development of endothelial cyst is extremely rare, and its association with other adrenal neoplasms is even rarer. The review by Erickson *et al.* included only one case of endothelial cyst associated with pheochromocytoma [8]. In 2009, Nigawara *et al.* reported the first case of adrenal endothelial cyst associated with adrenocortical adenoma [9]. Herein, we report a second similar case of adrenal endothelial cyst associated with adrenocortical adenoma, which was almost indistinguishable from AC.

The main challenge of managing adrenal mass is to correctly distinguish the rare unexpected malignant lesion or hyperfunctioning adenoma from a benign, clinically insignificant disease. Adrenalectomy is required in hormonally active tumors responsible for syndromes and symptoms of uncontrolled release of hormones. The Adrenal Subcommittee of the American College of Radiology Incidental Findings Committee has presented the algorithm for evaluation of an incidentally detected adrenal mass. The algorithm was applied to patients who are aged > 18 years, asymptomatic, and referred to imaging for a reason that is unrelated to potential adrenal pathology. Moreover, it recommended that patients with adrenal mass > 4 cm in size without cancer history may consider resection [1]. Smaller tumors, growing over the period of observation, or those that do not fulfill the criteria of benign adenoma in imaging studies should also be excised [4].

Therefore, we presented a case of adrenal endothelial cyst associated with adrenocortical adenoma, which could not be clearly discriminated from AC in preoperative imaging studies. Suspicious large adrenal mass (> 4 cm)

should always be closely characterized and considered for resection because it may compress surrounding organs. Moreover, there is a potential risk of malignancy that requires detailed histological exploration. When we do not attempt to distinguish clinically significant from insignificant disease, we are at risk for overdiagnosis or even misdiagnosis.

### Conflicts of interest

The authors indicated no potential conflicts of interest.

### References

1. Mayo-Smith WW, Song JH, Boland GL, *et al.* Management of incidental adrenal masses: a white paper of the ACR incidental findings committee. *J Am Coll Radiol*, 2017, 14: 1038–1044.
2. Ctvrtlik F, Koranda P, Tichy T. Adrenal disease: a clinical update and overview of imaging. A review. *Biomed Pap Med Fac Univ Palacky Olomouc Czech Repub*, 2014, 158: 23–34.
3. Korobkin M, Giordano TJ, Brodeur FJ, *et al.* Adrenal adenomas: relationship between histologic lipid and CT and MR findings. *Radiology*, 1996, 200: 743–747.
4. Major P, Pędziwiatr M, Matlok M, *et al.* Cystic adrenal lesions - analysis of indications and results of treatment. *Pol Przegl Chir*, 2012, 84: 184–189.
5. Chien HP, Chang YS, Hsu PS, *et al.* Adrenal cystic lesions: a clinicopathological analysis of 25 cases with proposed histogenesis and review of the literature. *Endocr Pathol*, 2008, 19: 274–281.
6. Akçay MN, Akçay G, Balik AA, *et al.* Hydatid cysts of the adrenal gland: review of nine patients. *World J Surg*, 2004, 28: 97–99.
7. Barron SH, Emanuel B. Adrenal cyst. A case report and a review of the pediatric literature. *J Pediatr*, 1961, 59: 592–599.
8. Erickson LA, Lloyd RV, Hartman R, *et al.* Cystic adrenal neoplasms. *Cancer*, 2004, 101: 1537–1544.
9. Nigawara T, Sakihara S, Kageyama K, *et al.* Endothelial cyst of the adrenal gland associated with adrenocortical adenoma: preoperative images simulate carcinoma. *Inter Med*, 2009, 48: 235–240.

DOI 10.1007/s10330-019-0378-8

Cite this article as: Hong YX, Yang QT, Zheng JH, *et al.* Adrenal endothelial cyst associated with adrenocortical adenoma: a case report and literature review. *Oncol Transl Med*, 2020, 6: 43–45.



# 中国科技核心期刊

(中国科技论文统计源期刊)

## 收录证书

CERTIFICATE OF SOURCE JOURNAL  
FOR CHINESE SCIENTIFIC AND TECHNICAL PAPERS AND CITATIONS

### ONCOLOGY AND TRANSLATIONAL MEDICINE

经过多项学术指标综合评定及同行专家  
评议推荐，贵刊被收录为“中国科技核心期  
刊”（中国科技论文统计源期刊）。

特颁发此证书。

中国科学院  
中国科学技术信息研究所

Institute of Scientific and Technical Information of China

北京复兴路 15 号 100038

www.istic.ac.cn

2019年11月





中国抗癌协会  
CHINA ANTI-CANCER ASSOCIATION

2020.4.15-21

第26届全国肿瘤防治宣传周

中国抗癌日

4.15

抗癌路上

你我同心

科技助力  规范诊治